SSD

SCIENCE FOR A SUSTAINABLE DEVELOPMENT

# " ROLE OF PELAGIC CALCIFICATION AND EXPORT OF CARBONATE PRODUCTION IN CLIMATE CHANGE"

## «PEACE»

L. CHOU, J. HARLAY, C. DE BODT, N. ROEVROS, J.-P. VANDERBORGNT, A.V. BORGES, K. SUYKENS, B. DELILLE, P. JOASSIN, S. SOLLBERGER, M. GRÉGOIRE, K. SABBE, N. VAN OOSTENDE, A. ENGEL, J. PIONTEK, N. HÄNDEL, C. BORCHARD, S. KOCH, A. BIERMANN AND M. LUNAU

ENERGY

TRANSPORT AND MOBILITY

AGRO-FOOD

HEALTH AND ENVIRONMENT

CLIMATE

BIODIVERSITY

ATMOSPHERE AND TERRESTRIAL AND MARINE ECOSYSTEMS

TRANSVERSAL ACTIONS

.be

**SCIENCE FOR A SUSTAINABLE DEVELOPMENT**
**(SSD)**

FINAL REPORT - Fase 1

# ROLE OF PELAGIC CALCIFICATION AND EXPORT OF CARBONATE PRODUCTION IN CLIMATE CHANGE
# "PEACE"

**SD/CS/03**


Promotors

**Lei Chou**
Université Libre de Bruxelles (ULB)
Laboratoire d'Océanographie Chimique et Géochimie des Eaux
Campus Plaine – CP 208, Boulevard du Triomphe, B-1050 Brussels

**Alberto V. Borges**
Université de Liège (ULg)
Unité d'Océanographie Chimique, B5
Allée du 6 Août 17, B-4000 Liège

**Koen Sabbe**
Universiteit Gent (UGent)
Protistologie & Aquatische Ecologie
Krijgslaan 281 S8, B-9000 Gent

**Anja Engel**
Alfred Wegener Institute for Polar and Marine Research (AWI)
'Global change and the future marine Carbon cycle' Group
Am Handelshafen 12, D-27515 Bremerhaven

Authors

L. Chou, J. Harlay, C. De Bodt, N. Roevros, J.-P. Vanderborght (ULB)
A.V. Borges, K. Suykens, B. Delille, P. Joassin, S. Sollberger, M. Grégoire (ULg)
K. Sabbe, N. Van Oostende (UGent)
A. Engel, J. Piontek, N. Händel, C. Borchard, S. Koch, A. Biermann,
M. Lunau (AWI)


BELGIAN SCIENCE POLICY


Avenue Louise 231
Louizalaan 231
B-1050 Brussels
Belgium
Tel: +32 (0)2 238 34 11 – Fax: +32 (0)2 230 59 12
http://www.belspo.be

Contact person: Martine Vanderstraeten
+32 (0)2 238 36 10



L. Chou, J. Harlay, C. De Bodt, N. Roevros, J.-P. Vanderborght, A.V. Borges, K. Suykens, B. Delille, P. Joassin, S. Sollberger, M. Grégoire, K. Sabbe, N. Van Oostende, A. Engel, J. Piontek, N. Händel, C. Borchard, S. Koch, A. Biermann and M. Lunau. ***Role of pelagic calcification and export of carbonate production in climate change « PEACE » (SD/CS/03).*** Final Report. Brussels Belgian Science Policy 2009 – 121 p. (Research Programme Science for a Sustainable Development)

## TABLE OF CONTENTS

## ACRONYMS, ABBREVIATIONS AND UNITS

$^{14}C$: radioactive carbon
AIMES: Analysis, Integration and Modelling of the Earth System
AWI: Alfred Wegener Institute for Polar and Marine Research
BBP: Bacterial biomass production
BCC: bacteria community composition
BCE: Bayesian Composition Estimator
BGE: Bacterial growth efficiency
CAL: Calcification
$CaCO_3$: calcium carbonate
Chl-a: Chlorophyll a
CFB: Cytophaga-Flavobacterium-Bacteroides
DAPI: 4'-6-Diamidino-2-phenylindole
DEA: Dissolved esterase activity
DCCHO: Dissolved combined carbohydrates
DIC: Dissolved inorganic carbon
$DIC_{35.5}$: Dissolved inorganic carbon normalized to a salinity of 35.5
DGGE: Denaturating Gradient Gel Electrophoresis
DMS: Dimethylsulfide
DMSP: Dimethylsulfoniopropionate
$DMSP_d$: dissolved dimethylsulfoniopropionate
$DMSP_p$: particulate dimethylsulfoniopropionate
DOC: Dissolved organic carbon
EA: Esterase activity
*E. huxleyi* / *E. hux*: *Emiliania huxleyi*
EGU: European Geoscience Union
EU: European Union
EPS: Exopolymer substances
ESD: Equivalent spherical diameter
F: Air-sea $CO_2$ fluxes
FDA: Fluorescein diacetate
FL: Free-living fraction
FTA : Benthic flux of total alkalinity
Fx: Fucoxantin
GC: Gas chromatograph
GLOBEC Global Ocean Ecosystem Dynamics
GPP: Gross primary production
HFx: Hexanoyl fucoxantin
HPAEC: High-Performance Anion-Exchange Chromatography
HPLC-IRMS: High-Performance Liquid Chromatography – Isotope Ratio Mass Spectrometry
HR: high reflectance
IGBP: International Geosphere Biosphere Programme
IMBER: Integrated Marine Biogeochemistry and Ecosystem Research
IOC: Intergovernmental Oceanographic Commission
IPCC: Intergovernmental Panel on Climate Change
*k* : gas transfer velocity
LOICZ: Land-Ocean Interactions in the Coastal Zone
MUF: methylumbelliferone

MWCO: Molecular weight cutoff
NCP: Net community production
NCC : Net community calcification
NEP: Net ecosystem production
NIOO-CEME: Netherlands Institute of Ecology - Centre for Estuarine and Marine Ecology
NOAA: National Oceanic and Atmospheric Administration (USA)
NPP: Net primary production
$\Omega_{calcite}$ / $\Omega_{CAL}$: Saturation state with respect to calcite
OMEX-I: Ocean Margin Exchange part I
PA: particle associated fraction
PAD: Pulsed amperometric detection
$pCO_2$: $CO_2$ partial pressure
$pCO_2$@13°C: $CO_2$ partial pressure normalized to a temperature of 13°C
$pCO_2$@SST: $CO_2$ partial pressure at in-situ temperature (SST)
PCA:
PCHO: Polysaccharide
PEA: Particulate esterase activity
Phaeo : phaeopigments
PIC: Particulate inorganic carbon
$PO_4$: dissolved phosphate
POC: Particulate organic carbon
POM : Particulate organic matter
PON: Particulate organic nitrogen
POP: Particulate organic phosphorus
PP: Primary production
ppm: parts per million
R : benthic respiration
Ra: autotrophic respiration
Rh: heterotrophic respiration
SCOR: Scientific Committee on Oceanic Research
SeaWiFS: Sea-viewing wide field-of-view sensor
SEM: Scanning electron microscopy
SOLAS: Surface Ocean-Lower Atmosphere Study.
SPM: Suspended particulate matter
SST: Sea-surface temperature
TA: Total alkalinity
$TA_{35.5}$: total alkalinity normalized to a salinity of 35.5
$TA_{anomaly}$: total alkalinity anomaly
TCCHO: Total combined carbohydrates
TDN: Total dissolved nitrogen
TEA: Total esterase activity
TEP: Transparent exopolymer particles
TEP-C: Carbon content of transparent exopolymer particles
TOC: Total organic carbon
TPC: Total particulate carbon
TR: Total Respiration
UGent: Universiteit Gent
ULB: Université Libre de Bruxelles
ULg: Université de Liège

UPGMA: Unweighted Pair Group Method with Arithmetic mean
α : solubility coefficient of $CO_2$
Δ $pCO_{2observed}$ : total change of observed $CO_2$ partial pressure
$\Delta DIC_{computed}$ : total change of computed Dissolved inorganic carbon
$\Delta DIC_{observed}$ : total change of observed Dissolved inorganic carbon
$\Delta DIC_{org}$: change of Dissolved inorganic carbon due to net community calcification
$\Delta DIC_{org}$: change of Dissolved inorganic carbon due to net community production
$\Delta pCO_{2air-sea}$ : $CO_2$ partial pressure air-sea gradient
$\Delta pCO_{2computed}$ : total change of computed $CO_2$ partial pressure
$\Delta pCO_{2inorg}$: change of $CO_2$ partial pressure due to net community calcification
$\Delta pCO_{2org}$: change of $CO_2$ partial pressure due to net community production
$\Delta pCO_{2SST}$: change of $CO_2$ partial pressure due to Sea-surface temperature change
wt/wt: weight to weight
Xeq: Gum Xanthan equivalents
µatm: micro-atmosphere

## 1. SUMMARY

In order to provide an accurate prediction of ocean organic and inorganic carbon storage, it is essential to understand the physical, chemical and biological controls governing the present and future marine ecosystem and ocean carbon dynamics. These also include biogeochemical responses to and feedbacks on climate change. One of the emerging and alarming issues concerns the ocean acidification, due to increasing atmospheric $CO_2$ concentration, and its impacts on marine ecosystems. The important role of calcification in the global carbon cycle has been increasingly recognized. A better understanding of the effects of changing pH and carbon system parameters on marine biogeochemical cycles and organisms is urgently needed to allow the evaluation of different scenarios of $CO_2$ increase and mitigation strategies. Redressing this concern should be of high priority within research agendas. This was especially important in the context of the preparation of the 2007 IPCC assessment report and will contribute to the scientific basis of the drafting of the second Kyoto Protocol (2012). As pointed out in a document prepared by a group of global change scientists on ocean acidification (The Royal Society of London, 2005), this issue also needs to be kept under review by international scientific bodies such as IOC, SCOR and IGBP. Furthermore, a bill was introduced recently to the US senate to establish an interagency committee to develop an ocean acidification research and monitoring plan and to establish an ocean acidification program within NOAA. The present research contributes to the core projects of the IGBP: AIMES, GLOBEC, IMBER, LOICZ and SOLAS.

The overall objective of the PEACE project is to evaluate the role in climate regulation of calcification, primary production and export processes during coccolithophorid blooms. We use a transdisciplinary approach that combines process-oriented field investigations with laboratory experiments and modelling tools. Specific objectives are:

1) to study the net ecosystem dynamics during coccolithophorid blooms,
2) to unravel the link between the bacterial community, grazing, transparent exopolymer particles (TEP) dynamics, carbon export and dimethylsulfide (DMS) cycling during coccolithophorid blooms,
3) to assess the effects of ocean acidification on coccolithophorid metabolism and TEP production, and
4) to model coccolithophorid dynamics and their impact on ocean dissolved inorganic carbon (DIC) chemistry.

The objectives of the project were met and major conclusions can be summarized hereafter.

In the period 2006-2008, intense phytoplankton blooms were observed and sampled along the shelf break of the Northern Bay of Biscay. These blooms were either

dominated by diatoms or coccolithophores (mainly *E. huxleyi*), with prasinophytes, dinoflagellates and cryptophytes as codominants, and were characterized by high spatial and (short-term and interannual) temporal variability in composition and biomass, as different phases of the spring bloom were sampled during the cruises. In general, the degree of water column stratification appeared to be a good predictor of bloom stage, with especially coccolithophores declining as stratification increased. Spatial and temporal patterns in bacterial community composition were complex and appeared to be highly station-specific; there was however little change with depth (0-80 m). While they roughly corresponded (directly or indirectly) to bloom composition, other factors (e.g. nutrients) also appeared to affect these communities.

Results from biogeochemical investigations showed that our study area acted as a sink for atmospheric $CO_2$. Hence, the balance of organic carbon fixation to inorganic carbon production during coccolithophorid blooms does not lead to a significant accumulation of $CO_2$ that would reverse the direction of the air-sea $CO_2$ flux (i.e. from a sink to a source of atmospheric $CO_2$). The impact of calcification on reducing the $CO_2$ sink in the study area is variable, but on average it is relatively small, ~12%. This implies that the potential feedback on atmospheric $CO_2$ of the projected decrease of pelagic calcification, due to the "production" of $CO_2$ from biogenic precipitation of $CaCO_3$, would probably be minor.

Our data also showed that benthic $CaCO_3$ dissolution rates over the continental shelf represent ~1% of the pelagic calcification rates. This suggests a decoupling of calcification by coccolithophores and the dissolution of $CaCO_3$ in the sediments. Particulate inorganic carbon (PIC) produced by coccolithophores is either stored in the sediments or exported out of the system, but does not seem to be significantly dissolved in the sediments.

Field investigations showed that the northern Biscay area is a zone of high calcite production as witnessed by reflectance images and $^{14}C$ incorporation measurements. Biogenic calcium carbonate may act as "ballast" and increases the transfer efficiency of particulate organic carbon (POC) from the surface ocean to the deep waters (Armstrong et al., 2002; Klaas and Archer, 2002). In addition, TEP production during coccolithophorid blooms has also been shown to enhance organic matter export (De la Rocha and Passow, 2007). During our cruises, the contribution of TEP-C to POC has been shown to be important. Thus, the ballast effect and the production of TEP could be responsible for a high export of particulate matter in the northern Bay of Biscay. The contribution of TEP in coccolithophore aggregates to the vertical export was not quantified in this study. Nevertheless, a large deposit of gelatinous matter was observed in late August 1995 along the slope of the N.W. European continental margin (de Wilde et al., 1998). Pigment analyses revealed that prymnesiophytes (coccolithophores, mainly *E. huxleyi*) were the major contributor to this mucus-rich

aggregates layer, which was confirmed by SEM examination (de Wilde et al., 1998). The production of TEP could thus constitute the first step within the process of coccolithophore aggregation, sedimentation and seafloor deposition in the Bay of Biscay.

Our field data showed that high lysis rates co-occurred with a high microplankton grazing rates, together forming key sources of phytoplankton mortality. Both processes tended to intensify with increasing water column stratification, suggesting an indirect bottom-up control on phytoplankton loss. These results can be paralleled with increasing community pelagic respiration, bacterial production, and an evolution towards net heterotrophy with increasing stratification. In addition to grazing and cell lysis, viral cell lysis was identified as an additional loss term that could be significant (in accodance with previous mesocosm experiements) yet poorly investigated and quantified in the field.

Finally, our biogeochmical investigations allowed a better understanding of the TEP dynamics under naturally occurring bloom conditions:

- Dissolved acidic sugars are an important source for TEP production during coccolithophorid blooms in the Bay of Biscay
- Analysis of size spectrum of particles suggests assembly of lager particles from smaller ones by aggregation.
- Important concentrations of TEP were observed at the sediment-water interface (up to 10% of the pelagic TEP stock), which suggests that sediment deposition and diagenetic degradation could be a major fate of pelagic TEP.

Our laboratory experiments yielded new results, which contribute to a better understanding of the future response of C cycling in pelagic calcifying communities to ocean acidification and other global change factors (e.g. temperature):

- Calcification per cell decreased by 34% in the culture at present $pCO_2$ and by 7% in the one at future $pCO_2$ with a temperature increase of 5°C
- Changes in polysaccharide composition indicate that the surplus of free glucose generated by higher glucosidase rates was efficiently metabolized by bacterioplankton and that the bacterial substrate supply was improved under simulated future-ocean pH
- Lowering of pH potentially changed the equilibrium between TEP-precursors and TEP for the benefit of TEP formation. Further investigations are needed to explore the underlying mechanisms of increased TEP formation in response to increasing $pCO_2$
- Net production of particulate organic matter (POM), such as POC and TEP, decreased significantly with increasing $pCO_2$ in contrast to previous studies. This is due to the increase in bacterial biomass production under nutrient deplete

conditions with increasing $pCO_2$, suggesting that the response to ocean acidification may depend on the ecosystem status, i.e. on the balance between autotrophic and heterotrophic communities.

- Rising $pCO_2$ induced a decrease in the PIC:POC ratio and reduced the sinking velocity of aggregates of *Emiliania huxleyi*. Our findings therefore suggest a reduced deep-export of organic matter in the ocean, if $pCO_2$ in seawater further increases.

Overall, the results obtained during PEACE reveal that our understanding of the effects of ocean acidification on marine biogeochemistry, carbon cycling and potential feedbacks on increasing atmospheric $CO_2$ is still in its infancy. Further research is required to reduce uncertainties and to improve our knowledge before a robust and credible implementation in mathematical models can be achieved, allowing the projection of a plausible future evolution of carbon biogeochemistry under global change. Such future research will necessitate a multitude of approaches, such as a combination of laboratory experiments, field measurements and modelling as carried out in the framework of the PEACE project.

Key words: marine carbon cycle, ocean acidification, pelagic calcification, biogenic calcium carbonate, carbon dioxide uptake by the oceans, air-sea fluxes

## 2. INTRODUCTION

The accumulation of anthropogenic $CO_2$ has altered carbonate chemistry in surface waters (ocean acidification) since pre-industrial times and is expected to continue to do so in the coming centuries (Orr et al., 2005). Changes in the carbonate chemistry of surface waters related to ocean acidification can alter the rates and fates of primary production and calcification of numerous marine organisms and communities (Kleypas et al., 2006; Doney et al., 2009). Such modifications can provide either positive or negative feedbacks on increasing atmospheric $CO_2$ by changing the flux of $CO_2$ between the ocean and the atmosphere.

Coccolithophores (also called coccolithophorids), among which *Emiliania huxleyi* (*E. huxleyi*) is the most abundant and widespread species, are considered to be the most productive calcifying organism on earth. *E. huxleyi* often forms massive blooms in temperate and sub-polar oceans and, in particular, at continental margins and shelf seas. The intrinsic coupling of organic matter production and calcification in coccolithophorid blooms underlines their biogeochemical importance in the marine carbon cycle. Primary production via photosynthesis in the photic zone and vertical export of organic matter to deep waters draw down $CO_2$:

$$CO_2 + H_2O \rightarrow CH_2O + O_2$$

This is the so-called "organic carbon pump". In contrast, calcification and thus formation of biogenic calcium carbonate ($CaCO_3$), consumes total and carbonate alkalinity and releases $CO_2$:

$$Ca^{2+} + 2HCO_3^- \rightarrow CaCO_3 \text{ (PIC)} + H_2O + CO_2$$

This is often named the "carbonate counter-pump" because it counteracts the effect on $CO_2$ fluxes. The rain ratio, defined here as the ratio of particulate inorganic carbon (PIC) to particulate organic carbon (POC) in exported biogenic matter, determines the relative strength of the two biological carbon pumps and consequently the flux of $CO_2$ across the surface ocean-atmosphere interface.

Several manipulative experiments to test the effect of ocean acidification on coccolithophorids have shown that calcification would decrease in the future, while export of organic carbon could increase (Riebesell et al., 2000; Engel et al., 2004b; Delille et al., 2005; Riebesell et al., 2007). This enhancement of POC was in part explained by higher production of transparent exopolymer particles (TEP) under future $CO_2$ conditions (Delille et al., 2005). TEP are formed from phytoplankton exudates such as polysaccharides. It has been shown that TEP enhance particle aggregation (Logan et al., 1995; Engel, 2000) and participate in marine snow formation and

sinking (Alldredge et al., 1993; Logan et al., 1995; Passow et al., 2001; Passow, 2002).

For a robust and credible implementation in mathematical models of feedback mechanisms to allow the projection of a plausible future evolution of carbon biogeochemistry under global change, it is required to understand present day biogeochemistry and ecology of pelagic calcifying communities under field conditions. This can only be achieved with comprehensive and multidisciplinary studies of carbon cycling during coccolithophorid blooms under natural conditions such as those carried out during the PEACE project. To further unravel the potential feedbacks of changes of marine carbon biogeochemistry and in particular pelagic calcification due to ocean acidification, laboratory experiments were undertaken to assess these effects under controlled conditions. Finally, based on knowledge acquired from experimental studies and with the contribution from the whole consortium a mathematical model was developed to evaluate the effects of ocean acidification on coccolithophorid physiology.

# 3. MATERIAL AND METHODS

## 3.1 Field study area and sampling

Interdisciplinary biogeochemical investigations, assisted by remote sensing data, were conducted in the Northern Bay of Biscay (one of the main European continental margins), where intense, frequent and recurrent coccolithophorid blooms are observed (Figure 1). Sampling campaigns were carried out onboard the *RV Belgica* in June 2006, May 2007 and May 2008 along the shelf break, characterized by a marked topographic discontinuity. Vertical mixing occurs along this northeastern Atlantic margin and is permanently maintained by turbulent dissipation from pronounced internal waves of tidal origin (Pingree and Le Cann, 1989 and 1990; Pingree and New, 1995). It is intermittently intensified by strong wind events and increases from Goban Spur to La Chapelle Bank (Wollast and Chou, 2001).

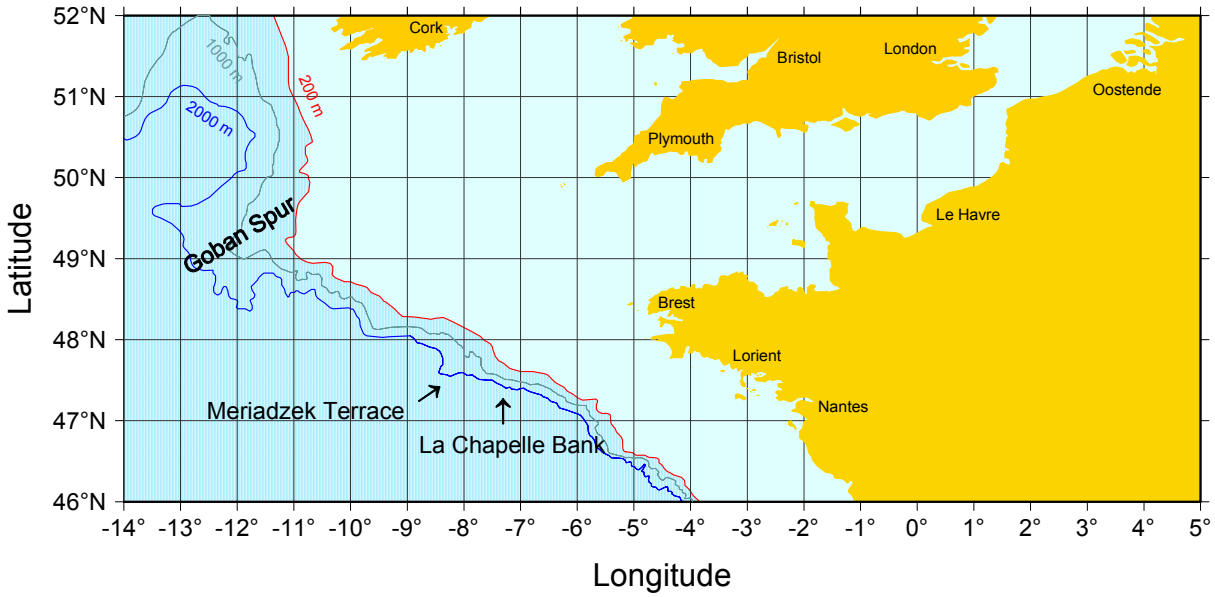


Figure 1. Sampling area along the shelf break in the Northern Bay of Biscay.

Discrete samples were taken from a CTD Rosette sampler equipped with twelve 10 L Niskin bottles. A suit of biogeochmical parameters were measured in the water column, including temperature, salinity, pH, total alkalinity (TA), dissolved organic (DOC) and inorganic carbon (DIC), dissolved oxygen ($O_2$) and inorganic nutrients. To decipher the impact of coccolithophores on climate relevant processes, key processes such as algal characterisation and bacterial community structure, rate of organic and inorganic carbon production, degradation and export, and air-sea exchange of $CO_2$ and DMS were investigated. In addition, we have assessed the role of TEP in carbon sequestration during coccolithophorid blooms.

## 3.2 Process studies during field investigations

### *3.2.1 Primary production and calcification by $^{14}C$ incorporation experiments*

Primary production (PP) is defined here as the potential fixation of dissolved inorganic carbon (DIC) into particulate organic carbon (POC) under ideal conditions of light without cloud coverage. Similarly, calcification (CAL) is the potential fixation of DIC into particulate inorganic carbon (PIC).

The rate of C fixation was estimated from the incorporation of $^{14}C$-bicarbonate. Surface seawater (3m depth) was collected at dawn in acid-clean carboys after filtering through a nylon sieve of 200 µm mesh size to remove zooplankton and then inoculated with $NaH^{14}CO_3$ (45 µCi $ml^{-1}$) to reach a final concentration of 20 µCi $L^{-1}$. For standardization, five aliquots of 500 µl of labelled seawater were placed in scintillation vials to which 500 µl NaOH (0.1N) were added; the standards were stored frozen until counting for radioactivity in the laboratory.

Incubations were carried out in sterile 250 ml culture flasks filled with labelled seawater. The bottles were incubated for about 6 h in a linear incubator reproducing a gradient of irradiance ranging from 5 to 400 µmol Photons $m^{-2}$ $s^{-1}$. During incubation, samples were kept at sea surface temperature (SST) with the ship's seawater supply circulating continuously through the incubator. One flask was wrapped in aluminium foil and another one was poisoned with 5% sodium azide (3 ml $L^{-1}$) and both were incubated in the dark for 6 h to correct the uptake rate for abiotic adsorption.

The incorporation was terminated by filtration of 125 ml of each sample at very low vacuum through 25 mm GF/F glassfiber filters. Duplicate filters (same filtration volume) were collected for each sample. One filter was left untreated and the other was acidified (about 2 minutes on the filtration set) by adding 500 µl of diluted acetic acid (~0.1 M) to eliminate the $^{14}C$ incorporated as PIC. All filters were rinsed with 25 ml of filtered natural seawater in order to remove the excess dissolved inorganic $^{14}C$ and stored frozen in 20 ml scintillation vials until radioactive counting in the laboratory. Radioactivity of the standards and the filters was determined in the laboratory by liquid scintillation counting (10 ml of ReadySafe scintillation cocktail per vial) and corrected for quenching with an external standard. The acidified filters were measured for radioactivity to quantify the incorporation of $^{14}C$ in the organic phase only and thus the PP. The amount of inorganic $^{14}C$ incorporated into PIC was obtained by difference between total $^{14}C$ incorporation and the assimilation of $^{14}C$ in POC. The $PO^{14}C$ and $PI^{14}C$ incorporation rates are presented as a function of irradiance (PPvE and CALvE, respectively) and expressed in µg C (µg Chl-a)$^{-1}$ $h^{-1}$ (Figure 2).

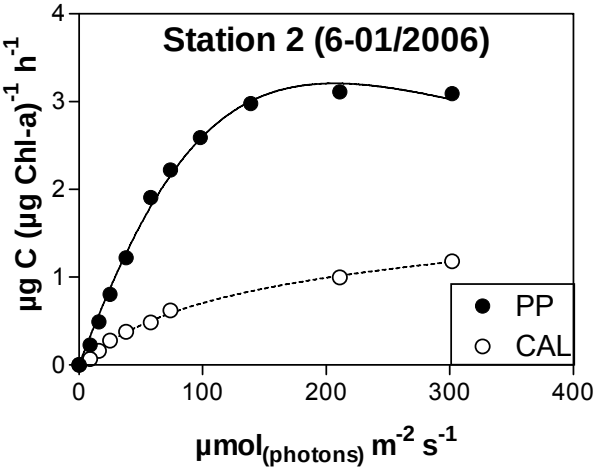


Figure2. Primary productivity (PP) and calcification (CAL) versus light intensity ($E_{(PAR)}$) determined for station 2 on June 1st, 2006. The corresponding PPvE and CALvE curves were established according to Eilers and Peeters (1988).

Daily potential depth-averaged PP ($PP_z$) was integrated and expressed in mg C $m^{-3}$ $d^{-1}$, following equation 1:

$$PP_z = \int_0^t Chl - a_z \times \frac{E_{z,t}}{AE_{z,t}^2 + BE_{z,t} + C} \times dt \quad (1)$$

with $E_{z,t} = E_{o,t} \times e^{-K_d(PAR)\,x\,Z}$ (2)

and $E_{0,t} = E_{max} \times \left( c_1 - c_2 \times cos \frac{2\pi \times t}{86400} \right)$ (3)

$$c_1 = 1 - c_2 \quad (4)$$

$$c_2 = \frac{1}{1 + cos(\alpha)} \quad (5)$$

$$\alpha = \pi \times \left( 1 - \frac{L_d}{24} \right) \quad (6)$$

In the equation 1, A, B and C are parameters determined with the model of Eilers and Peeters (1988) when fitting the PPvE curves. Chl-a concentration was calculated for

each depth (Chl-$a_z$) using a linear interpolation between two consecutive depths and this value was assumed constant over the day. The irradiance (PAR), $E_z$, was computed using the diffuse attenuation coefficient of light, $K_d$(PAR), in the water column, as determined from the vertical profile of PAR (not shown). The equation 3 was used to compute the variation of the irradiance below the surface during the photoperiod. The maximum irradiance at noon ($E_{max}$) and the day-length ($L_d$) were set to values representative of the study area during the period of the sampling campaign (1260 µmol photon $m^{-2}$ $s^{-1}$ and 13.5 hours, respectively).

Assuming a light dependency of PP and CAL during coccolithophores blooms, the Eilers and Peeters (1988) equation was also used to fit CALvE curves and to determine depth-averaged calcification rates ($CAL_z$) in mg C $m^{-2}$ $d^{-1}$ (Equation 7).

$$CAL_Z = \int_0^t chl - a_z \frac{E_{z,t}}{A' E_{z,t}^2 + B' E_{z,t} + C'} \times dt \qquad (7)$$

where A', B' and C' are the parameters determined with Eilers and Peeters (1988) by fitting the CALvE curves.

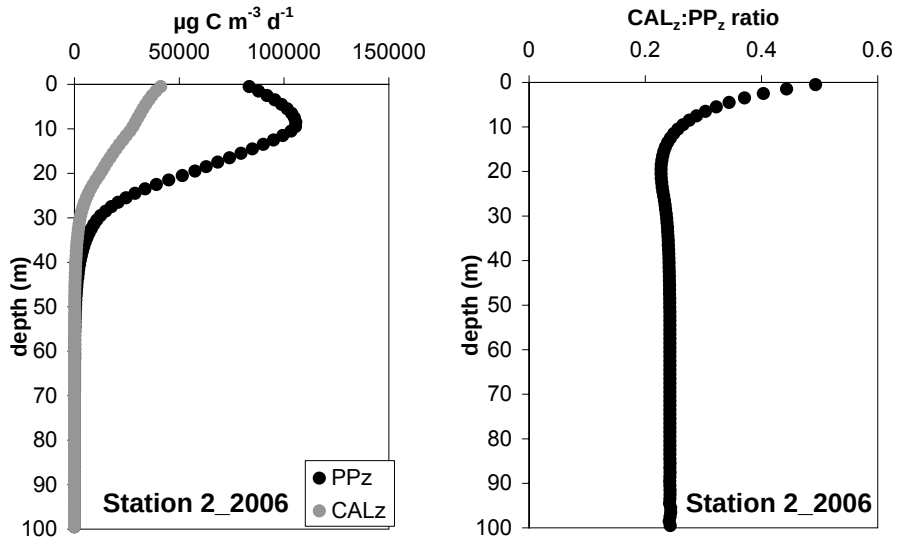


**Figure 3**. Predicted levels of potential $PP_z$ and $CAL_z$ in the water column at station 2 (1st June 2006) (left panel) and the profile of $CAL_z$:$PP_z$ ratio (right panel).

The predicted PPz and CALz based on the PPvE and CALvE parameters (Eilers and Peeters, 1988) exhibit a maximum level corresponding to the Chl-a maximum and indicate that PPz became light-limited at shallower depth than CAL (Figure 3). This pattern coincided with a decrease of $CAL_z$:$PP_z$ ratio in the first 20 meters of the water column.

The daily rate of integrated primary production (PP) was computed according to equation 8.

$$PP = \int_{0}^{z} PP_z \times dz \qquad (8)$$

The daily rate of integrated calcification (CAL) was computed according to equation 9.

$$CAL = \int_{0}^{z} CAL_z \times dz \qquad (9)$$

The daily production of organic and inorganic C was computed over the water column, down to 100 m, with a time-step of 20 seconds and a vertical resolution of 0.1 m. Daily integrated PP and CAL are given in mg C $m^{-2}$ $d^{-1}$.

### *3.2.2 Phytoplankton cell lysis rates*

The specific lysis rate, $\mu_L$, was determined using an improved version (Riegman et al., 2002; Riegman and Winter, 2003) of the esterase method (van Boekel et al., 1992). The release of esterases following cell lysis results in the hydrolysis of fluorescein diacetate (FDA), a nonfluorescent compound which is added as a substrate, causing the release of fluorescein (F), a fluorescent compound (Riegman et al., 2002). FDA is not stable in seawater and its decay rate is dependent on its concentration, temperature, salinity, pH and on the alkalinity of the sample (Riegman et al., 2002). The esterase activity (EA in nmol F $L^{-1}$ $h^{-1}$) is measured fluorimetrically in triplicate samples. The total esterase activity (TEA) is measured on untreated samples, the dissolved esterase activity (DEA) is measured on 0.2 µm filtrate. In order to correct the signal in regard to the nonenzymatic hydrolysis of FDA, EA is also measured on samples filtered on < 10 kDa MWCO to remove esterase.

To determine $\mu_L$ of a natural phytoplankton community, 3 components have to be measured: (1) intracellular amount of EA in the phytoplankton (PEA), which corresponds to TEA-$DEA_c$ where $DEA_c$ stands for the DEA corrected for nonenzymatic hydrolysis of FDA, (2) amount of extracellular DEA and (3) decay rate of $DEA_c$ in the sample (expressed as $t_{1/2}$, i.e. the half-life of EA in seawater). The rate of EA decrease was calculated from the changes in $DEA_c$ with time (t, in hours) by fitting the exponential decay equation. $\mu_L$ is defined here as the ratio of the DEA produced ($DEA_{prod}$) to PEA in a natural assemblage on an hourly basis and expressed per day ($d^{-1}$). It assumes that (1) the decay rate of DEA in a natural sample incubated in the dark at *in situ* temperature equals $DEA_{prod}$ ($DEA_{prod}$ = 0.5 (DEA/ $t_{1/2}$)) and (2) DEA is predominantly attributed to phytoplankton rather than

heterotrophic organisms (van Boekel et al., 1992; Brussaard et al., 1996; Agusti et al., 1998).

### *3.2.3 Phytoplankton growth and mortality rates*

The seawater dilution method (Landry and Hasset, 1982) was used to simultaneously determine the phytoplankton growth and mortality rates. The experimental set-up was largely based upon that of Olson and Strom (2002) and included HPLC pigment analysis allowing the determination of phytoplankton group specific dynamics. Microzooplankton grazing was determined from measurements of the apparent growth rate of phytoplankton, assuming the exponential growth equation of Landry and Hasset (1982). Values of growth and mortality were determined from linear regression analysis between the apparent growth rate of a particular pigment (Chl-a, Hfx, and Fx) and the fraction of undiluted seawater. The proportion of initial Chl-a standing stock turned over daily by the microzooplankton was calculated according to Stelfox-Widdicombe et al. (2000).

### *3.2.4 Bacterial biomass production (BBP)*

Bacterial biomass production (BBP) was estimated from incorporation rates of radiolabelled tracers assessed by liquid scintillation counting. The radiotracer ($^{3}$H-thymidine and $^{14}$C-leucine in 2006 and 2007, respectively) was added to samples of 10 ml volume at a saturating final concentration of 10 nmol $L^{-1}$. Samples were incubated at near *in situ* temperature in the dark. Incubation time ranged from 1 to 2 hours, depending on the bacterial activity. After incubation, samples were poisoned with formalin at a final concentration of 4% to stop bacterial growth. Formalin-killed controls were run for each sampling. Samples were further processed according to Smith and Azam (1992). Briefly, subsamples of 2 ml were centrifuged at approximately 1400 rpm for 20 minutes to obtain a cell pellet that was washed with ice-cold 5% trichloroacetic acid. The supernatant was carefully removed and scintillation cocktail (Ultima Gold AB, Perkin Elmer) was added. Samples were then radio-assayed by liquid scintillation counting. Rates of radiotracer incorporation were converted into BBP applying the factors of 1.15 x $10^{17}$ cells $mol^{-1}$ leucine incorporated (Kirchman, 1992) and 2 x $10^{18}$ cells $mol^{-1}$ thymidine (Ducklow and Carlson, 1992).

### *3.2.5 Activities of extracellular enzymes*

The reaction velocity of extracellular α-glucosidase and β-glucosidase was determined using substrate analogues labelled with the fluorescent marker 4-methylumbelliferone (MUF) (Hoppe, 1983). Subsamples of 200 µl were incubated with MUF-α-glucopyranosid and MUF-β-glucopyranosid at a final concentration of 1 µmol $L^{-1}$. Fluorescence was measured immediately after addition of the substrate

analogue and after 3 hours of incubation in the dark at close to *in situ* temperature with a plate reader (FLUOstar OPTIMA, BMG Labtech). Analysis of triplicate subsamples revealed a mean standard deviation of 5%. Calibration was carried out with MUF standard solutions. Rate constants for glucosidase activity were calculated assuming a linear relationship between non-saturating substrate concentrations and enzymatic reaction velocities according to Michaelis-Menten kinetics.

The bacterial uptake of glucose was estimated from the assimilation of [$^3$H]-glucose. Samples of 10 ml volume were incubated with [$^3$H]-glucose at a final concentration of 10 nmol $L^{-1}$ in the dark at 14°C for 1 to 2 hours, depending on the bacterial activity. Incubations were stopped by the addition of formalin at a final concentration of 4%. Formalin-killed controls were run for each sampling. Samples were further processed according to the microcentrifuge method as described by Smith and Azam (1992). Samples were then radio-assayed by liquid scintillation counting. Analysis of triplicate subsamples revealed a mean standard deviation of <5%.

### *3.2.6 Effect of pH on bacterial activity and degradation of organic matter*

During the 2007 cruise, effects of decreasing seawater pH on bacterial activity and on the degradation of polysaccharides were investigated. Particulate and dissolved organic matter was collected at station 2 at 5 m depth. Organic matter was incubated with the *in situ* bacterioplankton assemblage in six 10 L-Nalgene bottles. In three Nalgene bottles the *in situ* pH of 8.3 was not modified. These incubations served as reference and are referred to as "present-day (PD) treatment". The three remaining bottles were acidified by the addition of 0.1 M hydrochloric acid. The *in situ* pH of 8.3 was decreased to 7.9, thereby increasing the partial pressure of $CO_2$ from 384 µatm to 600 µatm. The treatment with lowered pH is referred to as "future-ocean (FO) treatment". Both series were incubated in the dark close to the ambient sea surface temperature of 12°C for 10 days.

### *3.2.7 Pelagic community respiration*

Water samples were collected from Niskin bottles in 60 ml biological oxygen demand (BOD) bottles (Wheaton). Three replicates were fixed immediately after collection while 3 other replicates were incubated during 24 h in the dark, thermostated with running seawater (surface water pumped at 2.5 m depth). Concentrations of dissolved $O_2$ were measured before and after incubation by the Winkler technique (§3.3.2.2).

### *3.2.8 Benthic fluxes of dissolved $O_2$, total alkalinity (TA) and nutrients*

Sediment cores were collected with a boxcorer and were incubated for approximately 42 hrs at *in situ* temperature. Fluxes of $O_2$, TA, DIC, $NO_3^-$, $NO_2^-$, $NH_4^+$, $PO_4^{3-}$ and Si were evaluated. $O_2$, pH, TA, dissolved nutrients and sediment content of POC and PIC

were were analyzed following the methods described in §3.3.2. The concentrations of Chl-a and Phaeo-pigments were determined fluorometrically according to the method described in §3.3.1. Granulometric analysis was performed by wet sediment sieving over 2000 µm, 500 µm, 250 µm, 125 µm and 63 µm sieves.

## 3.3 Analytical methods

### *3.3.1 Biological parameters*

#### *3.3.1.1 Chlorophyll a partitioning between phytoplankton groups*

Pigment samples (surface/10/20-30/40/50-60/80 m) of the three cruises were analysed using an improved HPLC method based on the method of Wright and Jeffrey (1997). A CHEMTAX routine based on pigment biomarker ratios from literature (Mackey et al., 1996; Gibb et al., 2001; Zapata et al., 2004) using multiple runs (Latasa, 2007). Depth bins was used to partition the Chl-a between the main phytoplankton groups identified by microscopic screening of selected samples. One of the type 6 haptophyte (*E. huxleyi*) pigment marker (Chl $c_2$ monogalactosyldiacylglyceride ester [18:4/14:0]) could not quantified in the 2006 samples due to bad chromatographic separation. This precluded the inclusion of HFx containing gymnodinioid dinoflagellates in the CHEMTAX partitioning routine. Nevertheless, gymnodinioids were not found to form a dominant phytoplankton group, making it safe to assume that most of the HFx can be attributed to coccolithophores in our samples.

Chl-a of water samples was also determined on GF/F filters after filtration of 250-ml seawater under low vacuum, following the fluorometric method of Yentsch & Menzel (1963). Filters were stored at -20°C until measurement. For analysis, the filters were extracted with 90% acetone at -20°C for 24 h. Samples were centrifuged (10 min, 5500 rpm) and the fluorescence of the extract was measured with a Shimadzu RF-150 fluorometer, using an excitation wavelength of 430 nm and an emission wavelength of 663 nm. The fluorescence was calibrated with a stock solution of pure chlorophyll *a* (Merck). The concentrations of Chl-a and Phaeo-pigments in the surface sediments were also determined fluorometrically according to Yentsch and Menzel (1963) with a TD-700 fluorometer.

#### *3.3.1.2 Microscopy*

Abundance and diversity of the microplankton was assessed by means of inverted microscopy (Utermöhl, 1958) in selected samples. Taxon-specific biomasses were calculated using biovolume (Hillebrand et al., 1999) and allometric carbon content equations (Menden-Deuer and Lessard, 2000). Bacterial cell abundance was determined using epifluorescence microscopic counts of DAPI-stained cells. At least

25 fields of view (1000x magnification) or 500 cells were counted per sample. Scanning electron micrographs were used to identify coccolithophores (Bollman et al., 2002).

Cell density of the batch culture experiments is estimated by haemocytometer counting (Malassez cell) using optical microscopy, which also allowed a visual check of the health of the culture.

#### *3.3.1.3 Cytometry*

The vertical distribution of phyto- and bacterio-plankton was determined by flow cytometery (FACSCalibur flow-cytometer, Becton Dickinson). Samples were preserved with glutardialdehyde (bacteria: 1% final concentration, phytoplankton: 0.1% final concentration) and stored at -20°C until analysis. Phytoplankton cell abundances were determined due to autofluorescence (orange and red) after excitation by a 488 nm laser. Bacteria where analyzed due to green fluorescence after DNA-specific staining. Nucleic acid was stained with SybrGreen I (Invitrogen). Bacterial abundances were estimated after visual inspection and manual gating of the bacterial subpopulation in the side scatter vs. green fluorescence - cell cytogram. Yellow-green fluorescent latex beads (diameter 0.94 µm, Polyscience) were used to normalize the counted events to a reference volume. TruCount beads (Becton Dickinson) were used for daily intercalibration and absolute volume calculation (Gasol and Del Giorgio, 2000).

#### *3.3.1.4 Mesozooplankton biomass*

Vertical net tows (depth: 80-100 m) were used to sample the mesozooplanktonic size fraction (> 200 µm) after sunset, according to the recommendations by Fraser (1968). We used a WP-2 net equipped with a flow meter. Aliquots of mesozooplankton samples were filtered onto pre-weighed combusted GF/D filters, dried onboard at 60°C for several days, and stored at room temperature before measuring the ash-free dry weight (Wishner et al., 1998). Carbon conversion was based on the equation of Bode et al. (1998).

#### *3.3.1.5 Bacterial community structure analysis*

Bacterial community composition (BCC) was sampled during the three cruises at different depths in the water column (surface, 20, 40, (60), 80 m). The total BCC was size-fractioned into the free-living (FL) (0.2 - 3 µm) and the particle-associated (PA) (> 3 µm) BCC. DNA of the samples was extracted following the method of Boström et al. (2004) with a bead beating step and the 16S rRNA gene amplified according to Muyzer et al. (1993) using the primers 357F with GC-clamp (5'-CGCCCGCCGCGCCCCGCGCCCGGCCCGCCGCCCCCGCCCCCCTACGGGAGG

CAGCAG-3') and 518R (5'-ATTACCGCGGCTGCTGG-3'). Denaturing Gradient Gel Electrophoresis (DGGE) was used as a molecular fingerprinting technique to compare bacterial community structure across samples. Sequencing of excised bands (150 bp) allowed the verification of band identity across gel patterns, which were digitised and analysed using the Bionumerics 4.61 software (Applied Maths, Belgium). For the 2006 samples, a clone library was constructed allowing more confident identification (full 16S rDNA) of the most abundant phylotypes in the banding patterns (Genbank accession numbers: EU394538-EU394678). Identified plast sequences were removed from the BCC datasets (2006). Multivariate analysis (ANOSIM, Primer 5.0, and ordination, Canoco 4.5) was used to analyse the patterns in BCC associated with phytoplankton composition and environmental variables.

### *3.3.2 Chemical parameters*

#### *3.3.2.1 Dissolved inorganic nutrients*

Dissolved silicate and phosphate were measured following the method of Grasshoff et al. (1983) adapted for automated analysis using a Skalar AutoAnalyser. When Si and $PO_4$ were analysed onboard the ship, manual determinations were made colorimetrically. Nitrate, nitrite and ammonium were measured colorimetrically. Nitrate and nitrite were analysed with a Technicon or Skalar AutoAnalyzer system following Grasshoff et al. (1983). Ammonium was measured manually with the indophenol blue technique according to Koroleff (1969).

#### *3.3.2.2 Dissolved inorganic carbon (DIC), dissolved $O_2$ and pH*

Measurements of $pCO_2$ in seawater were carried out by equilibration (Frankignoulle et al., 2001) with an infrared gas analyzer (Li-6262). Dissolved oxygen ($O_2$) concentration was measured by Winkler titration using a potentiometric endpoint determination (Knap et al., 1996). pH was measured with a combined electrode (METROHM 6.0232.100), calibrated on the Total Hydrogen Ion Concentration Scale, using TRIS (2-amino-2-hydroxymethyl-1,3-propanediol) and AMP (2-aminopyridine) buffers prepared at a salinity of 35. Total alkalinity (TA) was measured by potentiometric titration using HCl 0.1 M as titrant based on Gran (1952), and data were quality checked with Certified Reference Material acquired from Andrew Dickson (Scripps Institution of Oceanography, University of California, San Diego). Dissolved inorganic carbon (DIC) was computed from pH and TA using the carbonic acid dissociation constants of Mehrbach et al. (1973) as refitted by Dickson and Millero (1987).

#### *3.3.2.3 DMS and DMSP*

For the 2006 and 2007 campaigns, the total concentrations of DMS, $DMSP_d$ and $DMSP_p$ were determined on unfiltered water samples and the dissolved species

(DMS+$DMSP_d$) were determined on GF/F filtered samples. Ten milliliter aliquot of filtered or unfiltered seawater was transferred to glass tubes designed for dissolved gas sampling, to which 200 µl of 5N NaOH was added. The addition of the base allowed the conversion of DMSP to DMS. The tubes were closed immediately with aluminium caps with Teflon-lined septa. The samples were stored at 4°C until analysis.

For the 2008 curise, a 10 ml aliquot of GF/F filtered sample was additionally collected and bubbled with nitrogen during 20 minutes to eliminate the DMS. The degassed sample was then added with 200 µl of 5N NaOH, closed with an aluminium cap with Teflon-lined septa and stored at 4°C until analysis of the $DMSP_d$.

For the analysis, two needles were placed in the septa, one was bubbling nitrogen through the sample for 30 minutes at a flow rate of 25 ml/min and the other was collecting the flushed gases that were cryotrapped with liquid nitrogen in a 0.16 mm diameter FEP-Teflon loop. The trap was then heated at 100°C and its content was immediately injected into a TRACE GC INTERSCIENCE device equipped with a Flame Photometric Detector (FPD). DMS was calibrated from DMS standards (Merck) prepared in the laboratory.

#### *3.3.2.4 Dissolved organic carbon (DOC) and nitrogen (TDN)*

Seawater samples of 20 ml were filtered through precombusted (500 °C for 12 h) GF/F filters (Whatman). The filtrate was stored in combusted (500 °C for 12h) glass vials and immediately acidified with phosphoric acid and stored at 4 °C. Analysis was carried out on a Shimadzu TOC-VCSH analyser following the procedure described by Qian and Mopper (1996). A four-point calibration curve was constructed for each day of measurement using potassium phtalate standards for DOC and potassium nitrate standards for TDN prepared freshly with UV-treated Milli-Q water. Additionally, two types of certified reference material, Low Carbon Water (LCW) and Deep Sea Water (DSW) (Hansell laboratory, RSMAS, University of Miami), were measured together with the standards and samples. Each sample was measured 3-5 times. The DOC and TDN concentration of the sample was calculated as the average of these values.

#### *3.3.2.5 Particulate carbon and nitrogen*

Measurements of total particulate carbon (TPC) and particulate nitrogen (PN) were performed on particulate matter collected by filtration of seawater on precombusted (4h, 500°C) GF/F filters. Particulate organic carbon (POC) was measured using a Fisons NA-1500 elemental analyser after carbonate removal from the filters by strong acid fumes overnight. The difference between TPC and POC was attributed to

particulate inorganic carbon (PIC). Certified reference stream sediment (STSD-2) from the Geological Survey of Canada was used for the calibration.

The percentage of POC and PIC in the sediments was estimated by difference in weight after ashing the samples at 550 °C for 4 hrs and at 1000 °C for 1 hr, respectively.

*3.3.2.6 Polysaccharide analysis*

Polysaccharide composition was determined by the use of high performance anion exchange chromatography (HPAEC) coupled with pulsed amperometric detection (PAD), a high precision method for the direct determination of carbohydrates without prior derivatisation. However, current protocols to analyze carbohydrates with HPAEC-PAD have been restricted to neutral and amino sugars in dissolved and particulate polysaccharides. Since acidic sugars contribute significantly to the pool of carbohydrates in seawater, a new protocol for HPAEC-PAD to simultaneously determine neutral as well as amino and acidic sugars in polysaccharides was developed that included desalination of samples. Briefly, seawater samples were desalted prior to analysis by membrane dialysis with a 1 kDa molecular weight cut-off membrane at 4°C in less than 5 hours. The desalted samples were hydrolyzed with 0.8M HCl for 20h at 100°C. After cooling, acid was evaporated under $N_2$ atmosphere at 50°C to neutralise the sample (Engel and Händel, submitted).

*3.3.2.7 Abundance and size distribution of transparent exopolymer particles*

For microscopic analysis of transparent exopolymer particles (TEP), slides were prepared by the CytoClear-slide technique (Logan et al., 1995) from samples filtered onto 0.4 µm Nuclepore filters and stained with 1 ml of Alcian Blue. CytoClear slides are glass slides that are glazed on one side. The purpose of the glaze is to remove interference with the filter pores under brightfield and epifluorescence microscopy. Filters containing the stained gel particles were placed, sample side up, onto the slide with a drop of 0.2 µm filtered immersion oil underneath. Another drop is placed on top of the filter and the filter was then covered by a glass slip. Two blank filters were prepared from Nuclepore filters moistened with Milli-Q water and stained with 1 ml of Alcian Blue. Slides containing the stained gel particles were transferred to a compound light microscope and analyzed with the aid of image analysis software. The filter was screened by a digital colour camera at 200-400x magnification. Photos were taken from 30 frames per filter area, chosen in a cross section, i.e. 15 photos along the horizontal and 15 photos along vertical axis. Because gels have nonregular shapes, pictures were analyzed by the image analysis program ImageJ that can automatically count and size individual particles (Engel, 2009).

Concentrations of TEP stained with Alcian Blue were also determined colorimetrically, here defined as $TEP_{color}$, following the method of Passow and Alldredge (1995) and Engel (2009). Gum Xanthan was used to standardize the quantity of dye bound to TEP (expressed in µgXeq $L^{-1}$). This method is semi quantitative because the quantity of Alcian Blue is directly bound to a specific polysaccharide (Rasmus, 1977). Nevertheless, this simple and fast method provides valuable indications about the presence of reactive polysaccharides. The carbon content of TEP derived from the colorimetric method (TEP-$C_{color}$) was also assessed using the relationship determined by Engel (2004) for an assemblage of diatoms and coccolithophores:

$$TEP\text{-}C_{color}\ (\mu g\ L^{-1}) = (0.63 \pm 0.03) \times [TEP_{color};\ \mu g\ X\ eq.\ L^{-1}]$$

Since diatoms and coccolithophores were the dominant phytoplanktonic species at the time of our cruises, we decided to use this equation to estimate TEP-$C_{color}$ for our samples.

## 3.4 Laboratory and shipboard culture experiments

### *3.4.1 Set-up of batch cultures at ULB and UGent*

Laboratory batch experiments were performed on monospecific cultures of *E. huxleyi* (strain AC481 from Normandie, France). Experiments were carried out in duplicates in an incubator under controlled temperature and light conditions (Figure 4). Culture medium consisted of filtered (0.2 µm) and autoclaved surface post-bloom seawater sampled in the northern Atlantic Ocean (47°45'N, 7°00'W), enriched with nitrates and phosphates to obtain final concentrations of 32 µmol $L^{-1}$ and 1 µmol $L^{-1}$, respectively. Incident photon flux density was 150 µmol $m^{-2}$ $s^{-1}$ and the light/dark cycle was 14h/10h. Cultures (8 L) were inoculated with cells in exponential growth phase and were grown in Nalgene polycarbonate carboys (10 L size). Experiments were monitored for a period of around 50 days, depending on the experiment. Samples were taken with a sterile syringe always at the same time in the light cycle.

For the first set of experiments, the carbonate system was set by acid addition at the beginning of each experiment and was allowed to evolve with biological activity during the course of the experiments. Various parameters were followed. They include pH, TA, Chl-a, dissolved nutrients ($NO_3$ and $PO_4$), cells density, POC, PIC and $TEP_{color}$ (see §3.3 for analytical methods).

For the second set of experiments at different controlled $pCO_2$ and temperature, cells were pre-adapted to the experimental conditions for 10 days to avoid measuring potential adaptation effects during the experiments. pH and TA were measured daily.

Chl-a, cell density, POC and PIC were monitored every two or three days depending on the growth phase of the cultures. Additional samples for SEM were taken as well.

**Figure 4**. Set-up of the batch culture experiments.

In order to study the interaction between the extracellular carbohydrate pool in an *E. huxleyi* bloom and associated bacterial communities, (triplicate) *E. huxleyi* batch cultures (16 L) were set up at UGent. These were either kept axenic or were inoculated with a natural bacterial community and monitored for cell densities and nutrient concentrations during 3 weeks, with samples for bacterial community composition (BCC), carbon and carbohydrate dynamics taken at the end of the exponential growth phase and twice during the stationary phase. The composition and dynamics of the active bacterial community in the bacterised cultures was assessed by (16S rRNA RT- PCR DGGE) fingerprinting, both for the total (> 0.2 µm) and the particle-associated (> 3 µm) community. HMW DOM were concentrated by means of tangential flow ultrafiltration (10 kDa cut-off membrane), and its neutral aldose concentration and (isotopic) composition was measured by HPLC-IRMS. TEP was measured by the colourimetric alcian blue method.

### *3.4.2 Set-up of a chemostat system at AWI*

A laboratory chemostat system to investigate combined effects of temperature and $CO_2$ on phytoplankton was set up at the AWI. First chemostat experiments in 2006 showed that, in principle, chemostat set-up and experimental processing were convenient to investigate effects of $CO_2$ on the physiological processes of coccolithophores. Nevertheless, maintaining the $CO_2$ concentrations of the gas mixtures at constant values turned out to be a difficult task. Therefore, a sophisticated $CO_2$ gas-mixing system was added to the chemostat system in August 2007. This device allows the precise control of $CO_2$ concentrations ranging from 0 to 5000 µatm $CO_2$ in the incubators (Figure 5). The equilibration of gas with pre-set $CO_2$ concentrations was followed by the evolution of pH (Figure 6).


**Figure 5**. Components of one chemostat connected to the $CO_2$ regulation system. Incubator (①), thermostat (②), peristaltic pump (④), 100 L nutrient medium reservoir (③) and overflow bottle (⑤).

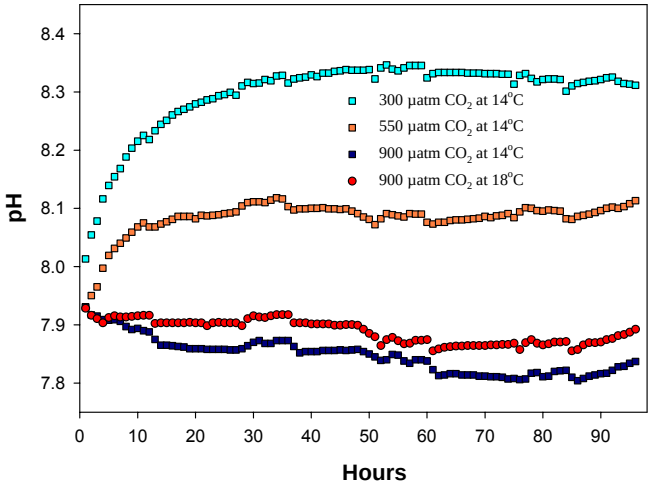


**Figure 6**. Evolution of pH during the *Emiliania huxleyi*-experiment at 14 and 18°C for the equilibration of gas with $pCO_2$ values of 300, 550 and 900 µatm.

### *3.4.3 Shipboard chemostat experiment*

To describe the influence of $CO_2$ concentration on coccolithophores, specifically on the kinetics of polysaccharide exudation and TEP production, an on-board chemostat study was performed during the 2006 cruise in the Bay of Biscay (Figure 7). The system applied 4 different $CO_2$ concentrations corresponding to ~180 µatm (glacial), ~370 µatm, ~750 µatm, and ~1400 µatm. $CO_2$ concentration in each reservoir was regulated by aeration with the defined $CO_2$/air mixtures. The experiments were performed in duplicate bottles of 2.0 L and at an irradiance of 200 µmol photons $m^{-2}$ $s^{-1}$ with a 16:8 light:dark cycle, and two different flow rates (0.6 and 0.13 $d^{-1}$) for 4 days each.


**Figure 7.** The Chemostat System onboard the RV Belgica during the 2006 cruise.

### *3.4.4 Aggregate experiments*

The influence of seawater $CO_2$ concentration on the aggregation and sinking of macroaggregates after an *E. huxleyi* bloom was investigated during a rollertable experiment. *E. huxleyi* cultures were first grown in batch cultures under three different $CO_2$-concentrations (~180 ppm, ~380 ppm and ~750 ppm), modified by a $CO_2$-aeration system. Aggregation of cells was promoted using the roller table approach of Shanks and Edmondson (1989). Samples were taken before and after the incubation as well as after seven days in the rollertanks. During the rolltertable-experiment video pictures were made for the calculation of the sinking velocity of individual aggregates. After the experiment, aggregates were isolated and analysed for mass, bacterial abundance, particulate organic and inorganic carbon (POC, PIC).

## 3.5 Procedure for estimation of impact of net ecosystem dynamics on air-sea $CO_2$ fluxes

The impact of net community production (NCP) and calcification (NCC) on DIC and $pCO_2$ was estimated based, respectively, on the changes of nutrients and the changes of TA, between the surface layer (top 20 m) and the deep layer (80 m to seafloor), as detailed hereafter.

TA was normalized to a salinity of 35.5 ($TA_{35.5}$) according to:
$TA_{35.5} = TA / S * 35.5$
where TA is the observed value at the observed salinity (S)

The anomaly of TA ($TA_{anomaly}$) was computed according to:

$TA_{anomaly} = <TA_{35.5}>_{0\text{-}20m} - 16(<PO_4>_{80m\text{-}bottom} - <PO_4>_{0\text{-}20m}) - (<PO_4>_{80m\text{-}bottom} - <PO_4>_{0\text{-}20m}) - <TA_{35.5}>_{80m\text{-}bottom}$

where $<TA_{35.5}>_{0\text{-}20m}$ is the average $TA_{35.5}$ between surface and 20 m depth, $<TA_{35.5}>_{80m\text{-}bottom}$ is the average $TA_{35.5}$ between 80m and the seafloor, $<PO_4>_{0\text{-}20m}$ is the average $PO_4$ between surface and 20 m depth, and $<PO_4>_{80m\text{-}bottom}$ is the average $PO_4$ between 80m and the seafloor.

For the $TA_{anomaly}$ to represent a change due to $CaCO_3$ production, TA values have to be corrected for $PO_4$ and $NO_3$ assimilation/release (Brewer and Goldman, 1976). $PO_4$ assimilation is given by the term $<PO_4>_{80m\text{-}bottom} - <PO_4>_{0\text{-}20m}$. In absence of the complete set of nitrate data for the 2006 cruise, $NO_3$ assimilation was computed from $PO_4$ assimilation using the Redfield ratio of 16:1 (Redfield et al., 1963). For stations on the shelf and slope, the averaging of deep layer samples was made between 80 m and 150 m.

The change of DIC in surface waters due to net organic carbon production ($\Delta DIC_{org}$) was computed from the change of $PO_4$ converted to carbon using the Redfield ratio (106:1), according to:

$\Delta DIC_{org} = 106 * (<PO_4>_{0\text{-}20m} - <PO_4>_{80m\text{-}bottom})$

The change of DIC in surface waters due to net $CaCO_3$ production ($\Delta DIC_{inorg}$) was computed using the TA anomaly technique (Smith and Key, 1975) according to:

$\Delta DIC_{inorg} = 0.5 * TA_{anomaly}$

To estimate the change of $pCO_2$ due to $\Delta DIC_{org}$ and $\Delta DIC_{inorg}$ (respectively, $\Delta pCO_{2org}$ and $\Delta pCO_{2inorg}$), we first computed DIC at atmospheric equilibrium ($DIC_{eq}$) from an average TA of 2340 µmol $kg^{-1}$, an average temperature of 13°C and an average salinity of 35.5.

$\Delta pCO_{2org}$ was computed as the difference between atmospheric equilibrium (380 ppm) and $pCO_2$ computed from $DIC_{org}$, a TA of 2340 µmol $kg^{-1}$, a temperature of 13°C and a salinity of 35.5, where $DIC_{org}$ is given by:

$DIC_{org} = DIC_{eq} + \Delta DIC_{org}$

$\Delta pCO_{2inorg}$ was computed as difference between atmospheric equilibrium (380 ppm) and $pCO_2$ computed from $DIC_{inorg}$, $TA_{inorg}$, a temperature of 13°C and a salinity of 35.5, according to:

$DIC_{inorg} = DIC_{eq} + \Delta DIC_{org}$

$TA_{inorg} = 2340 + TA_{anomaly}$

The change of $pCO_2$ due to SST change ($\Delta pCO_{2SST}$) was computed from the change of SST ($\Delta SST$) and the algorithm of Takahashi et al. (1993), where $\Delta SST$ is computed according to:

$\Delta SST = <SST>_{0\text{-}20m} - <SST>_{80m\text{-}bottom}$

The total computed change of DIC ($\Delta DIC_{computed}$) was calculated according to:
$\Delta DIC_{computed} = \Delta DIC_{org} + \Delta DIC_{inorg}$

The observed change of DIC ($\Delta DIC_{observed}$) was computed according to:
$\Delta DIC_{observed} = <DIC_{35.5}>_{0\text{-}20m} - <DIC_{35.5}>_{80m\text{-}bottom}$
where $<DIC_{35.5}>_{0\text{-}20m}$ is the average of measured DIC normalized to a salinity of 35.5 ($DIC_{35.5}$) between surface and 20 m depth, $<DIC_{35.5}>_{80m\text{-}bottom}$ is the average measured $DIC_{35.5}$ between 80m and the seafloor.

Normalization of DIC to a salinity of 35.5 was computed according to:
$DIC_{35.5} = DIC / S * 35.5$

The total computed change of $pCO_2$ ($\Delta pCO_{2computed}$) was calculated according to :
$\Delta pCO_{2computed} = \Delta pCO_{2org} + \Delta pCO_{2inorg}$

The observed change of $pCO_2$ ($\Delta pCO_{2observed}$) was computed according to:
$\Delta pCO_{2observed} = pCO_2@13°C - 380$
where $pCO_2@13°C$ is the measured $pCO_2$ normalized to a temperature of 13°C with the algorithm of Takahashi et al. (1993)

Air-sea $CO_2$ fluxes (F) were computed according to:
$F = \alpha\, k\, \Delta pCO_{2air\text{-}sea}$
where $\Delta pCO_{2air\text{-}sea}$ is the $pCO_2$ air-sea gradient, α is the solubility coefficient of $CO_2$, and *k* is the gas transfer velocity computed from the wind speed using the *k*-wind parameterization given by Wanninkhof (1992).

### 3.6 Mathematical modeling of coccolithophorid dynamics

A dynamic model was developed to represent the coccolithophorid blooms (*E. huxleyi*) and validated with data obtained during the Bergen 2001 mesocosm experiment (Delille et al., 2005; Engel et al., 2004a; 2005). Mesocosm experiments provide an ideal framework for the conceptualization and calibration of a biogeochemical model because they cover the duration of bloom development and decline, and offer a large set of diversified data for model parameterization and calibration that are not usually available from field studies. The 19-days dataset includes data on the production of TEP, primary production, calcification, inorganic nutrients (nitrate, ammonium and phosphate), TA, DIC and $pCO_2$, $O_2$, pigments, DOC, POC/N and PIC. Compared to existing models of coccolithophorid development, the present tool is innovative because it describes carbon and nitrogen cycling. Indeed, existing models of coccolithophorid dynamics (e.g. Tyrrell and Taylor, 1996; Merico et al., 2004) describe nitrogen cycling using a balanced growth model in carbon and nitrogen. This approach does not allow one to simulate temporal decoupling of carbon and nutrient dynamics repeatedly reported after bloom events

and reflected notably in the temporal accumulation of carbon-rich dissolved organic matter and the formation of TEP. Moreover, a thorough representation of the calcification process requires the simulation of carbon flows through coccolithophorids. Finally, the above-mentioned mathematical models do not address the impact of coccolithoporid development, and in particular of calcification, on the DIC dynamics. The model developed in the framework of this project addresses these limitations and explicitly simulates carbon (inorganic and organic) cycling including the exchanges of $CO_2$ at the air-sea interface and carbonate chemistry. It is based on unbalanced algal growth and balanced growth for bacteria as described in Van den Meersche et al. (2004). In order to adequately reproduce the observations, the present model has been extended to obtain an explicit and thorough representation of coccolithophorid specialized processes such as calcification and TEP production from carbon over-consumption as described by Engel et al. (2004b). These processes have been considered co-jointly in a global biogeochemical context reproducing carbon fluxes from DIC to microbial loop. In addition, the present model considers also contingencies affecting typically an enclosed-space experiment such the potential action of viruses.

# 4. RESULTS AND DISCUSSION

## 4.1 Net ecosystem dynamics during coccolithophorid blooms

### *4.1.1 General settings of field investigations*

During the three yearly cruises, several patches of cold water (SST <14°C) were observed along the shelf break in the entire study area (Figure 8). They corresponded to the signature of enhanced vertical mixing due to turbulent dissipation related to the generation of internal tides (Pingree et al., 1999; Wollast and Chou, 2001). These patches of cold waters were characterised by lower Chl-a values (~0.4 µg $L^{-1}$) and were surrounded by water masses both on-shelf and off-shore exhibitin higher Chl-a values (>0.8 µg $L^{-1}$). This was related to the propagation of the nutrient rich colder waters from the shelf break both off-shore and on-shore, leading to enhanced biological activity as they warm and stratify. As these water masses propagated further onto the shelf, phytoplankton development leads to nutrient exhaustion. Hence, the high Chl-a waters were confined close to the shelf break. Waters high in Chl-a were also associated with high reflectance patches indicating the presence of coccolithophorids (Figure 8).

Figure 9 shows, as an example, the vertical distributions of Chl-a concentration at station 12 sampled on the 19$^{th}$ of May during the 2008 cruise. The vertical profiles are similar at each station visited during the three cruises. The Chl-a exhibited higher concentrations in the upper 40 m of the water column, with a subsurface maximum situated at a depth between 20 m and 40 m and was close to 0 below 80 m. Phytoplankton development in surface waters led to the depletion of inorganic nutrients (Figure 9). $PO_4$ exhibited concentrations close to 0 (< 0.1 µmol $L^{-1}$) in surface waters and around 0.5 µmol $L^{-1}$ below the photic zone. The photic depth (1% of the incoming irradiance) ranged between 26 m and 45 m during the surveys (data not shown). While $PO_4$, $NO_x$ and Si were assimilated in surface water, they reached constant concentrations below the thermocline.

Data on temperature, Chl-a and nutrient concentrations in surface waters at stations visited during the three yearly cruises in the Bay of Biscay are summarized in Table 1. Surface Chl-a concentration did not exceed 2 µg $L^{-1}$ during the cruises and the lowest values (< 1 µg $L^{-1}$) were found during the May 2008 cruise in the Goban Spur area. $PO_4$ concentrations ranged between 0 and 0.2 µmol $L^{-1}$ in surface waters. $NO_x$ concentration varied between 0.14 and 2.45 µmol $L^{-1}$ at 3 m depth. Si exhibited concentrations < 2 µmol $L^{-1}$ at surface of each stations.

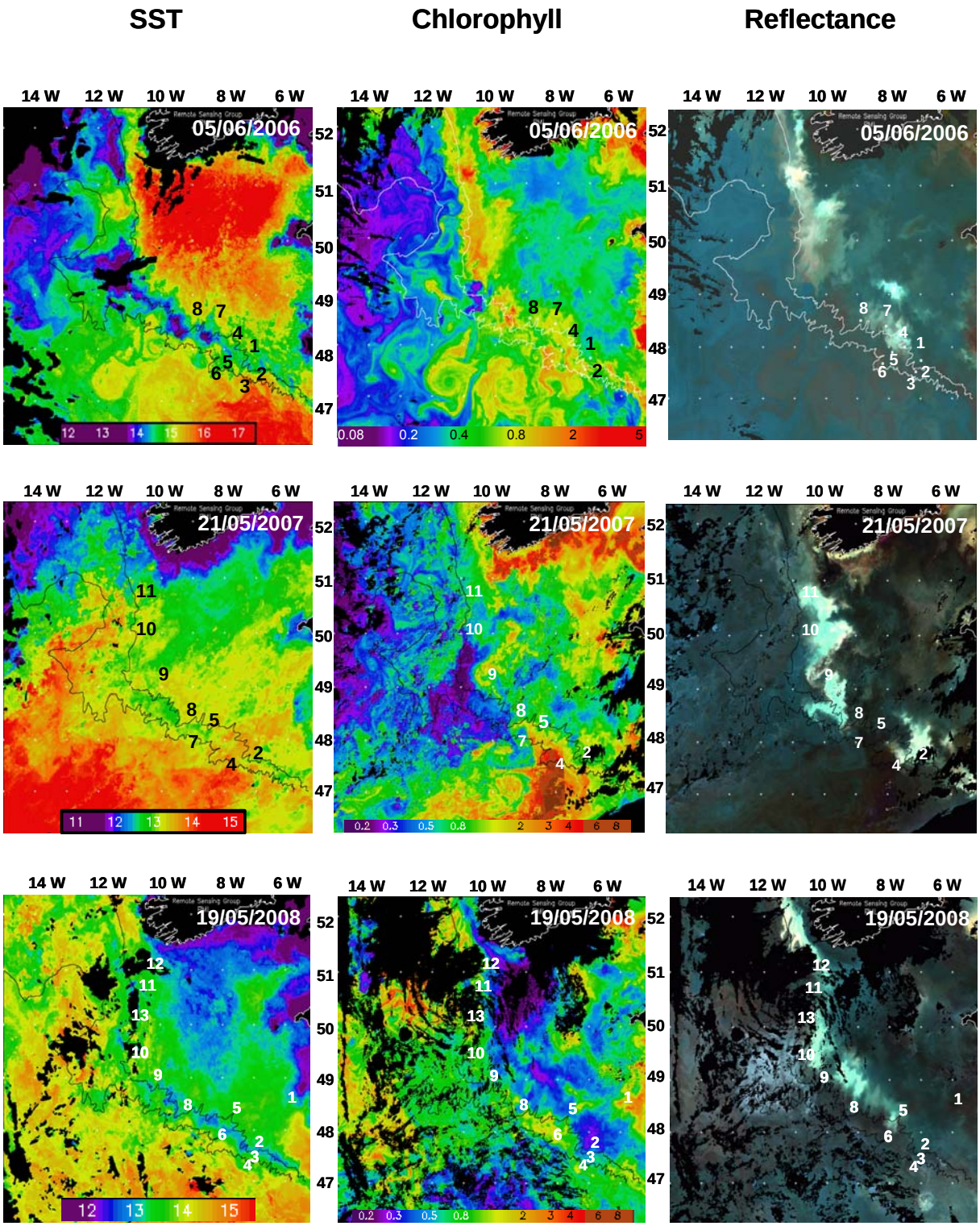


**Figure 8.** Remote sensing images of SST, chlorophyll a and reflectance contemporary to the May 2006 (top panel), June 2007 (middle panel) and 2008 (bottom panel) cruises in the Bay of Biscay (courtesy of Steve Groom, RSG, PML). Locations of the sampling stations are also indicated.

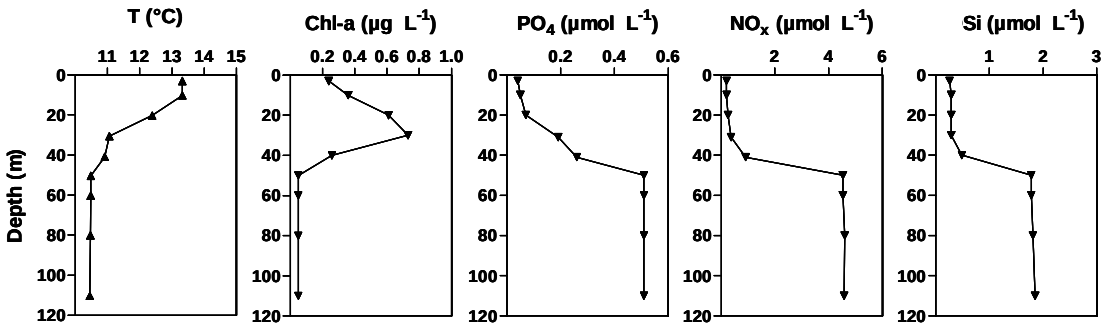


**Figure 9.** Vertical profiles of temperature, Chl-a, phosphates ($PO_4$), nitrates+nitrites ($NO_x$) and dissolved silicate (Si) concentration at station 12 on the 19th of May 2008.

Table 1. Temperature, Chl-a and nutrient concentrations in surface waters at stations visited during the three yearly field cruises in the Bay of Biscay. See Figure 8 for sampling locations. The asterisk indicates stations located over the shelf. n.d.: not determined.

| Stations | Date | Lat (°N) | Long (°W) | T (°C) | Chl-a (µg $L^{-1}$) | $PO_4$ (µM) | $NO_x$ (µM) | DSi (µM) |
|---|---|---|---|---|---|---|---|---|
| 1* | 31/05/2006 | 47.75 | 7.00 | 13.04 | 0.98 | 0.00 | 0.00 | 0.97 |
| 2 | 1/06/2006 | 47.53 | 7.17 | 13.11 | 1.76 | 0.08 | 1.01 | 1.66 |
| 3 | 1/06/2006 | 47.42 | 7.27 | 14.01 | 0.67 | 0.16 | 1.99 | n.d. |
| 5 | 2/06/2006 | 47.90 | 7.90 | 13.26 | 1.22 | 0.12 | 2.32 | 0.35 |
| 4* | 2/06/2006 | 48.10 | 7.50 | 13.29 | 1.27 | 0.04 | 0.17 | 1.14 |
| 8* | 6/06/2006 | 48.50 | 8.90 | 14.47 | 0.80 | 0.04 | 0.12 | 1.57 |
| 7* | 7/06/2006 | 48.40 | 8.10 | 14.51 | 0.96 | 0.01 | 0.12 | 0.31 |
| 6 | 7/06/2006 | 47.69 | 8.21 | 14.90 | 1.39 | 0.04 | 0.48 | 0.16 |
| 4b* | 8/06/2006 | 48.10 | 7.50 | 14.21 | 0.91 | 0.04 | 0.00 | 0.09 |
| 1b* | 9/06/2006 | 47.75 | 7.00 | 14.33 | 0.39 | 0.03 | 0.07 | 0.52 |
| 2* | 10/05/2007 | 47.79 | 6.90 | 13.40 | 0.48 | 0.09 | 1.19 | 1.15 |
| 5* | 12/05/2007 | 48.20 | 7.62 | 12.96 | 1.03 | 0.09 | 0.80 | 0.26 |
| 8* | 13/05/2007 | 48.50 | 8.50 | 13.24 | 1.39 | 0.06 | 0.89 | 0.14 |
| 9* | 14/05/2007 | 49.20 | 9.49 | 13.00 | 0.96 | 0.07 | 0.68 | 0.48 |
| 10* | 15/05/2007 | 49.50 | 10.51 | 12.73 | 0.39 | 0.07 | 1.21 | 0.18 |
| 11* | 16/05/2007 | 51.34 | 10.50 | 12.29 | 1.40 | 0.06 | 0.49 | 0.76 |
| 8b* | 21/05/2007 | 48.50 | 8.50 | 13.25 | 1.25 | 0.07 | 0.49 | 0.11 |
| 5b* | 22/05/2007 | 48.22 | 7.59 | 13.30 | 0.50 | 0.10 | 0.38 | 0.17 |
| 4 | 23/05/2007 | 47.42 | 7.27 | 13.38 | 1.27 | 0.14 | 2.15 | 1.17 |
| 7 | 23/05/2007 | 47.68 | 8.20 | 13.50 | 1.52 | 0.10 | 0.51 | 0.18 |
| 2b* | 24/05/2007 | 47.80 | 6.89 | 13.39 | 0.92 | 0.06 | 1.47 | 1.95 |
| 1 | 7/05/2008 | 48.50 | 6.00 | 12.42 | 1.06 | 0.07 | 0.22 | 1.00 |
| 3 | 7/05/2008 | 47.53 | 7.16 | 12.71 | 0.19 | 0.20 | 2.45 | 1.04 |
| 2* | 8/05/2008 | 47.80 | 6.90 | 12.82 | 0.78 | 0.06 | 0.24 | 0.73 |
| 6 | 9/05/2008 | 47.90 | 7.91 | 12.27 | 0.42 | 0.26 | 3.51 | 1.01 |
| 5* | 10/05/2008 | 48.20 | 7.59 | 12.92 | 0.34 | 0.06 | 0.25 | 0.21 |
| 8* | 11/05/2008 | 48.50 | 8.50 | 12.95 | 0.30 | 0.06 | 0.23 | 0.03 |
| 9* | 12/05/2008 | 49.20 | 9.50 | 13.33 | 0.11 | 0.01 | 0.23 | 0.07 |
| 10* | 13/05/2008 | 49.50 | 10.50 | 13.13 | 0.14 | 0.02 | 0.18 | 0.10 |
| 11* | 14/05/2008 | 50.50 | 10.50 | 13.63 | 0.27 | 0.02 | 0.27 | 0.16 |
| 12* | 19/05/2008 | 51.00 | 10.00 | 13.32 | 0.24 | 0.04 | 0.21 | 0.26 |
| 13* | 20/05/2008 | 50.00 | 10.34 | 13.41 | 0.63 | 0.03 | 0.14 | 0.03 |
| 9b* | 21/05/2008 | 49.20 | 9.50 | 13.63 | 0.46 | 0.03 | 0.24 | 0.00 |
| 5b* | 22/05/2008 | 48.20 | 7.60 | 13.50 | 0.94 | 0.05 | 0.20 | 0.37 |
| 4 | 23/05/2008 | 47.42 | 7.27 | 14.31 | 0.86 | 0.06 | 0.14 | 0.03 |

Comparison of concentrations of dissolved nitrate and nitrite (NOx) with those of dissolved phosphate ($PO_4$) yields N/P ratios of 16.7 and 15.7, respectively, for the 2007 and 2008 campaigns, which are very close to the Redfield ratio of 16:1 (Figure 10). For the 2006 cruise, only limited NOx data are available due to sample conservation problems. The negative intercepts suggest that nitrogen was the limiting inorganic nutrient compared to phosphorus. Note that coccolithophorids can assimilate N and P as organic nutrients (Paasche, 2002). Figure 10 also shows that surface waters were more depleted in $NO_x$ during the May 2008 cruise compared to the May 2007 cruise. Comparison of $NO_x$ concentrations with Si data shows a typical deep regeneration profile due to the slower dissolution process of biogenic silica (Figure 11).

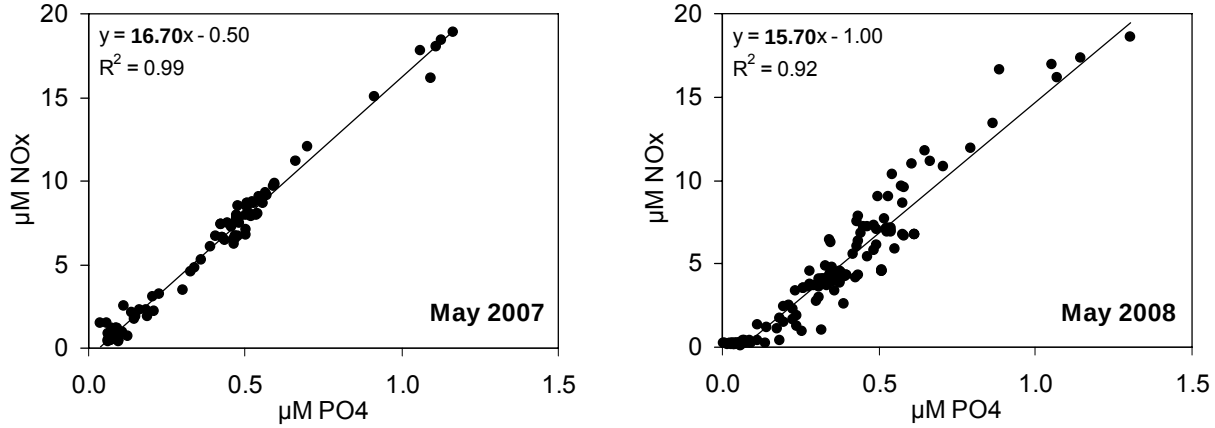


**Figure 10**. Nitrate and nitrite (NOx) vs. phosphate (PO4) for the 2007 and 2008 cruises in the Bay of Biscay. The straight lines denote the linear regressions. All data have been included.

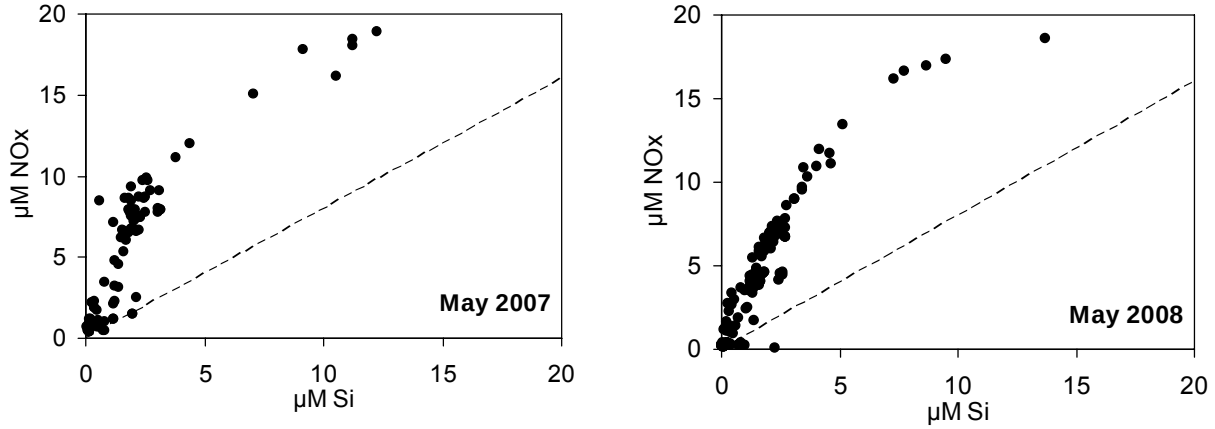


**Figure 11**. Nitrate and nitrite (NOx) vs. silicate (Si) for the 2007 and 2008 cruises in the Bay of Biscay. The dashed lines indicate the average N:Si ratio of 0.8:1 found in marine diatoms (Brezenski, 1985). All data have been included.

Coccolithophorid blooms have been shown to occur after the spring diatom blooms (Head et al., 1998) or co-occur with diatoms (Lampert et al., 2002). Surface levels of inorganic nutrients are generally low at the end of a diatom bloom. *E. huxleyi* does not require Si compared to diatoms that require at least 2 µmol $L^{-1}$ (Egge and Aksnes, 1992) and it can thus bloom at low or depleted $PO_4$ concentrations (Egge and Heimdal, 1994; Riegman et al., 2000). Moreover, one observes several high reflectance (HR) patches over the shelf each year, which indicate the presence of coccolithophorids, among which *E. huxleyi* is thought to be the dominant species (Figure 8), as cofirmed by SEM observations in May 2007 (Figure 27) and May 2008 (Figure 30). Zones of HR often reflect a later stage of the coccolithophorid bloom, as HR patches are caused principally by enhanced light reflection due to detached coccoliths in suspension, accumulated during the calcifying phase.

A highly resolved sampling procedure for dissolved organic carbon (DOC) and total dissolved nitrogen (TDN) was conducted during the cruises in the Bay of Biscay 2006-2008. Samples were taken at all stations in vertical profiles. DOC concentrations ranged from 78 to 124 µmol $L^{-1}$ during the cruise 2007. Neither the vertical distribution of DOC nor horizontal concentrations along the transect showed clear trends. Concentrations of TDN ranged from 7 to 14 µmol $L^{-1}$ along the 2007 transect. The mean molar C:N-ratio of dissolved organic matter was 10.7.

### *4.1.2 Plankton dynamics*

In 2008, the vertical distribution of phyto- and bacterio-plankton abundance and of average phytoplankton size in the range 0.5-10 µm equivalent shperical diameter (ESD) was determined by flow cytometery. Figure 12 illustrates the variability in cell abundance over the shelf, where a bloom patch was encountered at Station 10 as indicated by high plankton abundance in the photic zone. Here, oxygen saturation, as well as bacterial abundance was highly correlated to phytoplankton abundance ($p<0.01$) Shown is also the increase in average size of phytoplankton with depth, summarized for all stations that were visited in 2008.

Based on the concentrations of marker pigments and on microscopic assessment of the dominant phytoplankton groups, HPLC determined Chl-a concentrations were partitioned over the various plankton groups using the CHEMTAX routine for the three years. Depth-integrated (upper 80 m) Chl-a concentrations were on average higher during the 2006 campaign (average: 63.8 mg chl *a* $m^{-2}$) than during the 2007 (average: 27.0 mg chl *a* $m^{-2}$) and 2008 (average: 41.3 mg chl *a* $m^{-2}$) cruises (Figure 13). In general, the phytoplankton assemblages during the three consecutive campaigns were dominated by diatoms (*Rhizosolenia* spp., *Thalassiosira* spp., *Thalassionema* sp., *Chaetoceros* spp., and *Pseudonitzschia* sp.) and/or coccolithophores (*E. huxleyi*), occasionally with dinoflagellates (*Ceratium* spp.,

*Protoperidinium* spp., *Dinophysis* sp., and Gymnodinioids), cryptophytes or prasinophytes as codominants. In 2006, the phytoplankton community was dominated by coccolithophores at stations 1, 2, 3, 6, and 1b, while stations 4, 7, and 4b were diatom-dominated, with a high share of prasinophytes at station 4. In 2007, the phytoplankton community was dominated by coccolithophores at stations 2, 4, 7, 9 and 11; stations 5, 8, 8b, and 5b were diatom-dominated. Station 10 exhibited a high prevalence of prasinophytes (together with coccolithophores), while station 2b was dominated by peridinin-containing dinoflagellates. Finally, in 2008, the phytoplankton community at stations 11, 12, 13, 9b, and 5b was dominated by coccolithophores, while stations 2, 3, 4, 5, 6, 9 and 10, and were diatom-dominated. At station 1 both cryptophytes and diatoms were dominant; station 8 showed a mixed assemblage with high relative abundances of dinoflagellates and coccolithophores.

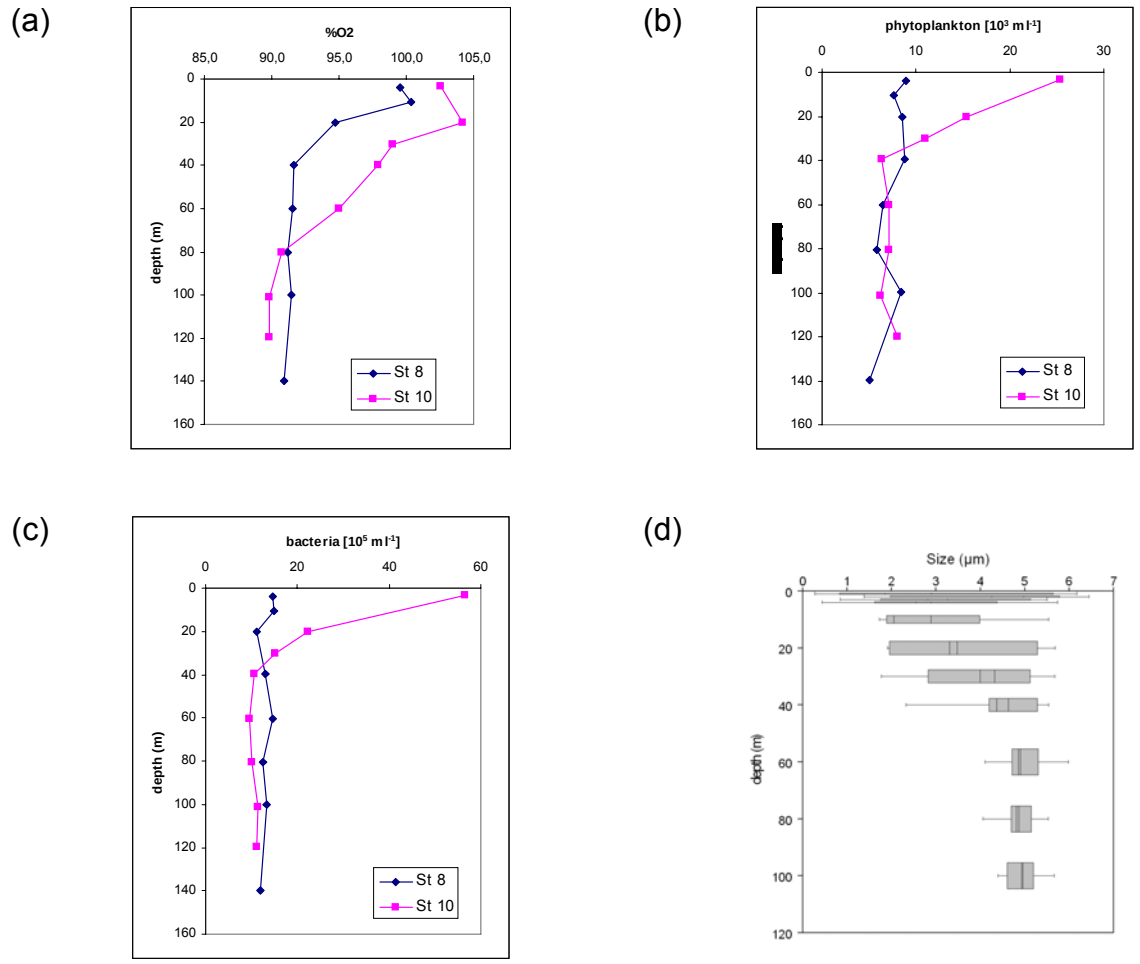


**Figure 12**. Vertical distribution of (a) oxygen saturation, and of (b) phytoplankton and (c) bacterioplankton abundance at stations 8 and 10, 2008. (d) Depth distribution of average phytoplankton size for all stations sampled in 2008. Each box encloses 50% of the data with the median and mean values of the variable displayed as thin lines. The bottom of the box marks the 25% limit, and the top the 75% limit, of the variable population. The lines extending from the top and bottom of each box marks the minimum and maximum values within the data set.

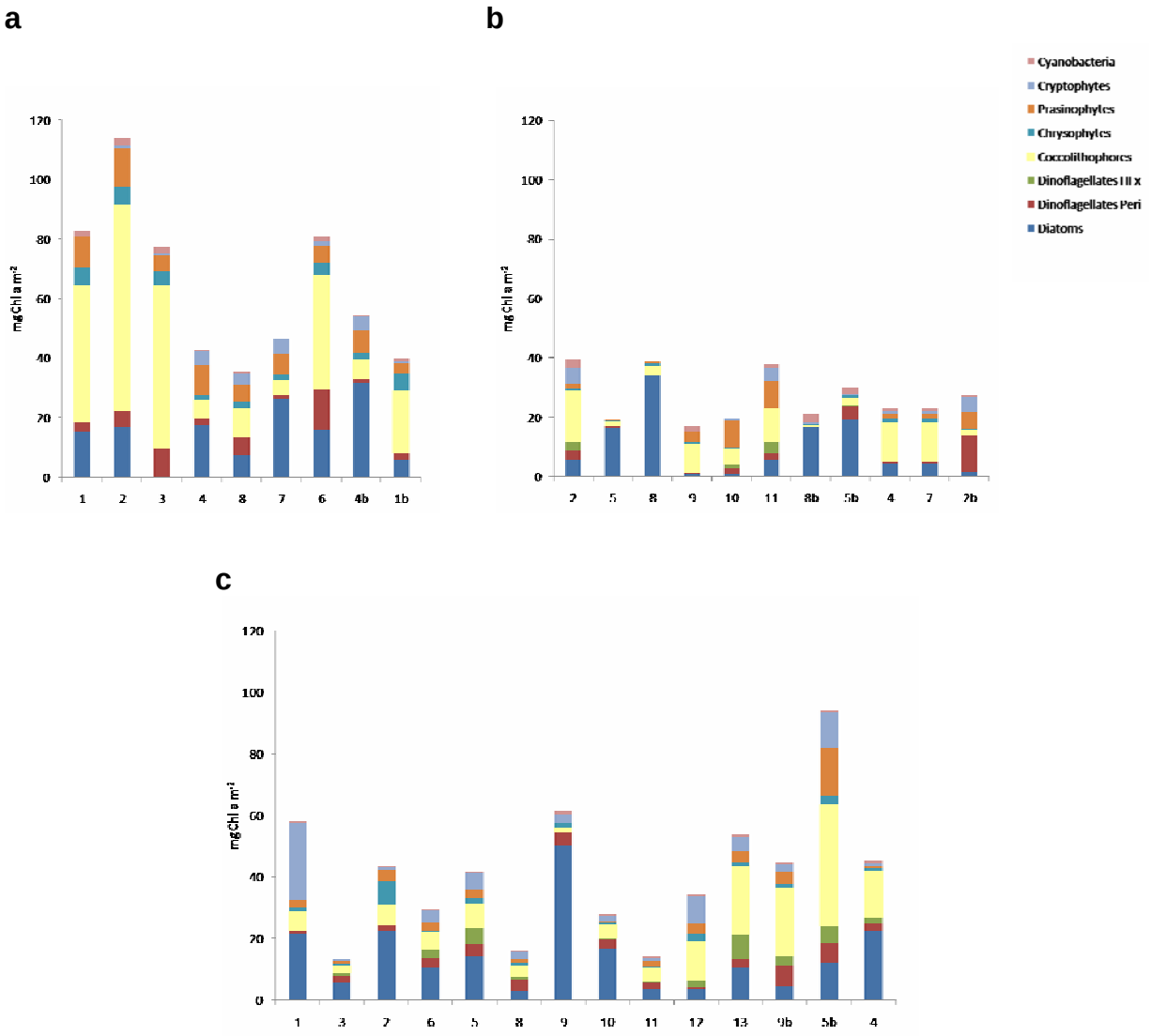


**Figure 13.** Depth-integrated Chl-a concentrations (partitioned over the dominant phytoplankton groups) for (a) 2006, (b) 2007 and (c) 2008 campaigns. Stations are ordered by date of sampling.

Multi-annual trends in phytoplankton community composition and biomass (symbol size) in the surface layers (upper 30 m) are shown in Figure 14a. The main trend in community composition (PC1) separates diatom- from coccolithophore-dominated samples over the three sampling years (note that biomass also tends to be higher in the latter samples). The second gradient (PC2) is related to the relative importance of coccolithophores vs codominant groups (such as prasinophytes, dinoflagellates and cryptophytes). In 2006, the coccolithophore blooms had a higher biomass and had few codominants, while in 2007 and 2008 the blooms were less intense and had more codominants. The positive relation between phosphate and coccolithophore (relative) abundance, and the negative correlation between diatoms and phosphate, is mainly driven by a strong, significant correlation in 2006. No major correlations

were observed during 2007 and 2008. Diatom (relative) abundance was negatively correlated with Si in 2006 and 2007, not in 2008, resulting in an overall negative relation between both variables.

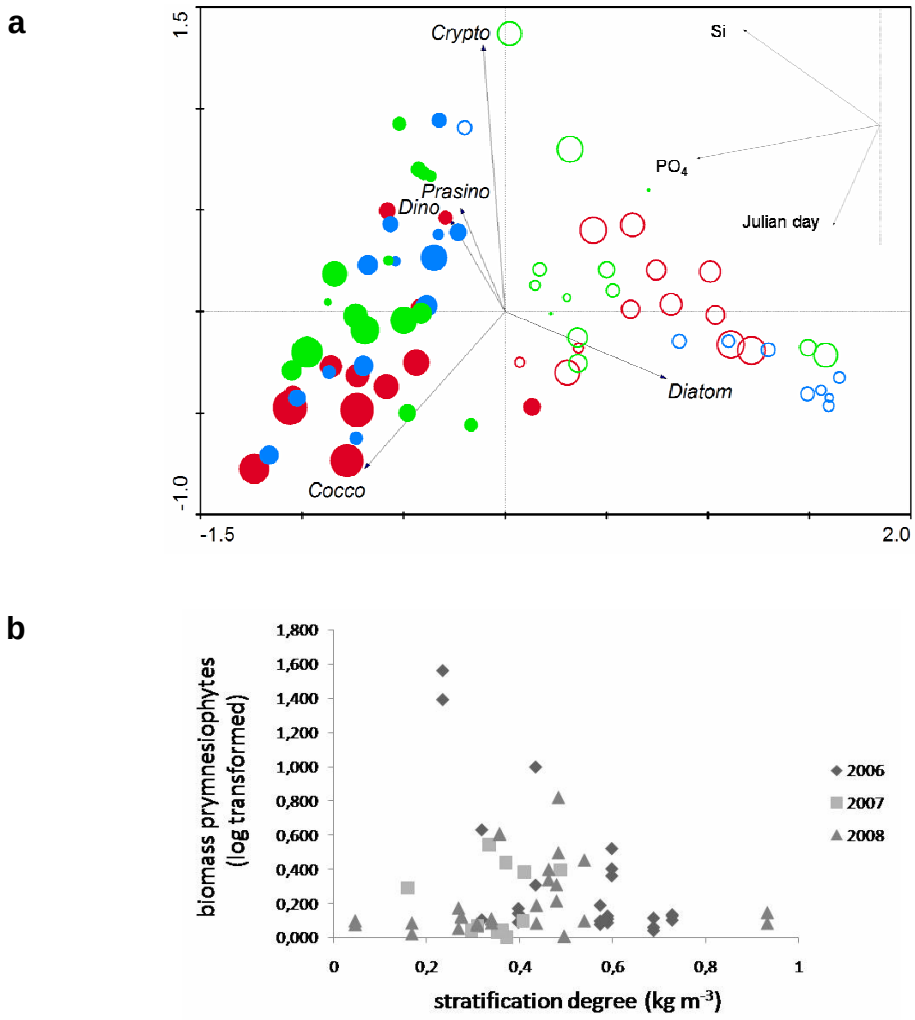


**Figure 14.** (a) PCA plot based on the relative abundance of phytoplankton groups at each sampling point above 30 m (station and depth). Sampling years are colour coded (2006: red, 2007: blue, 2008: green). Filled symbols represent sampling points where coccolithophores are dominant, empty symbols represent diatom-dominated samples. Phytoplankton arrows indicate the direction of steepest increase in relative abundance for the corresponding group. The size of the symbols is proportional to the chl *a* concentration. Julian day, Si and $PO_4$ concentrations are plotted as supplementary variables (inset), indicating the main direction of change with respect to the PCA axes. (b) Prymnesiophyte biomass vs stratification degree for the three sampling years.

Figure 14b shows that prymnesiophyte biomass (mainly *E. huxleyi*) is related to the degree of stratification of the water column, with biomass steadily declining as stratification becomes more pronounced (and nutrients depleted, see Figure 33). Diatom biomass showed no clear trend with this parameter, while several

codominants (prasinophytes, chrysophytes) tended to first increase as waters stratified, only to decrease again (not shown).

Microplankton (> 20 µm) abundance and diversity was determined only for samples from 20 m depth (roughly corresponding to the Chl-a maximum) for 2006 and diversity in 2008 (dilution experiment stations). In total, 72 taxa or morphotypes were identified. Total microplanktonic biomass values ranged from 2.48 µgC $L^{-1}$ to 34.02 µgC $L^{-1}$ in 2006. In all the samples that were analysed the autotrophic biomass was dominated by diatoms (*Bacteriastrum* sp. and *Rhizosolenia* spp.). In 2008, *Dinophysis acuminata* and *Ceratium kofoidii* were the dominant armored dinoflagellates at station 5. The heterotrophic biomass (> 20 µm) in 2006, which was dominant in samples from stations 2, 3, 4, 8, & 1bis, was primarily composed of ciliates. In all stations oligotrichous and choreotrichous ciliates made up most of the ciliate biomass.

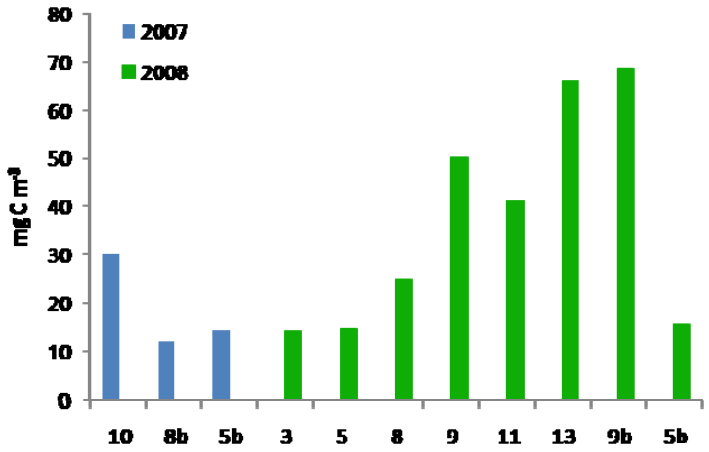


**Figure 15.** Mesozooplankton biomass concentration for stations of the 2007 and 2008 campaigns.

Mesozooplankton biomass was measured to provide an additional trophic level carbon estimate of the northern Bay of Biscay shelf break ecosystem (Figure 15). Mesozooplankton carbon concentrations varied more than 6-fold across sampling sites, but were in the same range or sometimes higher (13 and 9b) than those reported by Huskin et al. (2006) off the NW coast of Spain. No correlations were found between mesozooplankton and phytoplankton biomass estimates, possibly indicating a lag period in response to the blooms. Moreover, in oligotrophic environments where smaller phytoplankton cells are favoured, microzooplankton cells are responsible for most of the grazing compared to mesozooplankton (Sautour et al. 1996). In this scenario, larger diatom cells could be preyed upon by mesozooplankon and help explaining the disappearance of the diatom bloom at station 9 (below 10 m) compared to the same station revisited one week later (Figure 13c). In addition, the generally low Si values in surface waters (< 2 µmol $L^{-1}$) did not

favour the development of diatoms during the time of sampling. This is in agreement with the general seasonal phytoplankton cycle in the area, whereby the main phytoplankton bloom of diatoms occurs in April (Figure 17a).

Bacteria are principally responsible for the respiration of organic matter in the oceans, thus influencing strongly the biogeochemical fluxes of carbon and other elements. We therefore investigated the bacterial community composition (BCC) by means of DGGE in order to identify the dominant bacterial phylotypes (which are assumed to be responsible for the bulk of these processes), to determine their spatial and temporal dynamics, and to elucidate possible relationships between their occurrence, phytoplankton dynamics and other environmental variables (nutrients, TEP, stratification, depth).

Exploratory analyses including all data revealed a pronounced distinction in BCC between the free-living (FL) and the particle associated (PA) fractions in all years. We therefore analyzed both fractions separately in order to assess whether different factors influence BCC in these fractions. We performed principal components analysis (PCA), a multivariate ordination technique, on the DGGE data, and added the phytoplankton and environmental data as supplementary (passive) variables (Figure 16). Species data (DGGE band numbers/phylotypes) are not shown to avoid cluttering of the diagrams. The most important phylotypes observed in 2006 are shown in Table 2.

The main variation in BCC within each year is related to the dominance of diatoms vs coccolithophores in the samples (note the opposing arrows for these organisms, and the separation of empty vs filled symbols), and hence reflects bloom stage. Co-dominance of other phytoplankton groups (e.g. cryptophytes in 2006 at station 8, and in 2008 at stations 1, 3 and 5b, all FL) may explain the isolated position of some samples. This contrast in BCC between diatom vs coccolithophore stations/samples is most pronounced in the FL bacterial fraction, and appears to be less clear-cut in the PA fraction (cf. also Sapp et al., 2007a). It is unclear what the reason is for this observation, which may suggest that BCC relates more strongly to plankton exudates (and derivates) than to the presence of the cells themselves (see also below) (cf. also Sapp et al., 2007b). In this respect, it is noteworthy that TEP (both the color and the surface measures) is always strongly related to the presence of coccolithophores, not diatoms. Except for the FL fraction in 2008, there is no clear relationship between BCC and depth. Instead, the different depths from the various stations tend to cluster together, being more similar within than between stations. BCC uniformity along the depth transects may be due to mixing (in the mixed layer) or sinking from the surface layers.

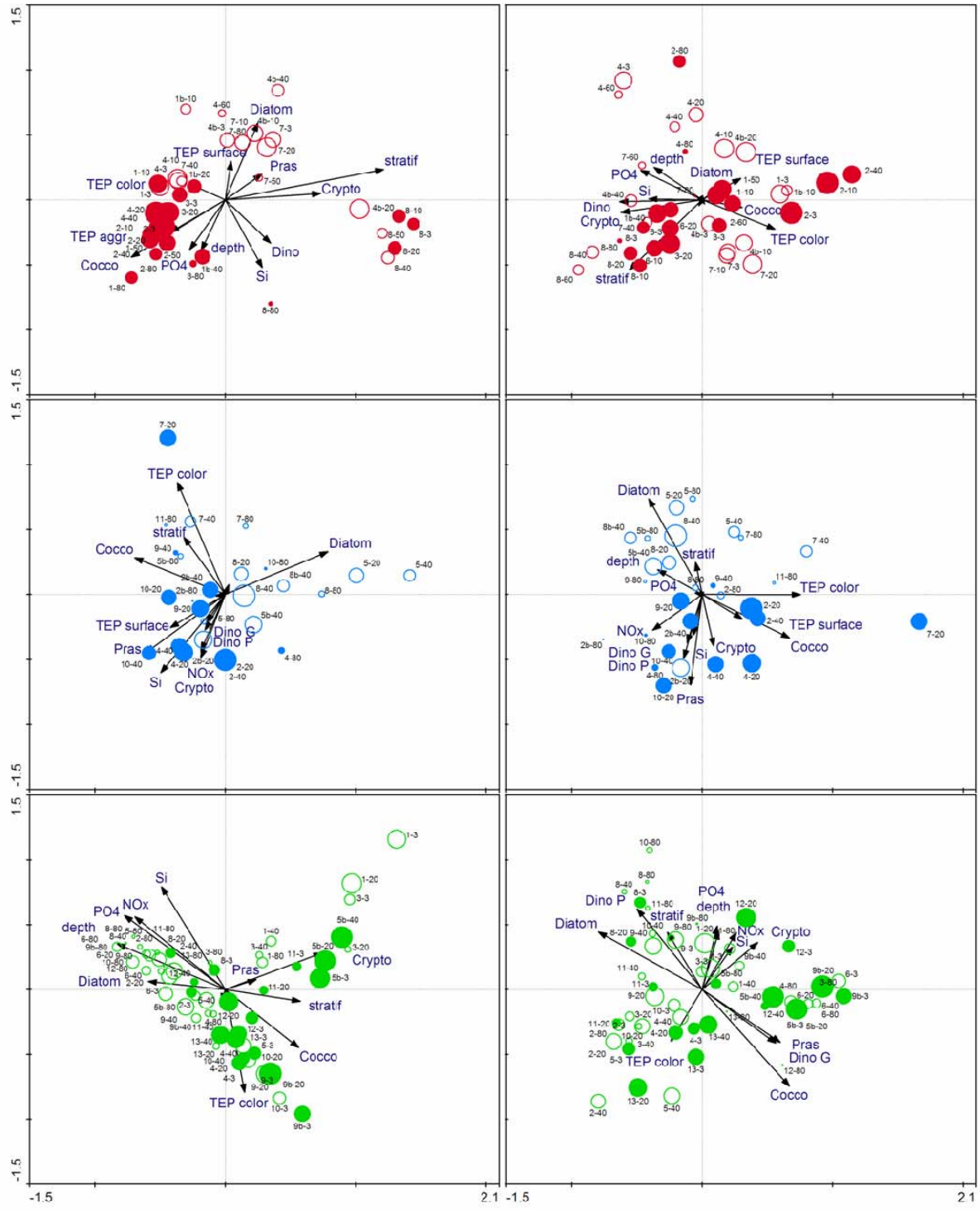


**Figure 16.** PCA diagrams summarizing variation in bacterial community structure for all stations and depths (> 80m) based on DGGE (2006: red, 2007: blue, 2008: green) (left: free-living; right: particle-associated). Filled symbols = coccolithophore-dominated; empty = diatom-dominated (note that this is based on relative values!). Symbol size is proportional to Chl-a concentration. Projection of phytoplankton and environmental arrows (added as supplementary variables) on axes is proportional to the correlation of these variables with the ordination axes.

**Table 2**. Phylotypes of both FL and PA BCC associated with *E. huxleyi* (blue), diatoms (green), dinoflagellates or cryptophytes (yellow), or high TEP concentration (pink). Phylotypes in bold represent the most abundant ones in each BCC. Genbank accession numbers are provided when sequence data are available.

| **FL BCC** | | **PA BCC** | |
|---|---|---|---|
| phylotypes | Accession n° | phylotypes | Accession n° |
| **aProt_5** | EU394545 | **24.2** | no seq |
| **Pubique** | EU394544 | **Pubique** | EU394544 |
| **18.2** | no seq | **SAR86_1** | EU394552 |
| **Sphingo** | EU394566 | **18.2** | no seq |
| **24.2** | no seq | **aProt_5** | EU394545 |
| **10.3** | no seq | **31.7** | no seq |
| 35.4 | no seq | **Flavo_3** | EU394543 |
| **aProt_2** | EU394547 | aProt_3 | EU394583 |
| **SAR86_1** | EU394552 | yProt_2 | EU394548 |
| **SAR86_2** | EU394540 | **Flavo_4** | EU394565 |
| **40.5** | EU394538 | **Sphingo** | EU394566 |
| **yProt_2** | EU394548 | **62.1** | no seq |
| aProt_3 | EU394583 | 19.2 | no seq |
| Flavo_3 | EU394543 | 62.1 | no seq |
| 27.0 | no seq | 29.0 | no seq |

While our analyses suggest strong relationships between phytoplankton and BCC, it is as yet not clear whether this relation is direct (e.g. via cell associations or exudates) or indirect (e.g. through nutrient depletion). We hope to further unravel these relationships using mesocosm experiments (see §4.2.2).

In Table 2 phylotypes (2006 data) for both FL and PA BCC contributing to most of the variation in composition are presented together with their association with certain phytoplankton regimes or environmental variables. Phylotypes in the FL BCC seem to be more commonly associated with *E. huxleyi* (blue) or codominant species (dinoflagellates and cryptophytes), diatoms (green), or pronounced water column stratification (yellow). The association with phytoplankton of the most abundant phylotypes in the PA BCC is shifted towards dinoflagellates (yellow) instead of the diatoms and *E. huxleyi* (blue) polarity. Moreover, some phylotypes are found to be associated with high TEP concentrations (pink), which would be expected of PA bacteria.

Bacterial abundances were determined for the 2006 and 2008 campaign (the 2007 samples were not usable due to bad preservation). In 2006, cell densities ranged from $0.60 \times 10^9$ to $2.57 \times 10^9$ cells $L^{-1}$ at the surface, and from $0.38 \times 10^9$ to $1.61 \times 10^9$

cells $L^{-1}$ at a depth of 80 m. Stations 4, 6 and 7 showed the highest overall cell densities. In 2008, cell densities ranged from $0.45x10^9$ cells $L^{-1}$ to $2.51x10^9$ cells $L^{-1}$ at the surface (station 5 and 10, respectively). In general, bacterial cell numbers decreased with increasing depth. Comparison of cell densities with the bacterial production values for the 2006 cruise showed good correlation for stations 2, 7, & 8 but no correlation for stations 1 and 4. The latter may be due to differences in cell activity or different mean cell size between samples, both of which were not assessed.

### *4.1.3 Primary production (PP) and calcification (CAL)*

Primary production (PP) and calcification (CAL) were determined based on the methodology described in §3.2.1. They represent respectively the potential fixation of DIC into POC and PIC under ideal conditions of light without cloud coverage. The results are summarised in Table 3 for the three field investigations.

**Table 3.** Daily rates of depth-integrated PP and CAL and depth-integrated Chl-a concentrations during the 2006, 2007 and 2008 cruises.

| Station | date | PP | CAL | Chl-a |
|---|---|---|---|---|
| | | mg C $m^{-2}$ $day^{-1}$ | mg C $m^{-2}$ $day^{-1}$ | mg Chl-a $m^{-2}$ |
| **1** | 31/05/2006 | 951 | 90 | 90.2 |
| **1bis** | 9/06/2006 | 710 | 189 | 36.6 |
| **2** | 1/06/2006 | 2160 | 617 | 130.3 |
| **4** | 2/06/2006 | 648 | 155 | 50.5 |
| **4bis** | 8/06/2006 | 655 | 150 | 57.1 |
| **5** | 2/06/2006 | 1168 | 290 | 74.8 |
| **7** | 7/06/2006 | 901 | 433 | 48.3 |
| **8** | 6/06/2006 | 426 | 160 | 34.9 |
| **2** | 10/05/2007 | 651 | 1685 | 22.0 |
| **2bis** | 24/05/2007 | 1149 | 292 | 58.6 |
| **4** | 23/05/2007 | 868 | 559 | 51.0 |
| **5** | 12/05/2007 | 358 | 117 | 49.3 |
| **5bis** | 22/05/2007 | 504 | 507 | 30.2 |
| **7** | 23/05/2007 | 487 | 436 | 85.8 |
| **8** | 13/05/2007 | 1411 | 984 | 70.7 |
| **8bis** | 21/05/2007 | 698 | 704 | 72.8 |
| **9** | 14/05/2007 | 1607 | 533 | 49.1 |
| **10** | 15/05/2007 | 667 | 1413 | 18.2 |
| **11** | 16/05/2007 | 2375 | 779 | 65.3 |
| **1** | 7/05/2008 | 1845 | 310 | 50.7 |
| **2** | 8/05/2008 | 187 | 23 | 47.9 |
| **4** | 23/05/2008 | 571 | 118 | 59.0 |
| **5** | 10/05/2008 | 314 | 69 | 15.8 |
| **5bis** | 22/05/2008 | 858 | 202 | 34.5 |
| **6** | 9/05/2008 | 431 | 171 | 18.3 |
| **8** | 11/05/2008 | 665 | 254 | 8.6 |
| **9** | 12/05/2008 | 490 | 371 | 99.6 |
| **9bis** | 21/05/2008 | 904 | 798 | 17.6 |
| **10** | 13/05/2008 | 542 | 125 | 14.1 |
| **11** | 14/05/2008 | 461 | 63 | 10.3 |
| **12** | 18/05/2008 | 521 | 177 | 21.8 |
| **13** | 20/05/2008 | 686 | 290 | 32.4 |

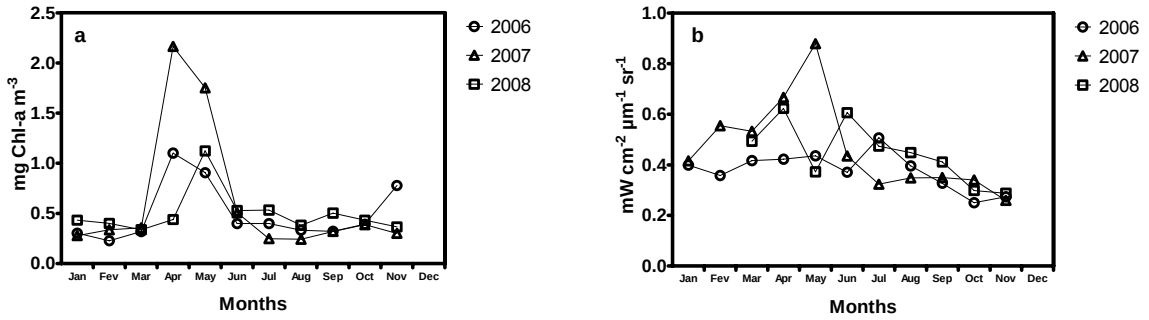


**Figure 17**. (a) Month-averaged surface MODIS Chl-a concentrations and (b) normalized water-leaving radiance at 555 nm at the La Chapelle Bank (latitude [48.0°N,48.5°N], longitude [7°W,6.5°W]) in 2006 (circles), 2007 (triangles) and 2008 (squares).

The analysis of remotely sensed parameters indicates that the spring bloom started in early April in 2006 and 2007 (Figure 17a). The phytoplankton biomass increased from <0.5 mg Chl-a $m^{-3}$ (winter levels) to their highest averaged levels of 1.1 mg Chl-a $m^{-3}$ and 2.1 mg Chl-a $m^{-3}$, respectively for 2006 and 2007. A phytoplankton biomass similar to the level determined in April 2006 was measured in May 2008 (1.1 mg Chl-a $m^{-3}$). A global decrease of biomass was observed in all years in June, where integrated Chl-a ranged between 0.4 mg Chl-a $m^{-3}$ and 0.5 mg Chl-a $m^{-3}$. The phytoplankton spring bloom was characterized, in 2007 and 2008, by an increase of the normalized water-leaving radiance signal to levels >0.5 mW $cm^{-2}$ $\mu m^{-1}$ $sr^{-1}$ corresponding to the winter averaged spectral signature of coccolithophores in surface waters (Figure 17b). A sudden decrease of this parameter was observed in May 2008 followed by a secondary increase in June. This was likely the consequence of storm events that occurred during this period in the Bay of Biscay. This led to the deepening of the mixed layer and resulted in a transfer of nutrients from deeper waters to the photic zone. The calcification rates in 2008, ranging between 23 mg C $m^{-2}$ $d^{-1}$ (station 2) and 798 mg C $m^{-2}$ $d^{-1}$ (station 9bis), were probably determined during the decline of the bloom (Figure 18a). The spectral signature of the coccolithophorid bloom was not observed on this monthly-averaged climatology during the year 2006 (Figure 17b), although apparent for the remote sensed images contemporary to the cruise (Figure 8). Our 2006 incubation results indicate, however, that coccolithophores were active, as suggested by significant calcification rates ranging between 90 mg C $m^{-2}$ $d^{-1}$ (station 1) and 617 mg C $m^{-2}$ $d^{-1}$ (station 2) (Table 3).

The highest rates of calcification were evaluated in the June 2007 (1685 mg C $m^{-2}$ $d^{-1}$ at station 2 and 1413 mg C $m^{-2}$ $d^{-1}$ at station 10), coinciding with the highest spectral signature of coccolithophores determined from remotely sensed parameters, in May-June 2007 (2.2 and 1.8 mW $cm^{-2}$ $\mu m^{-1}$ $sr^{-1}$) (Figure 17b). No clear relationship was observed between PP and CAL, as suggested by the Figure 18a.

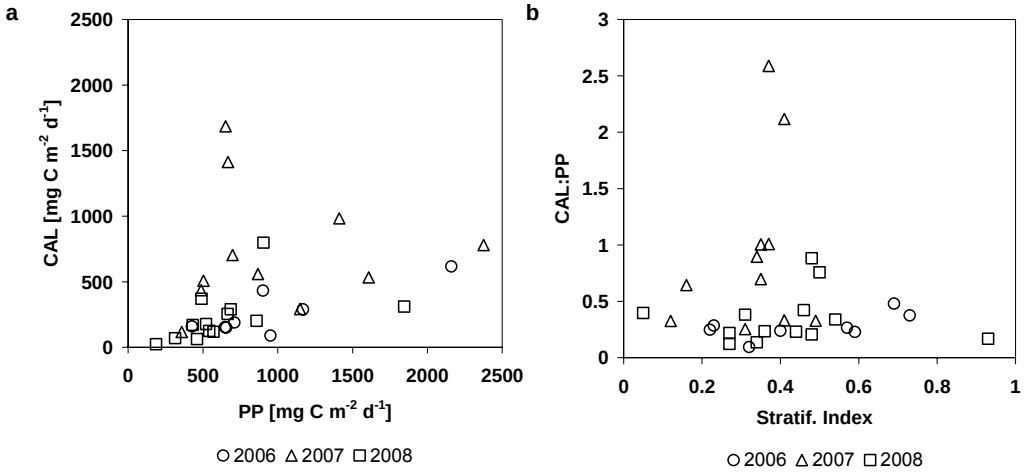


**Figure 18**. (a) Calcification rates (CAL) as a function of primary production (PP) and (b) the CAL:PP ratio as a function of the stratification index, computed from the difference of seawater density between 3 m (or 10 m) and 100 m depth for the 2006, 2007 and 2008 cruises.

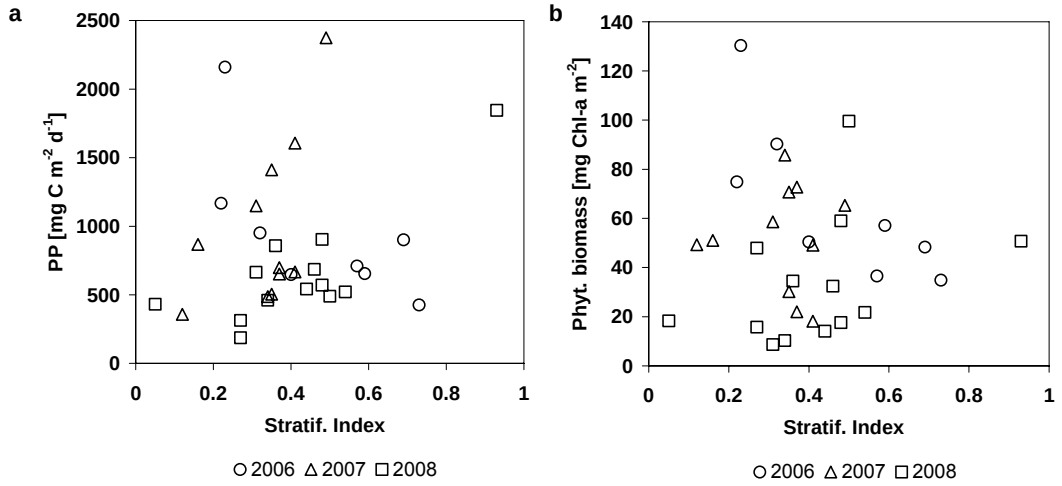


**Figure 19.** (a) PP and (b) phytoplankton biomass (vertically integrated Chl-a) as a function of the stratification index, computed from the difference of seawater density between 3 and 100 m depth, in 2006, 2007 and 2008.

The SST increased globally through spring and summer, reaching its maximum value in August over the continental shelf. This increase was paralleled by a deepening of the thermocline and a strengthening of the stratification, resulting in favourable conditions for the bloom development of coccoliothophores. However, punctual events like storms or internal waves induce a shoaling of the thermocline leading, in some cases, to a complete destratification of the surface layer. The link between stratification and rates of biological processes can be made by examining the ratio of CAL:PP as a function of the stratification index (the highest the index, the strongest is the stratification), computed as the difference of seawater density between 3 m (or 10 m) and 100 m (Figure 18b). The CAL:PP ratio ranged between 0.09 (station 1, 2006)

up to 2.59 (station 2, 2007) with an average of 0.53 (n= 32) over the 3 cruises. CAL:PP ratios remained below or close to the average in 2006 while they were above this value for several stations in 2007 and 2008. The highest values coincided with an index ranging between 0.35 and 0.5, as observed for 2007 and 2008.

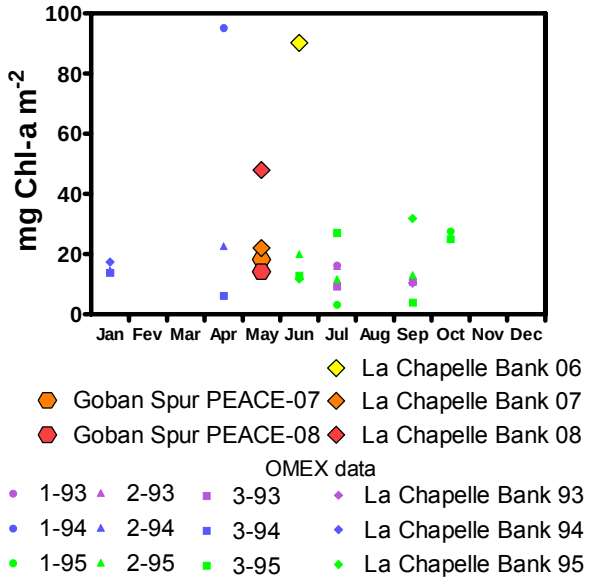


**Figure 20**. Depth-integrated Chl-a at Goban Spur (OMEX 1-3) and La Chapelle Bank, in 1993, 1994 and 1995 (Joint et al., 2001) and and during the June 2006, May 2007 and May 2008 PEACE cruise.

PP did not exhibit any particular trend regarding the stratification index (Figure 19a), as expected from the specific composition of natural phytoplankton assemblages with different ecological niche for environmental conditions: from pioneer diatom species, dinoflagellates to late-bloom unidentified flagellates (Joint et al., 2001). High rates of PP (above 1500 mg C $m^{-2}$ $d^{-1}$) were determined in either mixed (stratification index of 0.23; PP= 2160 mg C $m^{-2}$ $d^{-1}$ at station 2 in 2006), moderately stratified (stratification index of 0.41; PP= 2375 mg C $m^{-2}$ $d^{-1}$ at station 11 in 2007) or highly stratified (stratification index of 0.93; PP= 1845 mg C $m^{-2}$ $d^{-1}$ at station 1 in 2008) conditions, while the integrated phytoplankton biomass was the highest in mixed to moderately stratified conditions (Figure 19b). The integrated biomass ranged between 8.6 mg Chl-a $m^{-2}$ and 130.3 mg Chl-a $m^{-2}$ (average 47.7 mg Chl-a $m^{-2}$, n= 32) and were globally higher than that determined during the OMEX study at Goban Spur and La Chapelle Bank (Figure 20). The average PP was 840 mg C $m^{-2}$ $d^{-1}$ (n=32) over the 3 years of study and, except for the extreme PP quoted here-above, the overall range of the values (from 187 mg C $m^{-2}$ $d^{-1}$ at station 2, 2008, to 1607 mg C $m^{-2}$ $d^{-1}$ at station 9, 2007) agreed with the OMEX uppermost estimate of 1400 mg C $m^{-2}$ $d^{-1}$ at La Chapelle Bank (Joint et al., 2001) (Figure 21).

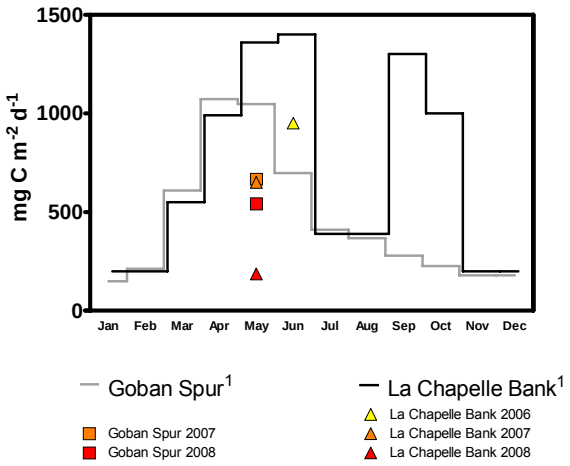


**Figure 21.** Climatology of estimated daily primary production at La Chapelle Bank (southern area) and Goban Spur (northern area) during the OMEX study (adapted from Joint *et al.*, 2001), and during the June 2006, May 2007 and May 2008 PEACE cruise.

### *4.1.4 Bacterial biomass production (BBP)*

Bacterial biomass production (BBP) in the Bay of Biscay was determined during the 2006 and 2007 cruises. BBP ranged from 5 to 27 nmol C $L^{-1}$ $h^{-1}$ at the surface along the transects of 2006 and 2007. In 2006, the maximum BBP of 13 nmol C $L^{-1}$ $h^{-1}$ was determined in surface and subsurface samples at station 2, the site nearest to the French coast. Stations located along the continental shelf break showed lower surface values, ranging from 7 to 9 nmol C $L^{-1}$ $h^{-1}$. BBP decreased strongly within the upper 50 m of the water column (Figure 22).

The highest BBP in 2007 was determined at the stations 5bis and 8bis, two sites along the shelf break. Results revealed that BBP increased during the duration of the cruise, since stations 5 and 8 showed clearly lower values during the first lag of the cruise conducted 8 -10 days earlier (Figure 23).

Rate constants for α- and β-glucosidase activity and for glucose uptake were calculated from Michaelis-Menten kinetics, assuming a linear relationship between non-saturating substrate concentration and enzymatic reaction velocity. Activities of α- and β-glucosidase were detected in all samples except for subsurface samples of stations 5bis and 8bis, revealing extracellular cleavage of polysaccharides by bacterioplankton along the transect. Extracellular glucosidase activity followed the vertical distribution of combined glucose, indicating the control of bacterial glucosidase expression by the availability of appropriate substrates (Figure 24).

No significant difference was observed between rate constants of α- and β-glucosidase and between glucosidase activity at the surface and at 40 m depth. The enzymatic polysaccharide breakdown was directly related to bacterial glucose uptake, when rate constants of α- and β-glucosidase did not exceed 0.0075 $d^{-1}$ and 0.020 $d^{-1}$, respectively (α-glucosidase: $r^2 = 0.66$, $p = 0.027$; β-glucosidase: $r^2 = 0.65$, $p = 0.002$) (Figure 25). Rate constants of bacterial glucose uptake ranged between

0.009 $d^{-1}$ and 0.062 $d^{-1}$, and were significantly higher than those of α-glucosidase ($p < 0.001$) and β-glucosidase ($p = 0.003$).

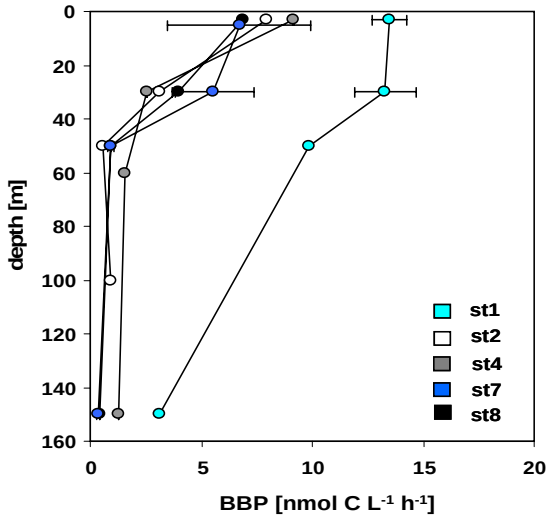


**Figure 22**. Depth profiles of bacterial biomass production in the Bay of Biscay, 2006. BBP was estimated from the incorporation of $^{3}H$- thymidine.

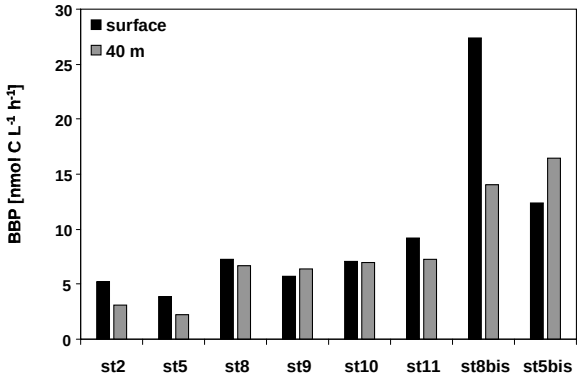


**Figure 23.** Bacterial biomass production at the surface and at 40 m depth (Bay of Biscay, 2007). BBP was estimated from the incorporation of leucine labelled with $^{14}C$.

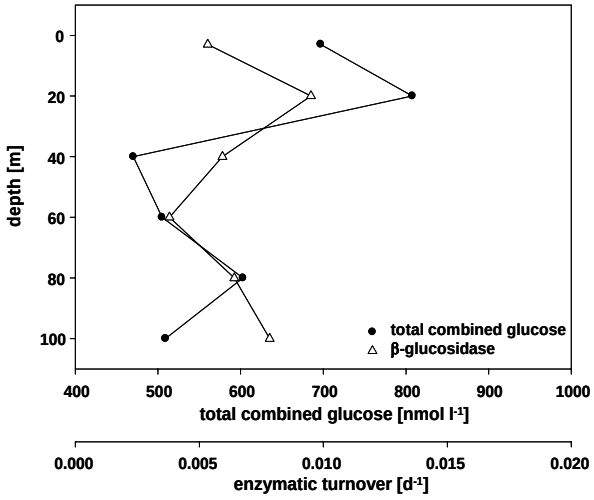


**Figure 24**. Vertical profile of total combined glucose and b-glucosidase activity at station 2 (Bay of Biscay, 2007).

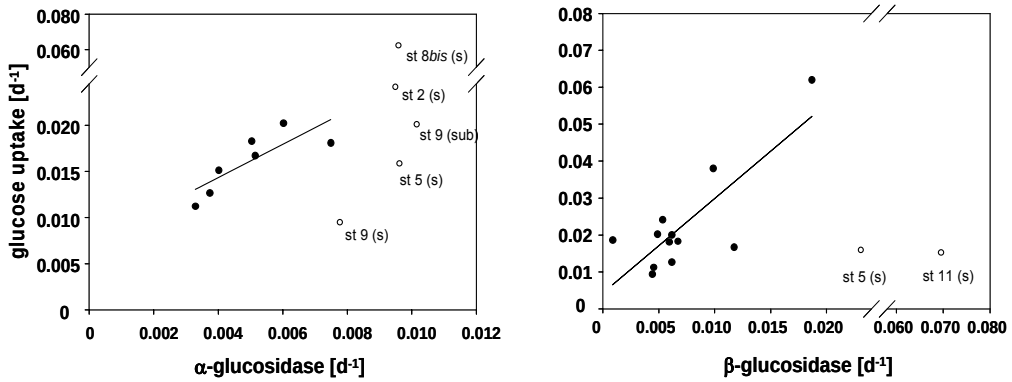


**Figure 25**. Glucose uptake rate constants as a function of α-glucosidase and β-glucosidase activity in the Bay of Biscay (α-glucosidase: $r^2 = 0.66$, $p = 0.027$, $n = 7$; β-glucosidase: $r^2 = 0.65$, $p = 0.002$, $n = 12$). Open symbols represent datapoints not included in the regression analysis (st=station, s=surface, sub= subsurface depth of 40 m).

Uptake rate constants were positively correlated with BBP along the transect ($r^2 = 0.63$, $p < 0.001$, $n = 16$) (Figure 26), indicating a direct relationship between glucose assimilation and biomass production of bacterioplankon.

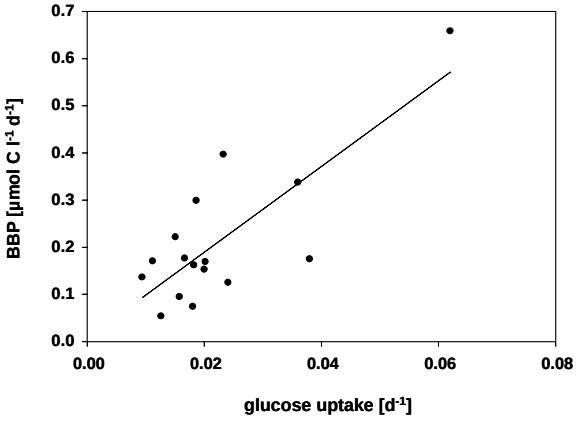


**Figure 26.** Bacterial biomass production (BBP) as a function of glucose uptake rate constants in the Bay of Biscay ($r^2 = 0.63$, $p < 0.001$, $n = 16$). Regression includes all data from surface and 40 m depth of all stations.

Our results revealed that bacterioplankton production in the Bay of Biscay was significantly related to the bacterial capacity of polysaccharide turnover that is determined by the efficiency of extracellular enzymatic hydrolysis and subsequent hydrolysate assimilation. However, highest glucosidase activities in the Bay of Biscay were not directly related to glucose uptake, showing that polysaccharide breakdown at high rates was not balanced by increasing bacterial glucose utilization (Figure 26).

During the 2007 cruise, effects of decreasing seawater pH on bacterial activity and on the degradation of polysaccharides were investigated. The natural phytoplankton community was dominated by *E. huxleyi* as observed by microscopic inspection. A large fraction of cells was included in fecal pellets and microaggregates (Figure 27),

suggesting that organic matter was not derived from freshly produced cells. The initial POC concentration was 14 µmol $L^{-1}$.

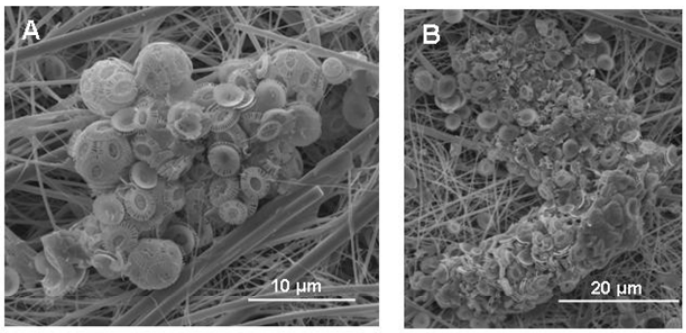


**Figure 27.** *E. huxleyi* collected at the surface of station 2 in the Bay of Biscay during the 2007 cruise. Cells are included in microaggregates (A) and fecal pellets (B).

Glucose was by far the most abundant neutral sugar in polysaccharides, accounting for up to 72% of combined carbohydrates. Other quantitatively important neutral sugars were galactose, mannose, and xylose. The deoxy-sugars fucose and rhamnose together accounted initially for 7%. The initial proportion of uronic acids, including the acidic sugars glucoronic acid and galacturonic acid, was 7 %. A high loss of combined glucose relative to other sugars led to a relative enrichment of uronic acids and deoxy-sugars during degradation (Figure 28). Both uronic acids and deoxy-sugars are known to be surface-active, influencing the stickiness of organic matter. Therefore, potential effects of changing polysaccharide composition induced by bacterial degradation on the stickiness of organic matter and consequences for aggregation processes need to be investigated.

The loss of polysaccharides is driven by the activity of bacterial extracellular enzymes. Macromolecules larger than 1 kDa cannot be taken up directly by bacteria and require extracellular enzymatic hydrolysis. Activity of β-glucosidase was higher in the future-ocean (FO) treatment relative to the present-day (PD) treatment (Figure 29). It can be assumed that higher rates of enzymatic polysaccharide hydrolysis at lowered seawater pH increased the availability of glucose for bacterioplankton. On day 5 of incubation, rates of glucose uptake and bacterial biomass production were 2.5 and 3.5 times higher, respectively, under FO conditions (Figure 29). This indicates that the surplus of free glucose generated by higher glucosidase rates was efficiently metabolized by bacterioplankton and that the bacterial substrate supply was improved under simulated future-ocean pH conditions.

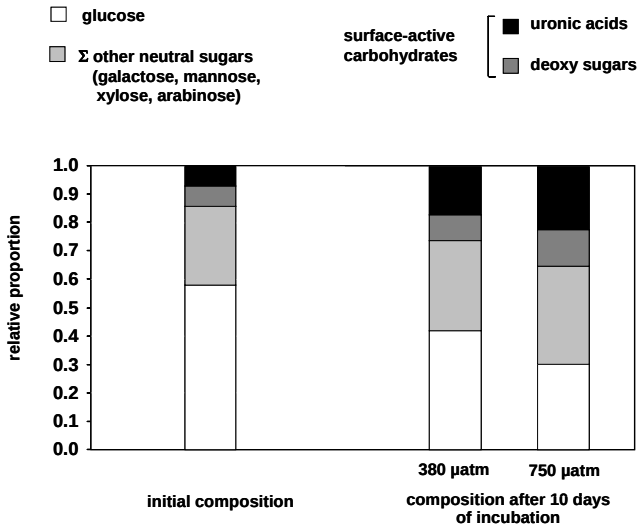


**Figure 28**. Changes in polysaccharide composition during degradation of organic matter sampled from the surface layer in the Bay of Biscay (station 2, 2007).

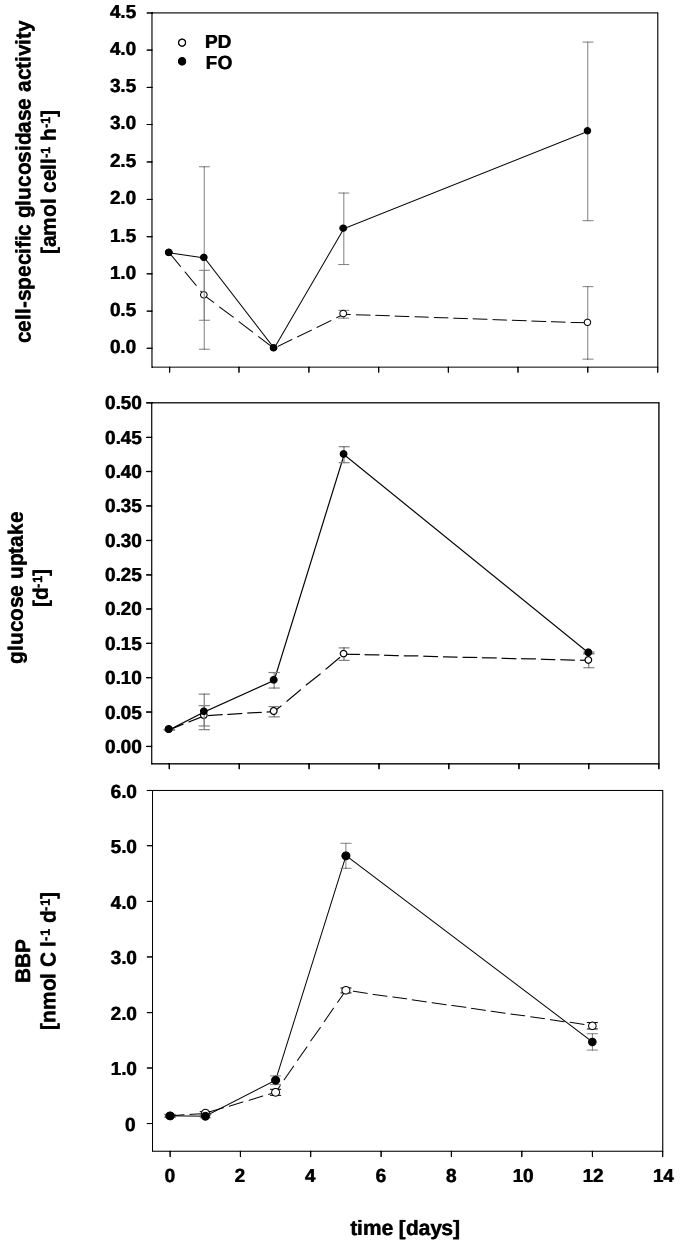


**Figure 29.** Cell-specific β-glucosidase activity, glucose uptake, and bacterial biomass production (BBP) in bottle incubations of present-day (PD) and future-ocean (FO) seawater pH.

### *4.1.5 Phytoplankton lysis rates and phytoplankton growth and mortality due to microplankton grazing*

The fate of the photosynthetic carbon production in marine ecosystem is a key parameter of the biological carbon pump. This carbon may be directly released extracellularly by the phytoplankton and/or transferred to higher trophic levels through grazing, to be ultimately exported to deeper waters by sedimentation. Phytoplankton cell lysis has to be considered as an important factor of loss such as extracellular release, grazing or sedimentation.

**Table 4.** Cell lysis rate ($\mu_L$) in surface waters during the June 2006, the May 2007 and the May 2008 cruises. $\mu_L$ was calculated as a function of the dissolved esterase activity (DEA) produced over 24 hours and the particulate esterase activity (PEA) following the method of Riegman and Winter (2003). The date of sampling was given as well as the temperature and the Chl-a concentration in surface waters.

| Stations | Date | Surface T °C | Surface Chl-a µg $L^{-1}$ | $\mu_L$ sf $d^{-1}$ |
|---|---|---|---|---|
| 2 | 1/06/2006 | 13.11 | 1.76 | 0.07 |
| 4 | 2/06/2006 | 13.29 | 1.27 | 0.25 |
| 8 | 6/06/2006 | 14.47 | 0.80 | 0.25 |
| 7 | 7/06/2006 | 14.51 | 0.96 | 0.11 |
| 1b | 9/06/2006 | 14.33 | 0.39 | 0.88 |
| 5 | 12/05/2007 | 12.96 | 1.03 | 0.35 |
| 8 | 13/05/2007 | 13.24 | 1.39 | 0.48 |
| 8b | 21/05/2007 | 13.25 | 1.25 | 0.60 |
| 2 | 8/05/2008 | 12.82 | 0.78 | 0.32 |
| 5 | 10/05/2008 | 12.92 | 0.34 | 0.25 |
| 11 | 14/05/2008 | 13.63 | 0.27 | 0.49 |
| 12 | 19/05/2008 | 13.32 | 0.24 | 0.81 |
| 13 | 20/05/2008 | 13.41 | 0.63 | 0.50 |
| 5b | 22/05/2008 | 13.50 | 0.94 | 0.38 |

Cell lysis rates were estimated in surface waters at some stations during the cruises (Table 4). Phytoplankton lysis rates ranged between 0.07 $d^{-1}$ (station 2, June 2006) and 0.88 $d^{-1}$ (station 1b, June 2006) (Table 4) and occurred at an average rate of 0.41±0.21 $d^{-1}$ (n=14) during our cruises. This level is consistent with previous studies (Riegman and Winter, 2003, Brussard et al., 1995, 1996) which reported lysis rates close to 0.3 $d^{-1}$ during *Phaeocystis* (Prymnesiophyte) blooms in the North Sea. The highest rates of cell lysis of 0.88 $d^{-1}$ at station 1b (2006) and 0.81 $d^{-1}$ at station 12 (2008), although significantly higher than other estimates determined in this study,

agree with values reported for a stratified Mediterranean Bay (Agusti and Duarte, 2000, 2002).

Dilution experiments were conducted at 5 stations where lysis rates were measured during the 2007 and 2008 cruises. Table 5 summarizes the estimates of phytoplankton growth and grazing coefficients for 3 marker pigments (Chl-a, HFx, and Fx). Nutrient-corrected phytoplankton growth rates and grazing rates ranged widely across the experiments. Total phytoplankton (Chl-a) growth and grazing rates ranged from 0.17 to 1.87 $d^{-1}$ and 0.32 to 1.54 $d^{-1}$, respectively. Coccolithophorid (HFx) growth and grazing rates ranged from 0.32 to 2.76 $d^{-1}$ and 0.23 to 2.13 $d^{-1}$, respectively, and diatom (Fx) growth and grazing rates ranged from 0.36 to 2.19 $d^{-1}$ and 0.48 to 2.09 $d^{-1}$, respectively. These rates are on average (Chl-a growth: 1.00 $d^{-1}$, SD = 0.51 and grazing: 0.76 $d^{-1}$, SD = 0.49) higher than the average growth and grazing rates compiled by Calbet and Landry (2004) for the open oceans (0.59 $d^{-1}$ and 0.39 $d^{-1}$, respectively), but in the same range as those measured by Stelfox-Widdicombe et al. (2000) and Olson and Strom (2002) during coccolithophorid blooms. In general, instantaneous nutrient-enhanced growth rates were higher than the nutrient-corrected growth rates, which may indicate a state of nutrient limitation among phytoplankton cells. Nonetheless this difference was not statistically significant (paired *t*-test for each marker pigment, all p>>0.05).

**Table 5.** Instantaneous growth rates ($\mu$), nutrient-corrected growth rates ($\mu_c$), rates of grazing mortality ($g$), and proportion of pigment standing stock grazed daily from linear regressions of Chl-a, 19'-hexanoyloxyfucoxanthin (HFx), and fucoxanthin (Fx) data for dilution experiments of the May 2007 and May 2008 cruises. r is the correlation coefficient of linear regression between apparent phytoplankton growth rate and dilution factor, ($^{*}p < 0.05$, $^{**}p < 0.01$).

| Station | Year | Growth $\mu$ ($d^{-1}$) | | | Nutrient corrected growth $\mu_c$ ($d^{-1}$) | | | Grazing $g$ ($d^{-1}$) | | | Proporion of stock grazed % ($d^{-1}$) | | | r | | |
|---|---|---|---|---|---|---|---|---|---|---|---|---|---|---|---|---|
| | | Chl-*a* | HFx | Fx | Chl-*a* | HFx | Fx | Chl-*a* | HFx | Fx | Chl-a | HFx | Fx | Chl-*a* | HFx | Fx |
| 5 | 2007 | 1.14 | 3.36 | 1.01 | 0.94 | 2.44 | 0.71 | 0.50 | 2.13 | 0.48 | 40 | 88 | 38 | 0.78$^{*}$ | 0.77$^{*}$ | 0.80$^{**}$ |
| 8b | 2007 | 0.92 | 0.80 | 0.67 | 0.88 | 0.76 | 0.57 | 0.97 | 0.44 | 0.81 | 62 | 36 | 55 | 0.76$^{*}$ | 0.44 | 0.70$^{*}$ |
| 5 | 2008 | 0.38 | 0.45 | 0.81 | 0.17 | 0.32 | 0.36 | 0.32 | 0.32 | 0.50 | 28 | 27 | 40 | 0.95$^{**}$ | 0.84$^{**}$ | 0.84$^{**}$ |
| 5b | 2008 | 1.,95 | 1.47 | 2.02 | 1.34 | 0.84 | 1.01 | 1.07 | 0.60 | 0.87 | 66 | 45 | 58 | 0.75$^{*}$ | 0.84$^{*}$ | 0.82$^{*}$ |
| 12 | 2008 | 2.16 | 1.94 | 2.44 | 1.87 | 1.61 | 2.19 | 1.54 | 1.45 | 2.09 | 79 | 77 | 88 | 0.97$^{**}$ | 0.98$^{**}$ | 0.97$^{**}$ |

In June 2006, a strong decrease in surface Chl-a was observed between the two legs. The pigments analysis indicated the disappearance of the coccolithophorid bloom at station 1 between the two legs (see Figure 13a). It is also at this station that the highest lysis rate was found (0.88 $d^{-1}$). Station 2, on the contrary, was located in a

zone of high Chl-a concentration and lower reflectance and exhibited the lowest lysis rate (0.07 $d^{-1}$) measured.

In 2007 diatoms dominated the phytoplankton assemblage (see Figure 13b). This is substantiated by the high Fx and low HFx concentrations measured and by microscopic observations (data not shown). Lysis rates exhibited a minimum value of 0.35 $d^{-1}$ at station 5 and a maximum value of 0.60 $d^{-1}$ at station 8b. An increase in cell lysis rate was observed between the two legs at station 8 (0.48 $d^{-1}$ to 0.60 $d^{-1}$, Table 4). Lysis rate were as important in 2007 as in 2006. This can be explained by the fact that concentrations of esterases in surface water are cumulative and that the decline of a diatoms bloom occurred before or even during the cruises. Total phytoplankton growth rate decreased while the grazing rate increased from station 5 to 8b, suggesting a higher control exerted onto phytoplankton by microzooplankton grazing.

In 2008, we sampled different stages of a coccolithophorid bloom. At station 5, low growth and grazing rates as well as low lysis rate were measured together with intermediate HFx concentrations, suggesting the very beginning of an *E. huxleyi* bloom (Figure 30a). At station 5b the onset of the bloom is marked by a higher growth than grazing rate, accompanied by a high HFx concentration and more numerous *E. huxleyi* cells (Figure 30b). In addition, a slight increase of lysis rate was observed at the revisited station 5, 12 days later (0.25 to 0.38 $d^{-1}$, Table 2). The same trend was observed at station 9, where low biomass and growth rate indicated a non-bloom situation as opposed to the revisited station 9b, where a full blown *E. huxleyi* bloom was happening (see fig. 4 c). Finally, at station 12 the prevalence of coccoliths and the much lower HFx concentration together with the high proportion of standing stock grazed daily, strongly suggest the demise of the bloom (Figure 30d). A higher lysis rate was also found at this station where the bloom was in a later stage than the southern areas (from reflectance images, Figure 8).

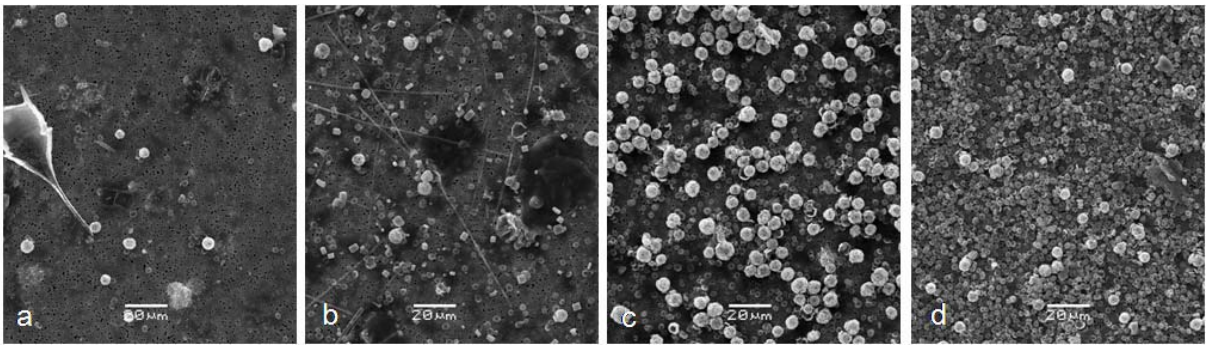


**Figure 30**. Scanning electron micrographs (UGent) of filtered surface water with *E. huxleyi* cells and coccoliths. (a) station 5; (b) station 5b; (c) station 9b; (d) station 12 of the May 2008 cruise. Equal volumes of water were filtered through each filter.

Our results indicate simultaneous occurrence of cell lysis and microzooplankton grazing. The levels of lysis rates measured during the cruises strongly suggest that cell lysis was occurring and that it could be attributed to, for example, viral activity or nutrients depletion. Algal cell lysis due to viral activity has the potential to compromise the assumption that phytoplankton growth is not limited in dilution experiments (Suffrian et al., 2008). This would be true when a critical "prey" cell or viral density, necessary for sustaining a significant infection rate, is maintained in the dilution series. This in turn would yield lowered instantaneous phytoplankton growth rates due to viral cell lysis and not necessarily due to grazing mortality. We therefore recommend to measure viral abundance as an additional variable to further distinguish both causes of phytoplankton mortality.

### *4.1.6 DIC dynamics and air-sea $CO_2$ fluxes*

#### *4.1.6.1 Distribution of $pCO_2$ and TA in surface waters*

The distribution of $pCO_2$ during the 3 cruises was patchy and strong horizontal gradients were observed (Figure 31). During the 3 cruises the range of $pCO_2$ variations in surface waters was similar (250 ppm to 360 ppm) and $pCO_2$ values were systematically below atmospheric equilibrium (~380 ppm), and hence the area acted as a sink for atmospheric $CO_2$.

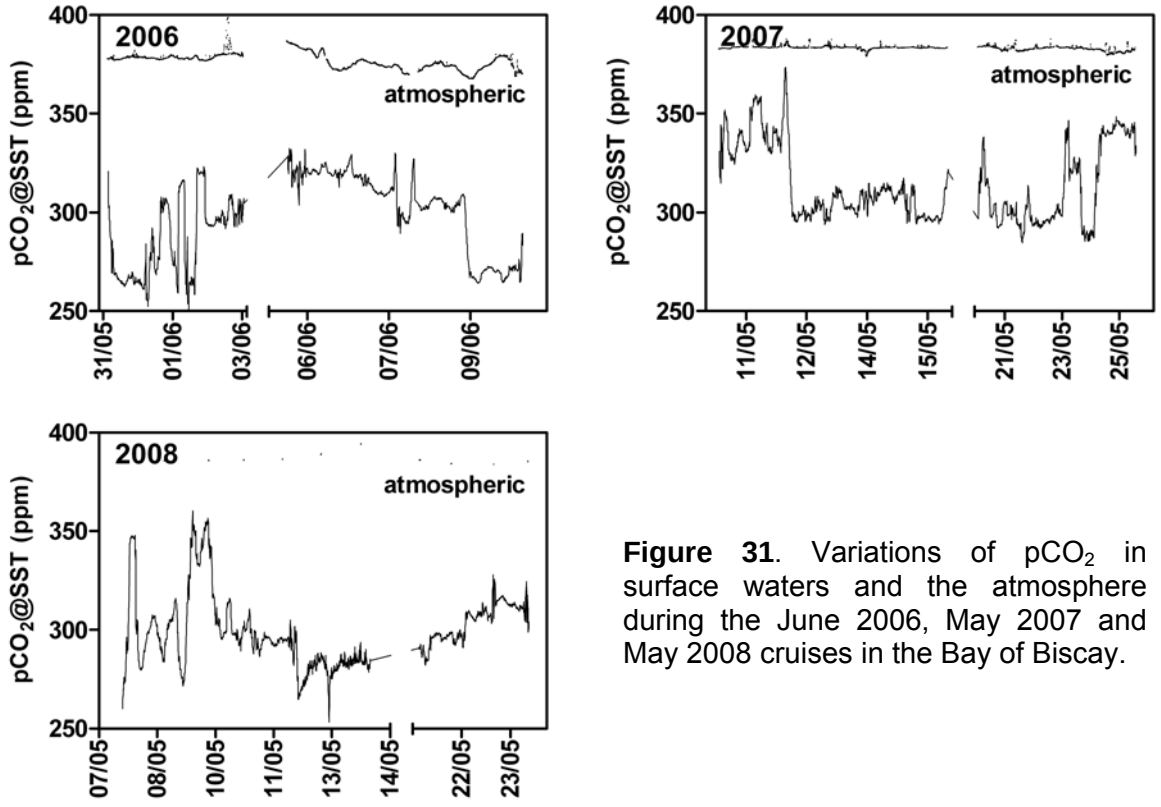


**Figure 31**. Variations of $pCO_2$ in surface waters and the atmosphere during the June 2006, May 2007 and May 2008 cruises in the Bay of Biscay.

TA data in surface waters (Figure 32) showed a systematic non-conservative behaviour during the 3 cruises as a function of salinity compared to the climatological TA-salinity relationship reported for North Atlantic Ocean surface waters (Millero et al., 1998). This indicates the drawdown of TA by calcification consistent with the presence of coccolithophorids in the area during the 3 cruises as indicated by the high reflectance patches from remotely sensed images (Figure 8), HPLC measurements (Figure 13), SEM images (Figure 30), and $^{14}C$ CAL measurements (Table 3).

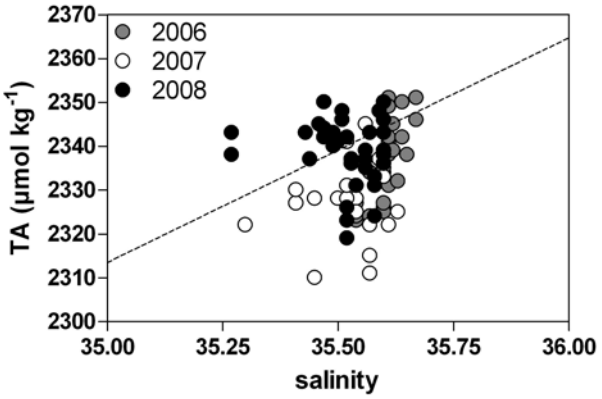


**Figure 32**. TA in the top 20 m versus salinity during the June 2006, May 2007 and May 2008 cruises in the Bay of Biscay. The dotted line corresponds to the climatological TA-salinity relationship given by Millero et al. (1998) for the North Atlantic Ocean surface waters.

### *4.1.6.2 DIC dynamics during the phytoplankton bloom development appraised by the degree of stratification*

Stratification is one of the most important variables controlling the intensity of primary production and the succession of phytoplankton communities (e.g. Margalef, 1997). The increase of stratification leads to the decrease of vertical inputs of inorganic nutrients but enhances light conditions for phytoplankton development, imposing a succession of phytoplankton communities with variable light and inorganic nutrient requirements. Variables were plotted as a function of the degree of stratification as a way of reconstructing the bloom sequence and succession of the mixed phytoplankton community (Figure 33). The degree of stratification was computed as the difference between density at 100m depth and 10m (or 3m) depth.

The trends of the variables as a function of the degree of stratification are remarkably consistent, considering that data from 3 cruises carried out in different years are compiled together. The increase of % $O_2$ saturation, and decrease of $PO_4$ are consistent with organic carbon production during the bloom development. The decrease of the TA anomaly is consistent with $CaCO_3$ production during the bloom development. The highest TA anomaly observed up to 32 µmol $kg^{-1}$ is comparable with maximum values of 28 µmol $kg^{-1}$ reported by Holligan et al. (1993) in the North Atlantic, and of 35 µmol $kg^{-1}$ reported by Bates et al. (1996) in the Sargasso Sea, but

lower than the value of 82 µmol $kg^{-1}$ reported by Murata and Takizawa (2002) in the Bering Sea. Both $pCO_2$@13°C and $pCO_2$@SST show a decreasing trend with stratification indicative that the net effect on $pCO_2$ of organic carbon production dominates over the net effect of calcification. The decreasing trend with stratification of $pCO_2$@SST shows more scatter than the one of $pCO_2$@13°C due to the increase of SST with stratification. It should be noted that changes of these variables as a function of stratification degree correspond to a cumulative signal of biological activity, and these trends do not necessarily indicate an increase of biological rates with stratification (see hereafter).

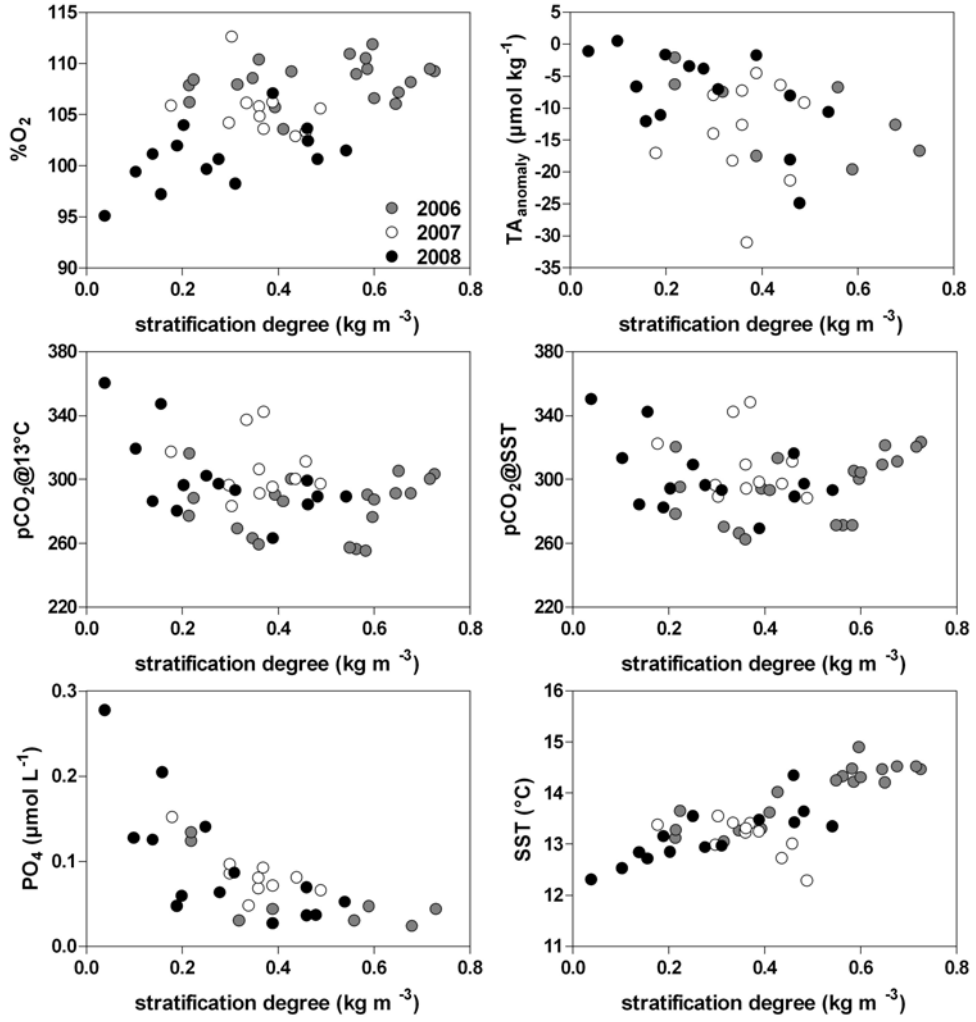


**Figure 33.** Average values in the top 20m of %O2, TA anomaly and PO4, of pCO2@13°C and pCO2@SST and SST as a function of the degree of stratification, during the June 2006, May 2007 and May 2008 cruises in the Bay of Biscay.

The cumulated impact of net community production (NCP), of calcification (NCC), and of SST change on DIC and $pCO_2$ were computed as described in §3.5. The cumulated impact of NCP on DIC was higher ($\Delta DIC_{org}$ up to -60 µmol $kg^{-1}$) than the

impact of calcification ($\Delta DIC_{inorg}$ up to -20 µmol $kg^{-1}$) (Figure 34). The cumulated impact of NCP on $pCO_2$ was higher ($\Delta pCO_{2org}$ up to -100 ppm) than the impact of calcification ($\Delta pCO_{2inorg}$ up to +20 ppm), the latter lower than the increase due to SST change ($\Delta pCO_{2SST}$ up to +60 ppm).

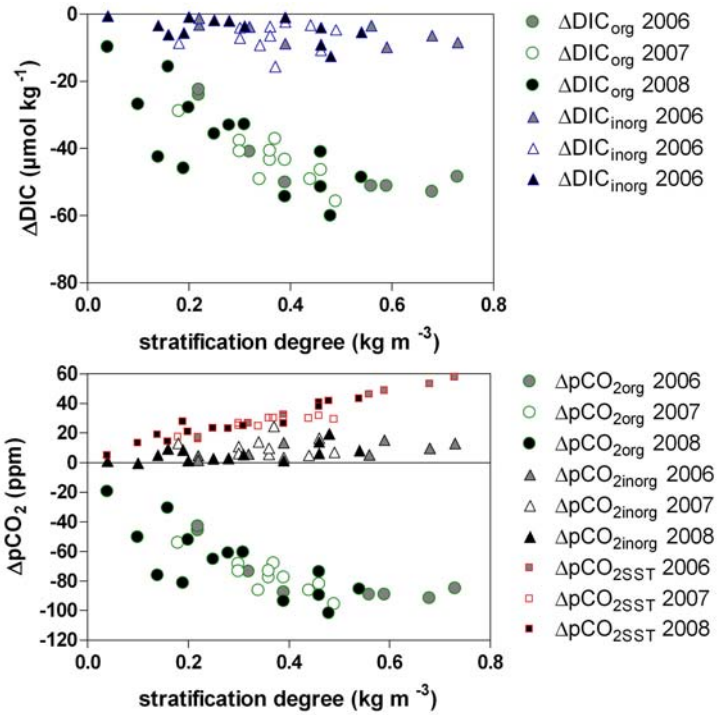


**Figure 34.** Trends of $\Delta DIC_{org}$ , $\Delta DIC_{inorg}$ , $\Delta pCO_{2org}$, $\Delta pCO_{2org}$ and $\Delta pCO_{2SST}$ as a function of the degree of stratification, during the June 2006, May 2007 and May 2008 cruises in the Bay of Biscay.

The $\Delta DIC_{inorg}$:$\Delta DIC_{org}$ ratio increased with stratification (Figure 35), in agreement with the life cycle of coccolitophorids. As the water mass stratifies and nutrients become exhausted, coccolithophorids shift from the organic carbon production and growth phase to the stationary calcification phase. $\Delta DIC_{inorg}$:$\Delta DIC_{org}$ and the ratio of $^{14}C$ calcification to $^{14}C$ primary production ($^{14}C$ CAL:$^{14}C$ PP) are not directly comparable because the ΔDIC signals correspond to the cumulated impact of biological activity on carbonate chemistry, while $^{14}C$ data are instantaneous rate measurements. Furthermore, $\Delta DIC_{org}$ corresponds to a cumulative effect of NCP while $^{14}C$ PP is a measure of primary production alone. Also the $^{14}C$ PP provides an estimate of particulate primary production, although there is evidence (see below) that dissolved primary production could be significant in the studied ecosystem. Yet, the $\Delta DIC_{inorg}$:$\Delta DIC_{org}$ and $^{14}C$ CAL:$^{14}C$ PP compare relatively well, as all $\Delta DIC_{inorg}$:$\Delta DIC_{org}$ values and 72% of all $^{14}C$ CAL:$^{14}C$ PP ratios are below 0.5. Furthermore, computed values of $\Delta DIC_{inorg}$:$\Delta DIC_{org}$ ratios (0.00 to 0.42, on average 0.13 for the three cruises) are in relatively good agreement with CAL:PP values

reported during several studies in the North Atlantic Ocean: 0.14-0.19 in the northeast North Atlantic Ocean in June 1991 (Fernández et al. 1993), 0.03-0.18 in the northern North Sea in July 1993 (Van der Wal et al. 1995), 0.14-0.16 in the northern North Sea in July 1994 (Marañon and González 1997), 0.03-0.18 in the northern North Sea June 1999 (Rees et al., 2002), 0.02-0.31 in the northern Bay of Biscay in June 2004 (Harlay et al., submitted).

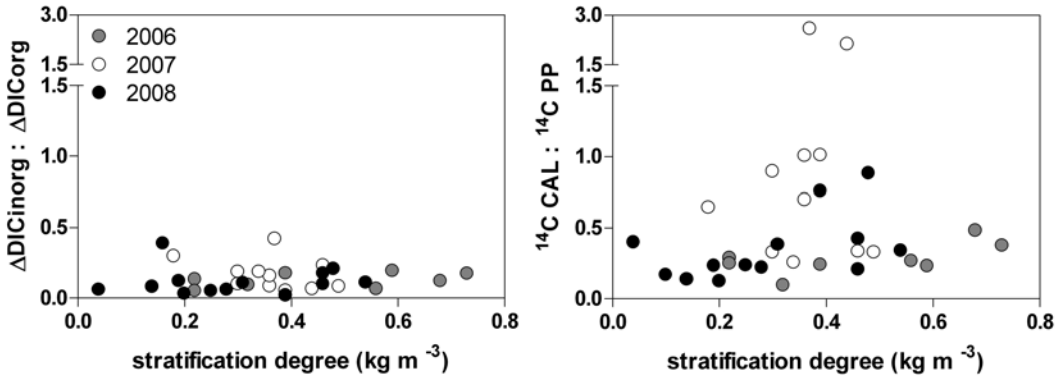


**Figure 35.** Trends of $\Delta DIC_{inorg}$:$\Delta DIC_{org}$ , and $^{14}C$ CAL:$^{14}C$ PP as a function of the degree of stratification, during the June 2006, May 2007 and May 2008 cruises in the Bay of Biscay.

The comparison of computed changes of DIC and $pCO_2$ ($\Delta DIC_{computed}$ and $\Delta pCO_{2computed}$) are remarkably consistent with the observed changes of DIC and $pCO_2$ ($\Delta DIC_{observed}$ and $\Delta pCO_{2observed}$), considering that these quantities were evaluated independently (Figure 36). Yet, $\Delta DIC_{observed}$ and $\Delta pCO_{2observed}$ values are almost always systematically lower than the $\Delta DIC_{computed}$ and $\Delta pCO_{2computed}$ values. This would indicate that additional processes affect DIC dynamics in surface waters that were not accounted for in the computations. Two processes could explain this discrepancy. We assumed that phosphorus was assimilated by phytoplankton only as $PO_4$, however coccolithophorids can rely on dissolved organic phosphorus (DOP) to meet part of their phosphorus requirements (Egge and Heimdal, 1994; Lessard et al., 2005). Second, in low nutrient environments a significant amount of carbon fixed by photosynthesis is released as DOC. This dissolved primary production cannot be accounted for in our computations since it is independent of nutrient assimilation (carbon overconsumption, e.g. Anderson and Sarmiento, 1994). Indeed, a significant dissolved primary production in the study area is consistent with the high TEP values reported during the cruises (Harlay et al., 2009), and with results of laboratory culture experiements showing increasing ratios of POC:PN after nutrient exhaustion (Figure 56e). Both explanations are consistent with the fact that the differences between observed and computed ΔDIC and $\Delta pCO_2$ increase towards the most negative values ΔDIC and $\Delta pCO_2$ corresponding to the most stratified and $PO_4$ depleted conditions.

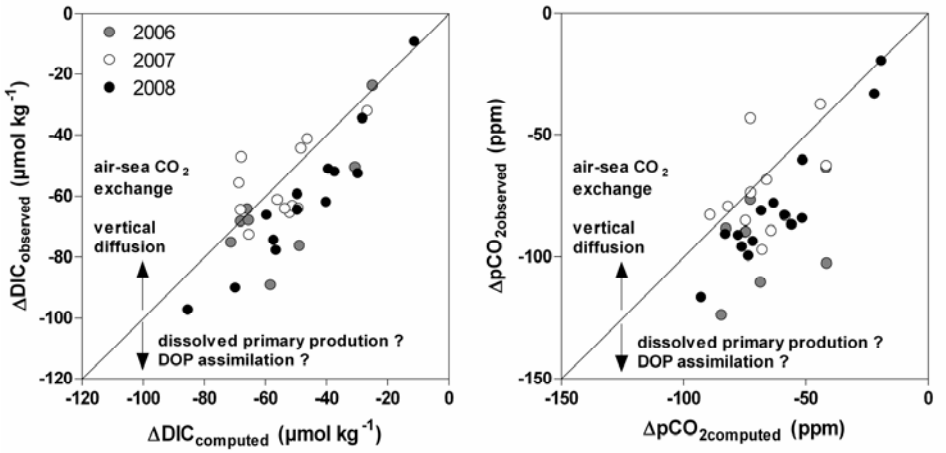


**Figure 36.** $\Delta DIC_{observed}$ versus $\Delta DIC_{computed}$ and $\Delta pCO_{2observed}$ versus $\Delta pCO_{2computed}$ during the June 2006, May 2007 and May 2008 cruises in the Bay of Biscay.

### *4.1.6.3 Rates of pelagic respiration and community trophic status during the bloom development*

Pelagic community respiration (PCR) increased with increasing stratification in parallel to an increase of bacterial production (BP) (Figure 37). The $^{14}C$ PP:PCR tended to decrease with increasing stratification showing an evolution from net autotrophic towards a net heterotrophic community status ($^{14}C$ PP:PCR > 1 corresponds to net community autotrophy; $^{14}C$ PP:PCR < 1 corresponds to net community heterotrophy). These trends are consistent with the overall evolution of the bloom as nutrients become increasingly exhausted with stratifying (aging) water masses.

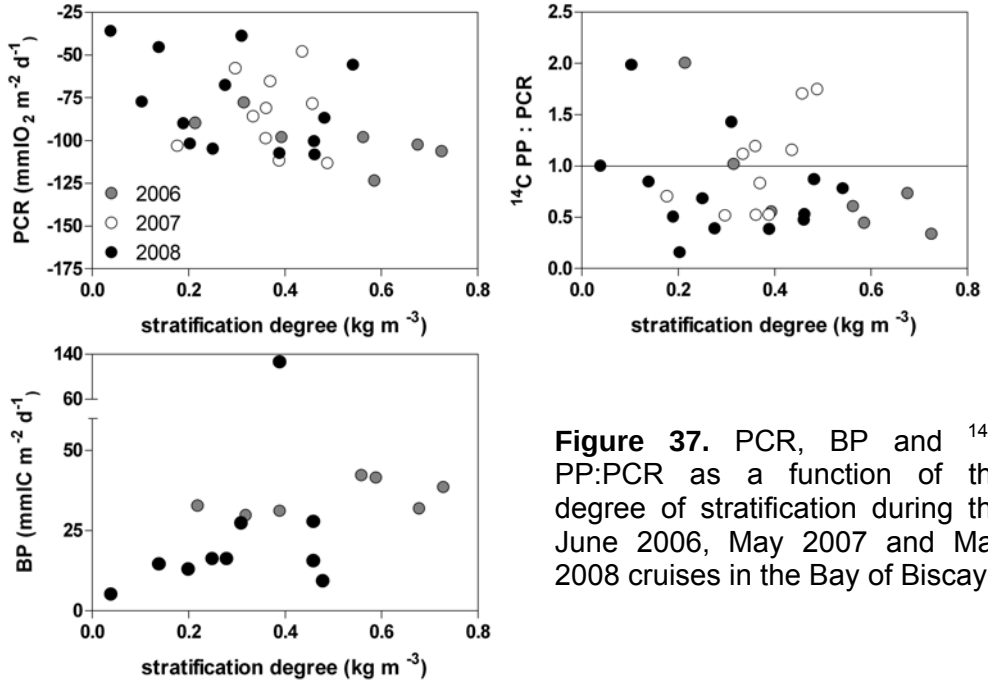


**Figure 37.** PCR, BP and $^{14}C$ PP:PCR as a function of the degree of stratification during the June 2006, May 2007 and May 2008 cruises in the Bay of Biscay.

### *4.1.6.4 Impact on air-sea $CO_2$ fluxes of calcification*

We computed the air-sea $CO_2$ fluxes on a station by station basis (Table 6). Air-sea $CO_2$ fluxes in June 2006, May 2007, and May 2008, averaged, respectively, -11.5, -19.4 and -7.9 mmol C $m^{-2}$ $d^{-1}$ (Table 6), in agreement with air-sea $CO_2$ flux values previously reported in the area at this time of the year (Frankignoulle and Borges 2001; Borges et al. 2006; Harlay et al. submitted). We evaluated the impact of calcification on air-sea $CO_2$ fluxes by re-computing the air-sea $CO_2$ fluxes from $\Delta pCO_{2air\text{-}sea}$ from which $\Delta pCO_{2inorg}$ was removed. The impact of calcification in decreasing the $CO_2$ sink in the study area ranges between 0 and 70% depending on the station, but on average it is small, ~12%. This would imply that the potential feedback on increasing atmospheric $CO_2$ of the projected decrease of pelagic calcification (Gehlen et al., 2007) due to thermodynamic $CO_2$ "production" from calcification is probably minor.

**Table 6.** Air-sea $CO_2$ flux (F) and the change of air-sea $CO_2$ flux due to $\Delta pCO_{2inorg}$ (calcification, in %).

| Cruise | Station | F (mmol $m^{-2}$ $d^{-1}$) | Change of flux due to calcification(%) |
|---|---|---|---|
| June 2006 | 1 | -15.4 | 5 |
| June 2006 | 2 | -14.1 | 5 |
| June 2006 | 5 | -8.1 | 3 |
| June 2006 | 4 | -11.9 | 16 |
| June 2006 | 8 | -7.7 | 24 |
| June 2006 | 7 | -9.4 | 15 |
| June 2006 | 4bis | -10.2 | 21 |
| June 2006 | 1bis | -15.2 | 5 |
| May 2007 | 2 | -9.1 | 70 |
| May 2007 | 5 | -22.7 | 12 |
| May 2007 | 8 | -19.4 | 7 |
| May 2007 | 9 | -18.7 | 23 |
| May 2007 | 10 | -22.6 | 6 |
| May 2007 | 11 | -24.9 | 7 |
| May 2007 | 8bis | -22.3 | 4 |
| May 2007 | 5bis | -23.2 | 11 |
| May 2007 | 4 | -15.8 | 22 |
| May 2007 | 7 | -24.5 | 6 |
| May 2007 | 2bis | -10.6 | 35 |
| May 2008 | 1 | -6.8 | 0 |
| May 2008 | 3 | -4.1 | 21 |
| May 2008 | 2 | -8.6 | 1 |
| May 2008 | 6 | -3.4 | 2 |

| Cruise | Station | F (mmol $m^{-2}$ $d^{-1}$) | Change of flux due to calcification(%) |
|---|---|---|---|
| May 2008 | 5 | -8.4 | 3 |
| May 2008 | 8 | -8.7 | 6 |
| May 2008 | 9 | -10.9 | 1 |
| May 2008 | 10 | -9.7 | 8 |
| May 2008 | 11 | -9.5 | 5 |
| May 2008 | 12 | -8.7 | 9 |
| May 2008 | 13 | -9.1 | 14 |
| May 2008 | 9bis | -8.3 | 22 |
| May 2008 | 5bis | -7.2 | 3 |
| May 2008 | 4 | -6.5 | 9 |

### *4.1.7 Benthic fluxes of oxygen, nutrients and TA*

Benthic respiration (R) rates ranged from -2 to -9 mmol $O_2$ $m^{-2}$ $d^{-1}$ (Figure 38), and were consistent with those reported by Lohse et al. (1998) at the continental shelf break at Goban Spur. They fall in the lower end of the range of those reported by Gazeau et (al. 2004) for continental shelves and estuaries in Europe (11-210 mmol $O_2$ $m^{-2}$ $d^{-1}$), and of the range of permeable sediments (10-120 mmol $O_2$ $m^{-2}$ $d^{-1}$) reported by Reimers et al. (2004) and Rusch et al. (2006). This is consistent with the fact that the study area is characterised by fine to medium sandy sediments, dominated by the 125 µm to < 500 µm fractions (not shown) with low organic matter content. Indeed, benthic Chl-a concentrations (range from 0 to 1 µg $g^{-1}$) are 10 times lower than those reported by Trimmer et al. (1999) in the Western Irish Sea in silt and clay sediments. All sediments were low in POC (ranging from 1.4 % to 4.0 %) and relatively rich in PIC (ranging from 1.3 % to 9.5 %). The comparison of the three cruises shows that overall R rates in June 2007 were less variable spatially, and were more intense during the June 2008 cruise (Figure 38).

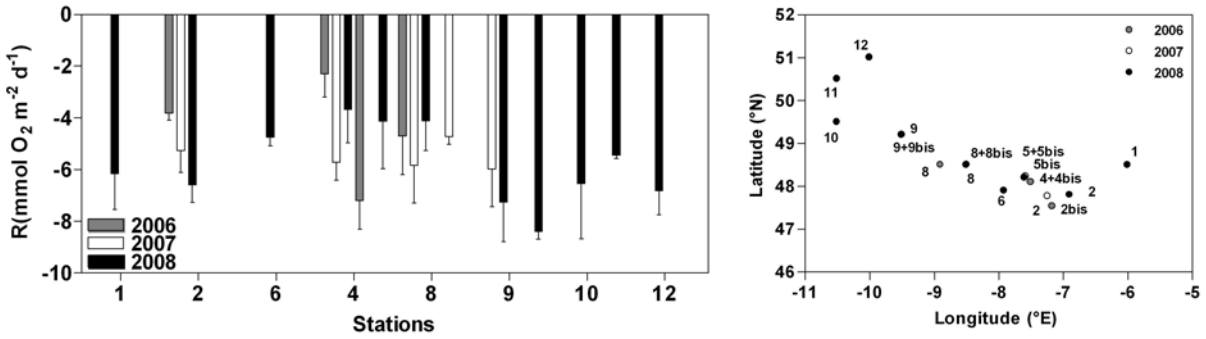


**Figure 38.** Benthic respiration rates during the June 2006, May 2007 and May 2008 cruises in the Bay of Biscay.

Benthic respiration was well correlated to the Chl-a content of the top 1 cm of the sediments, as well as to the % POC content (Figure 39). No relationship was found between R and the freshness of the organic material (represented by the Chl-a : Phaeo ratio), which suggests that there was no significant preference in fresh to "older" organic matter during remineralization. The deposition of fresh material seemed to be related to the local physics at the benthic boundary layer as indicated by the strong correlation between Chl-a in the top cm and the grain size content < 63 µm (in low turbulent regions high concentrations of fine sediments and high Chl-a were present).

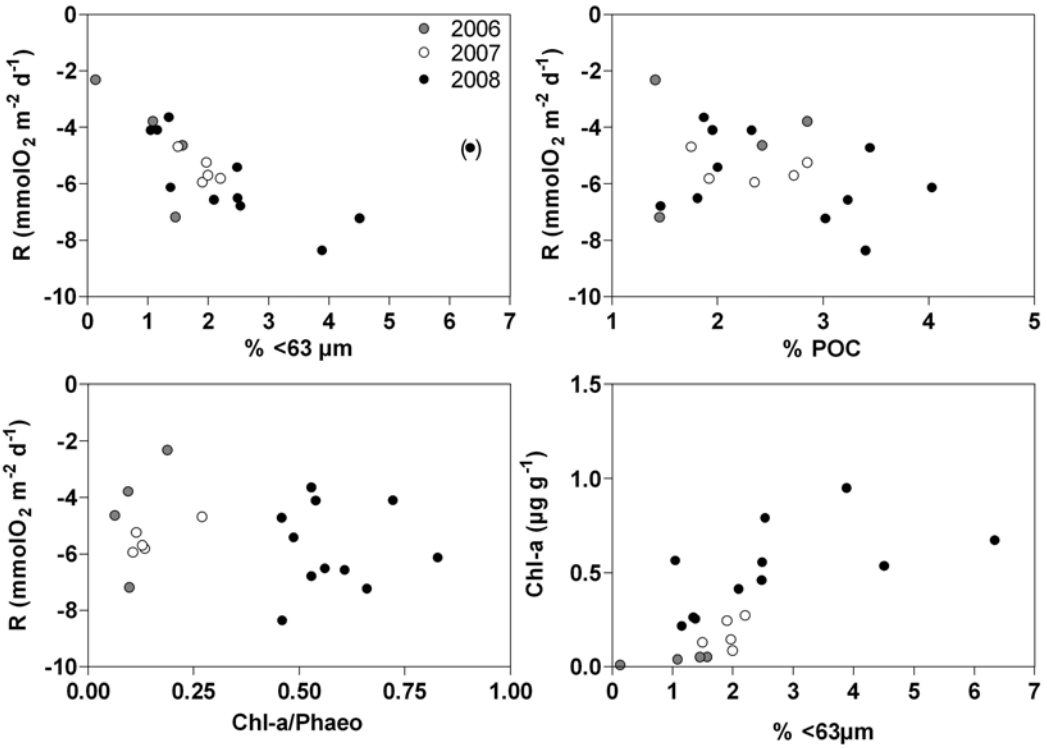


**Figure 39**. Respiration (R) versus Chl-a of the top 1 cm, the % POC content of the top 1 cm and the Chl-a:Phaeo ratio, and the Chl-a content of the top 1 cm versus the grain size content < 63 µm, for June 2006, May 2007 and May 2008 cruises in the Bay of Biscay.

At the last 3 stations of the May 2008 cruise, TEP-C was sampled in the surface of sediments. TEP-C values were as high as 29 mmolC $m^{-2}$ which corresponds to ~10% of the average pelagic integrated TEP at these 3 stations (Figure 40). TEP-C in the surface of the sediments was correlated to Chl-a and to benthic respiration. Hence, TEP-C export to the sediments and further diagenetic degradation could be a major sink for pelagic TEP in the area, which needs to be confirmed by further measurements.

Overall, a (possibly non linear) relationship between benthic production of TA (FTA) and R was observed (Figure 41a), showing a coupling between organic matter

degradation and $CaCO_3$ dissolution in the sediments (metabolic driven $CaCO_3$ dissolution) as also reported, for instance, in the US Mid-Atlantic continental slope (Jahnke and Jahnke, 2000).

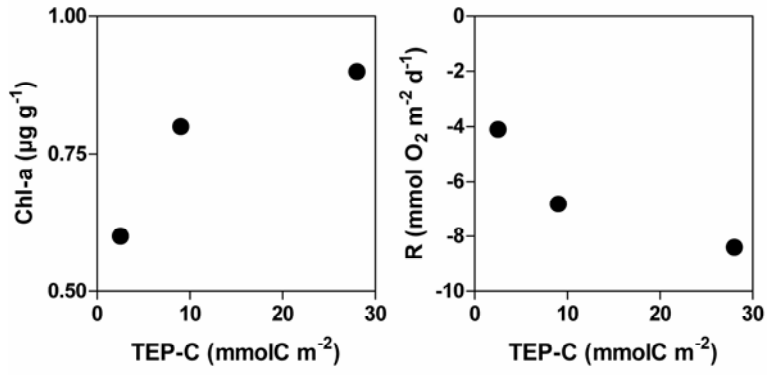


**Figure 40**. Chl-a in the top 1 cm and benthic respiration (R) versus TEP-C in surface sediments at stations 5bis, 9bis and 12 of the May 2008 cruise in the Bay of Biscay.

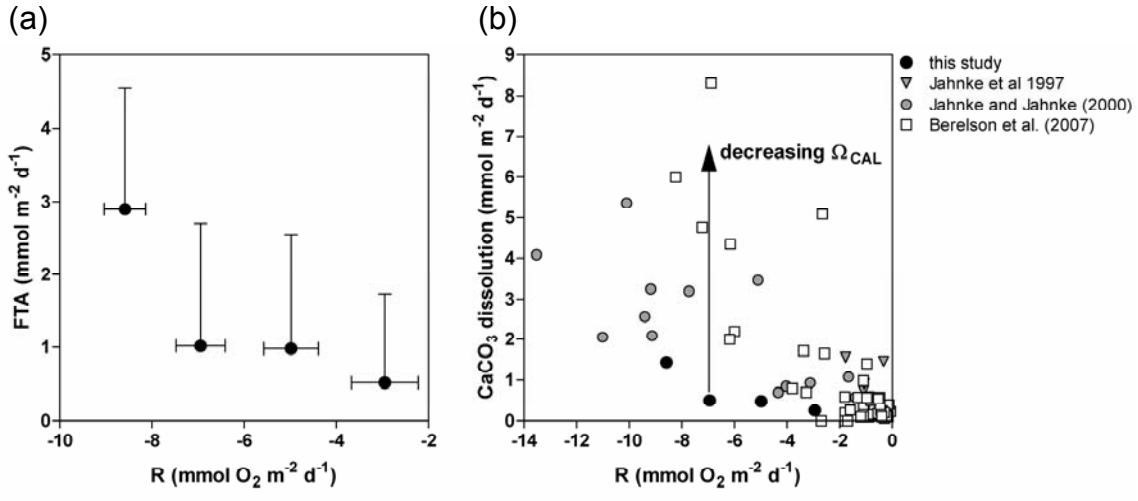


**Figure 41**. (a) Benthic flux of TA (FTA) versus benthic respiration (R) for the June 2006, May 2007 and May 2008 cruises in the Bay of Biscay. Data were bin-averaged by intervals of 2 mmol $O_2$ $m^{-2}$ $d^{-1}$ of R. (b) Benthic $CaCO_3$ dissolution (mmol $m^{-2}$ $d^{-1}$) versus R (mmol $O_2$ $m^{-2}$ $d^{-1}$) in northern Bay of Biscay (this study), in the California continental slope (Jahnke et al., 1997), in the US Mid-Atlantic continental slope (Jahnke and Jahnke, 2000), and from a compilation in deep ocean sediments (Berelson et al., 2007).

Figure 41b shows the comparison of benthic dissolution of $CaCO_3$ rates as a function of R in the northern Bay of Biscay, with data from the California continental slope (Jahnke et al., 1997), the US Mid-Atlantic continental slope (Jahnke and Jahnke, 2000), and from a compilation in deep sea sediments (Berelson et al., 2007). At a given R, benthic dissolution of $CaCO_3$ rates in the northern Bay of Biscay are systematically lower than those reported in the US Mid-Atlantic continental slope, themselves lower than those in deep ocean sediments. The saturation state of calcite ($\Omega_{CAL}$) values in the bottom water overlying the sediments in the northern Bay of Biscay averaged for the three cruise 3.5±0.3, ranged between 2.5 and 1.4 at the

sampling depths of the California continental slope (extracted from the Global Ocean Data Analysis Project (Key et al., 2004)), and 1.3±0.9 at the stations of the data compilation given by Berelson et al. (2007). This suggests that trend of the much lower benthic dissolution of $CaCO_3$ rates in the continental shelf sediments of the northern Bay of Biscay at similar R values than in the US Mid-Atlantic continental slope, themselves lower than those in deep ocean sediments, is related to decreasing $\Omega_{CAL}$ of the bottom waters overlying the sediments that facilitates $CaCO_3$ dissolution, in general agreement with the findings of the modelling study of Hales (2003). Rates of $CaCO_3$ dissolution averaged for the three cruises ~0.5±0.5 mmol $m^{-2}$ $d^{-1}$ which represents ~1% of the pelagic calcification rates due to coccolithophores measured during the cruises of ~34±32 mmol $m^{-2}$ $d^{-1}$. Considering also that visual inspection of sediments indicates that most of the PIC was related to bivalve shells (most probably driving the bulk of benthic $CaCO_3$ dissolution), this implies a decoupling of calcification by coccolithophores and the dissolution in the sediments of $CaCO_3$. Hence, PIC produced by coccolithophores is either stored in the sediments or exported out of the system, but does not seem to be significantly dissolved in the sediments.

## 4.2 Unraveling the link between the bacterial community, TEP dynamics, DMS cycling, and carbon export during coccolithophrid calcification

### *4.2.1 Temporal and spatial distribution of TEP and their polysaccharide precursors during coccolithophorid blooms*

Carbohydrates comprise a large fraction (~30 %) of organic matter in the ocean (Pakulski and Benner, 1994). The production of polysaccharides in seawater is mainly linked to autotrophic processes. Polysaccharides are included in structural cell components of phytoplankton and serve for energy storage in plankton species. Through exudation from phyto- and bacterioplankton cells, herbivorous grazing, microbial degradation and lysis of cells, polysaccharides are released into seawater (Carlson, 2002; Benner, 2002).

The determination of polysaccharide composition of samples collected in the Bay of Biscay 2006-2008 was carried out by the use of high performance anion exchange chromatography (HPAEC) coupled with pulsed amperometric detection (PAD).

The composition of dissolved polysaccharides in the Bay of Biscay sampled during 2006 was dominated by neutral sugars (60 - 80%) followed by acidic sugars (up to 40%). The relative proportion of amino sugars was low (<3%) at all stations. The depth profile of neutral sugars deviated from those of acidic and amino sugars, as the relative contribution of acidic sugars generally increased below the photic zone. This

points towards differences in biogeochemical cycling between the different classes of sugars.

In the year of 2006, concentrations of dissolved polysaccharides ranged from 700 to 2000 nM and decreased with depth at all stations (Figures 42-44).

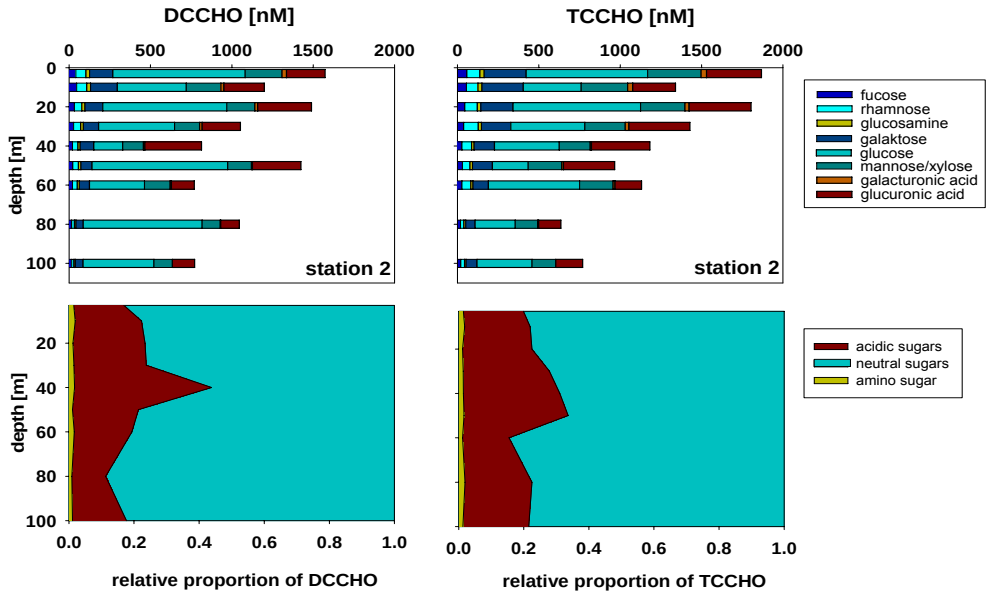


**Figure 42**. Concentration and composition of dissolved polysaccharides (DCCHO) (upper panel) and relative proportions of neutral, amino and acidic sugars (lower panel) in the Bay of Biscay (station 2, 2006).

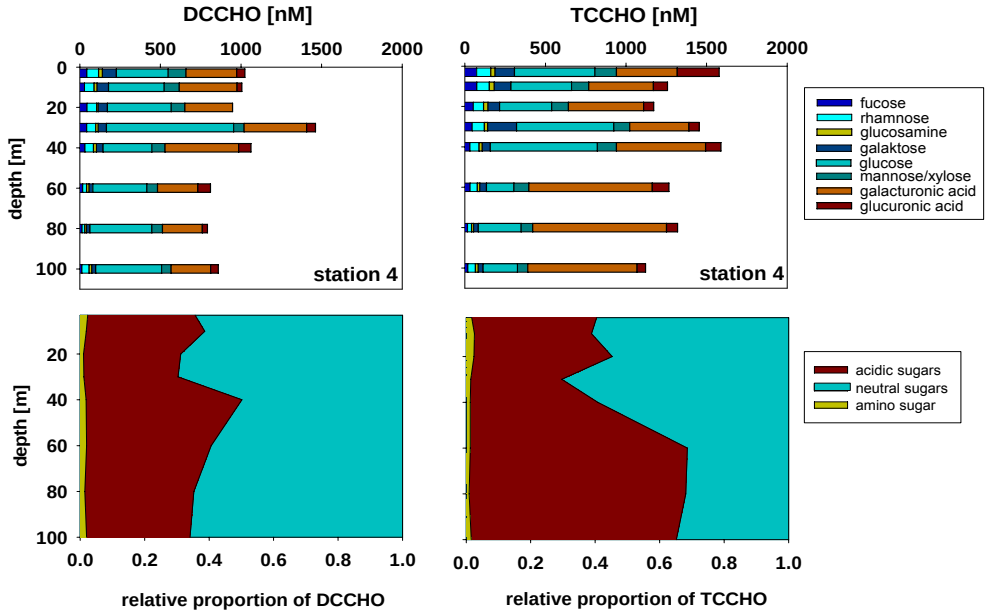


**Figure 43**. Concentration and composition of dissolved polysaccharides (DCCHO) (upper panel) and relative proportions of neutral, amino and acidic sugars (lower panel) in the Bay of Biscay (station 4, 2006).

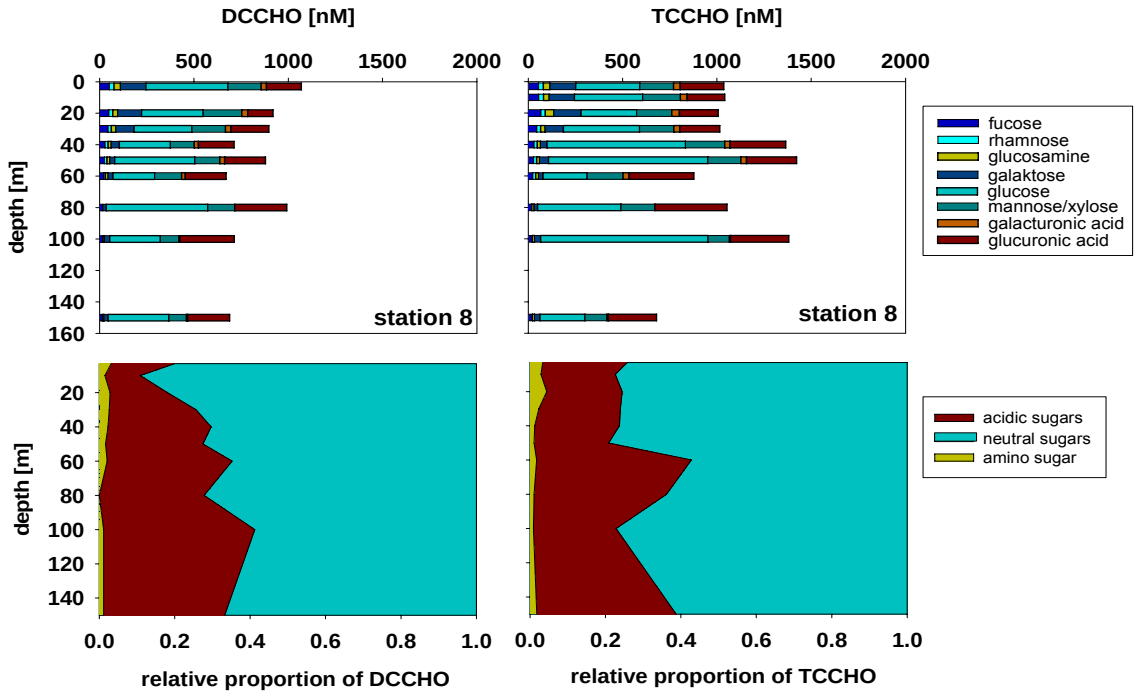


**Figure 44**. Concentration and composition of dissolved polysaccharides (DCCHO) (upper panel) and relative proportions of neutral, amino and acidic sugars (lower panel in the Bay of Biscay (station 8, 2006).

Comparing data from different depths and stations revealed that TEP concentration increased exponentially with dissolved acidic sugar concentration, suggesting that dissolved acidic sugars are an important source for TEP production during coccolithophorid blooms in the Bay of Biscay (Figure 45).

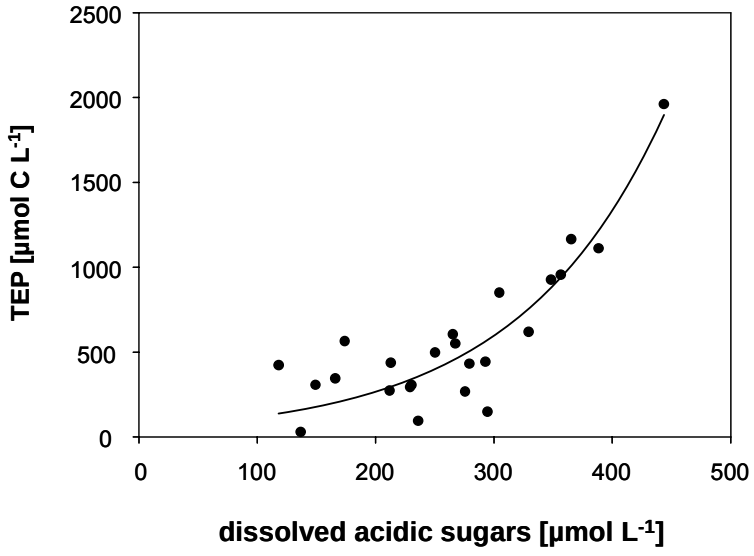


**Figure 45**. TEP concentration as a function of dissolved acidic sugars concentration in the Bay of Biscay ($r^2 = 0.81$, $p < 0.001$).

TEP size distribution was determined by a highly resolved sampling procedure during the cruises in the Bay of Biscay in 2006-2008 (Figures 46-47). For 2006 cruise, all TEP samples have been examined using both microscopy (and digital image analyses) and colorimetry and results are the object of an article (Harlay et al., 2009).

Results revealed that the concentration and vertical distribution of TEP particles in the years 2006 and 2007 were similar, ranging from 0.14 to 27.2*$10^6$ particles $L^{-1}$. Most depth profiles show maximum abundances at the surface or in subsurface depths of 10 to 40 m (Figures 46-47). The larger particles ranged between 20 and 30 µm and were abundant in the upper part of the water column. The concentration of large particles strongly decreased with depth to become insignificant below 80 m. The coincidence of large and small particles in the first 30 meters can be considered as the result of the assembly of lager particles from smaller ones by aggregation (Harlay et al., 2009).

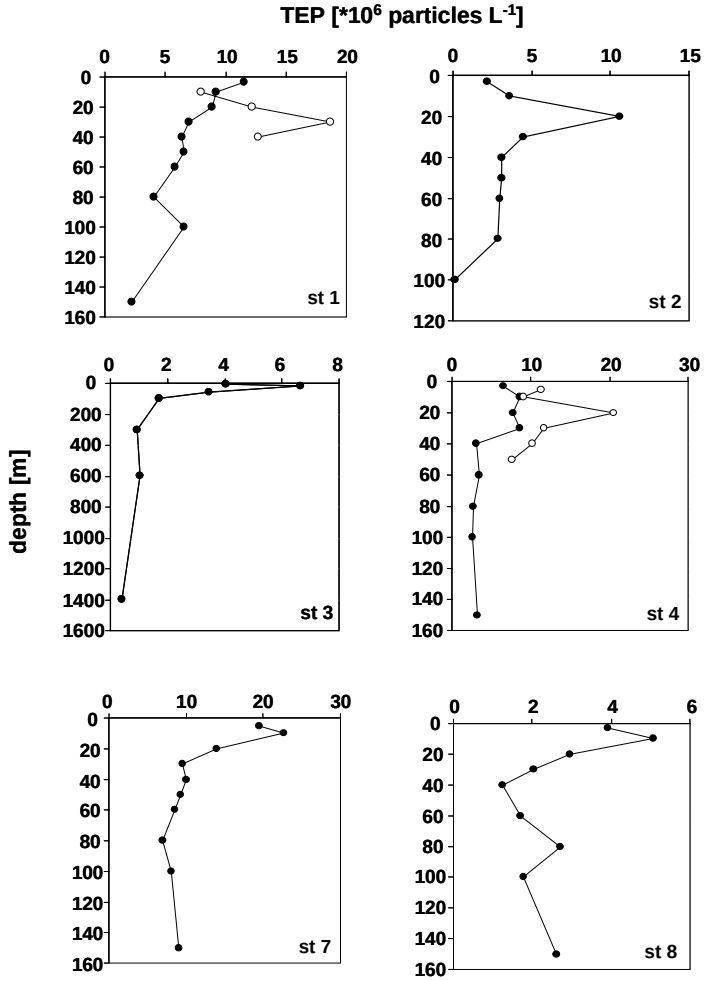


**Figure 46.** Vertical distribution of transparent exopolymer particles (TEP) in the Bay of Biscay 2006 as determined by microscopic analysis (stations 1 and 4: filled circles, first cruise lag; open circles, second cruise lag).

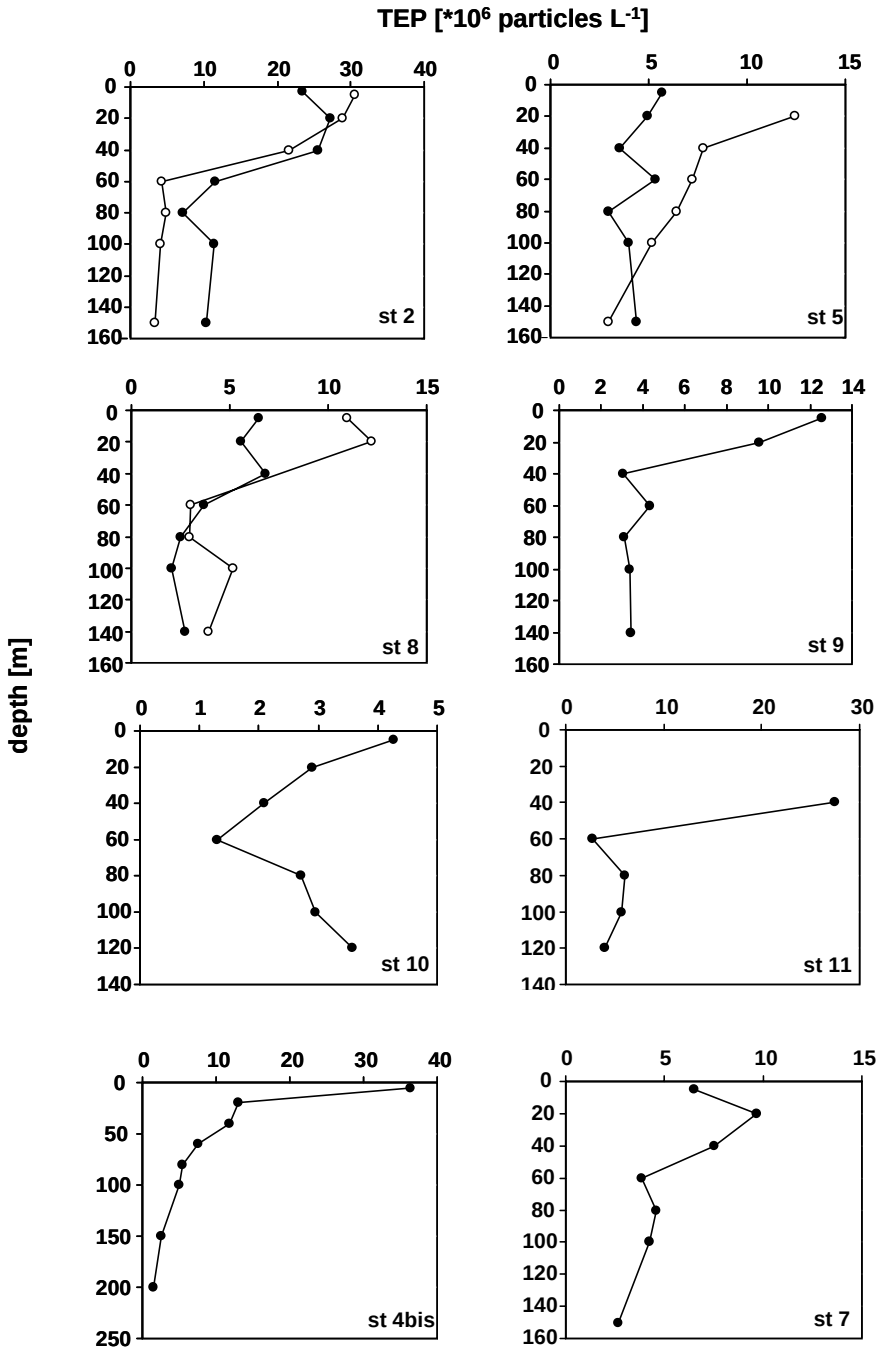


**Figure 47.** Vertical distribution of transparent exopolymer particles (TEP) in the Bay of Biscay 2007 as determined by microscopic analysis (stations 2 and 5: filled circles, first cruise lag; open circles, second cruise lag).

Vertical distributions of $TEP_{color}$ determined by colorimetry are shown in Figures 48 and 49 for the May 2007 and the May 2008 cruises, respectively. The profiles of TEP-$C_{color}$ estimated according to the method described in §3.3.2.7 are also indicated.

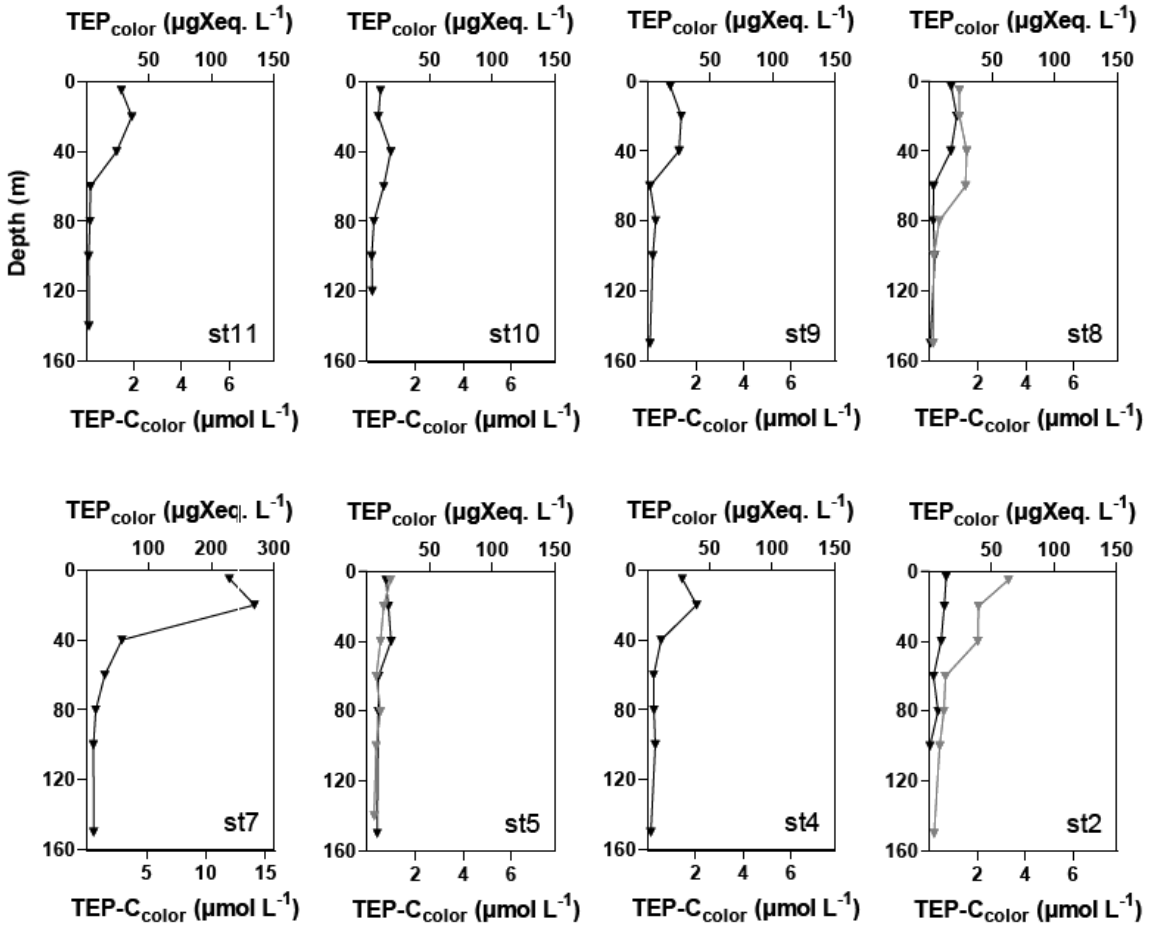


**Figure 48.** Vertical profiles of $TEP_{color}$ concentrations (upper axe) and estimated TEP-$C_{color}$ (lower axe) during the May 2007 cruise. Grey symbols represent values at the revisited stations 8b, 5b and 2b. Note that the scale is different for station 7.

For the 2007 campaign, surface $TEP_{color}$ concentrations ranged between a minimum of 10.54±0.36 µg X eq. $L^{-1}$ (average±SD of triplicate measurements) at station 10 and a maximum of 228.8±106.5 µg X eq. $L^{-1}$ at station 7 (Figure 48). Pigment data show that phytoplankton at station 7 was dominated by coccolithophores (Figure 13b). Higher concentrations were found in surface waters and decrease with depth. From 60 or 80 m, $TEP_{color}$ reached a constant value. Along the continental slope, we observed concentrations close to 20 µg X eq. $L^{-1}$ in surface waters. No difference between the two legs were observed at station 8 and 5 while at station 2, the concentrations increased up to 60 µg X eq. $L^{-1}$ 14 days later. Surface TEP-$C_{color}$ ranged between 0.55 (station 10) to 12.01 (station 7) µmol C $L^{-1}$ (Figure 48).

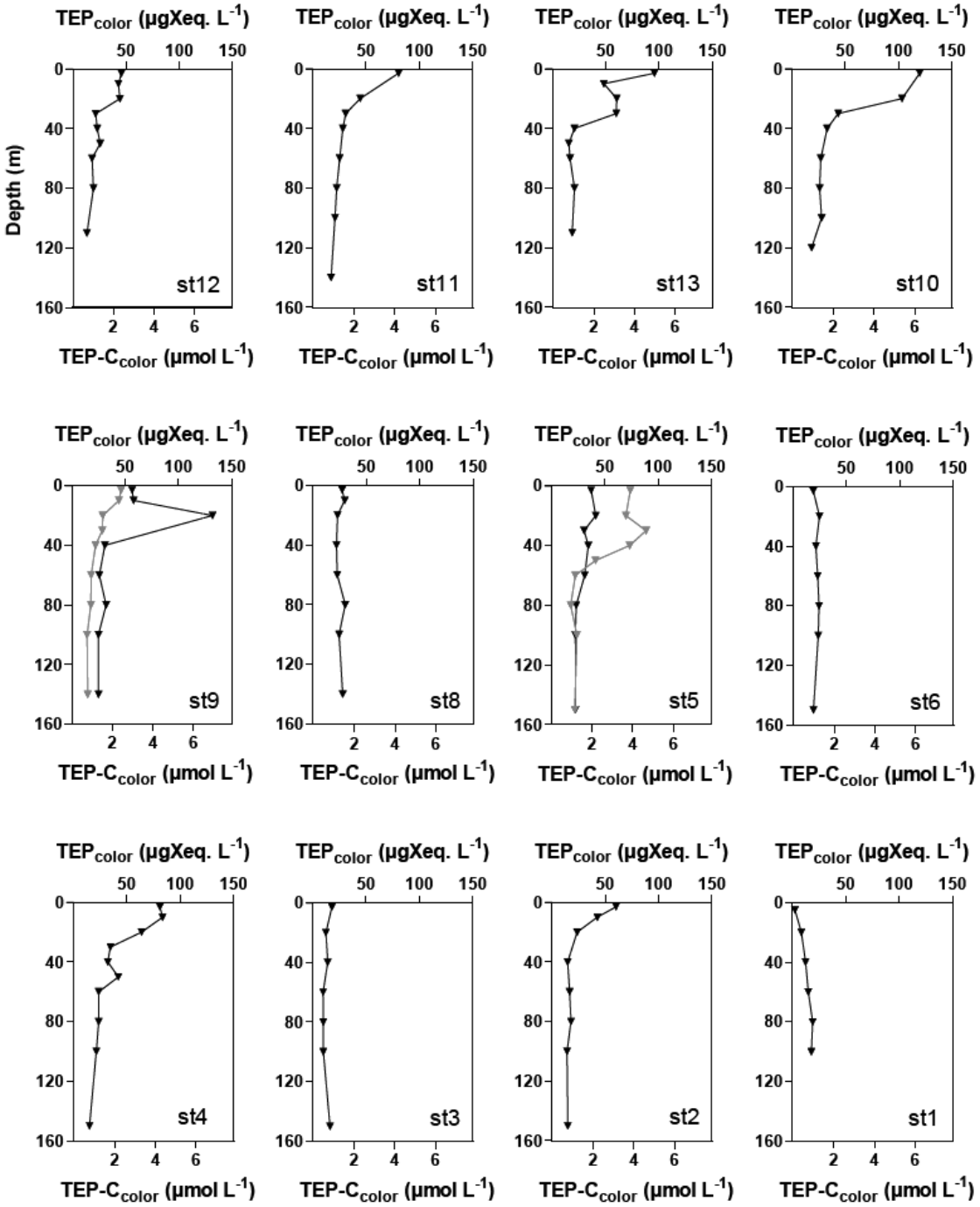


**Figure 49**. Vertical profiles of $TEP_{color}$ concentrations (upper axe) and estimated TEP-$C_{color}$ (lower axe) during the May 2008 cruise. Grey symbols represent values at the revisited stations 9b and 5b.

For the 2008 cruise, except at station 1, $TEP_{color}$ concentrations were higher in surface waters and presented stable value at depth (Figure 49). Concentrations ranged between 17.9 (station 3) to 120 (station 10) µg X eq. $L^{-1}$ at surface while from 40 or 60 m, they presented concentrations close to 20 µg X eq. $L^{-1}$. Stations 8, 6 and

3 presented a stable concentration close to 20 µg X eq. $L^{-1}$ along the entire water column. An increase in TEP surface concentrations was observed at the revisited station 5b (37.1 to 73.7 µg X eq. $L^{-1}$) whereas at the revisited station 9b a decrease was observed (56.6 to 46.2 µg X eq. $L^{-1}$). Surface $TEP_{color}$ concentrations were more important at stations located at Goban Spur in the HR patch (stations 9, 10, 11, 12 and 13). TEP-$C_{color}$ concentrations presented a minimum of 0.12 µmol C $L^{-1}$ at station 1 and a maximum of 6.28 µmol C $L^{-1}$ at station 10 at 3 m depth (Figure 49).

### *4.2.2 Bacteria community structure and TEP dynamics*

The interaction between the extracellular PCHO pool of *E. huxleyi* blooms and associated bacterial communities was studied by comparing the sugar composition of freshly produced, TEP-rich, extracellular PCHO in bacterised and axenic *E. huxleyi* batch cultures (collaboration with NIOO-CEME, Yerseke, The Netherlands), . The cultures were sampled during the late exponential and stationary growth phase, when extracellular carbohydrate accumulates. Of the active bacterial community (16S rRNA RT-PCR DGGE) only 3 out of the 8 phylotypes detected were prominently active. One phylotype increased its relative abundance in the PA fraction towards the end of the stationary growth phase, but overall the relative abundance of the active members of the bacterial community remained more or less stable over the 23 day sampling period. Rhamnose and galactose concentrations were significantly higher than those of xylose, fucose, mannose, glucose, and fructose (neutral sugars). Nonetheless, all showed a 4 to 9-fold increase in concentration during the stationary phase (Figure 50). High rhamnose concentrations found in HMW DOM do not agree with literature data (or with the field data, see 4.2.1) where glucose, fucose, and xylose are found to be relatively more abundant. It is as yet unclear what cause this observation. TEP probably contains several neutral aldoses in addition to the stainable acidic sugars used for its determination, as suggested by the strong positive correlation between $TEP_{color}$ concentrations and all individual neutral aldoses measured. The sugar and particle dynamics data of the bacterised cultures will be compared with those of axenic *E. huxleyi* cultures (which had to be set up again due to contamination). The first resulst indicate that $TEP_{color}$ appeared to be produced in lower amounts (or with a lower stainable acidic sugar content) in bacterised versus axenic cultures (Figure 51).

In 2010 (i.e. not part of the PEACE program) stable carbon isotope pulse-chase experiments using compound-specific (PLFA & neutral aldose) isotope analysis will focus on the carbon flows between the sugars in extracellular carbohydrates and bacterial communities in experimental *E. huxleyi* blooms.

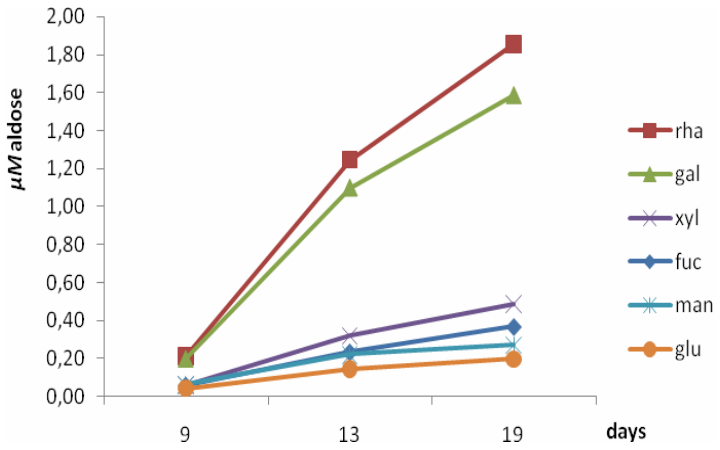


**Figure 50**. The average sugar composition of HMW DOM during the stationary growth phase.

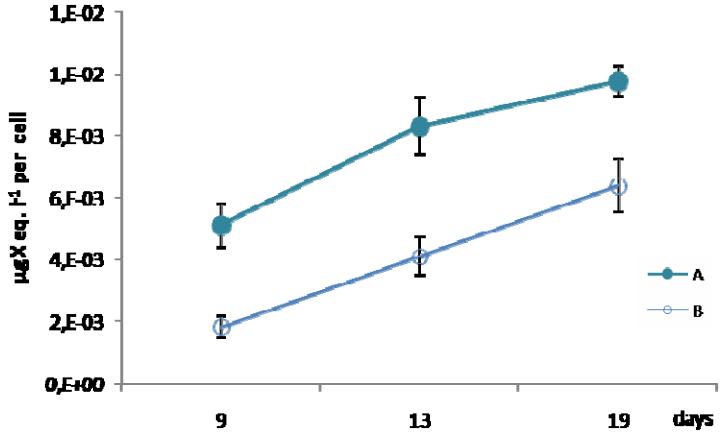


**Figure 51**. Cell abundance normalized TEP concentration in axenic (dots) and bacterised (circles) cultures.

### *4.2.3 DMSP production and its transformation in DMS*

DMSP synthesized by marine phytoplankton is the major precursor of DMS that is considered to play a significant role in the natural sulfur cycle and climate regulation (Charlson et al., 1987). In seawater, the enzymatic cleavage of DMSP produces DMS along with acrylic acid. The main DMS producers are confined to certain taxa, especially dinoflagellates and prymnesiophytes (including coccolithophores), while diatoms are minor contributors to DMS. The mechanisms for the production of DMS from DMSP is still unclear, but is thought to involve macrozooplankton grazing and bacterial conversion (see Stefels, 2000 for review).

High DMSP and DMS concentrations in the surface waters of the North Atlantic are often associated with blooms of coccolithophorids, especially *E. huxleyi* (e.g. Holligan

et al., 1993), rather than high-chlorophyll concentrations. During the June 2006 cruise, samples for DMS and DMSP were taken to investigate their stock level during a coccolithophore bloom in the northern Bay of Biscay.

The 2006 results indicate higher concentrations of DMS, $DMS_d$ and $DMSP_p$ in the upper 40 m of the water column with $DMSP_p$ being the most abundant fraction (data not shown). The highest concentration of $DMSP_p$ measured was at station 2 reaching 110 nM at 20 m where coccolithophores were identified as the dominant phytoplankton species based on HPLC pigment data (Figure 13a). For the 2007 cruise, high $DMSP_p$ also observed in the upper photic zone at stations 2 and 11 (data not shown) where the presence of high abundance of coccolithophores were also determined (Figure 13b).

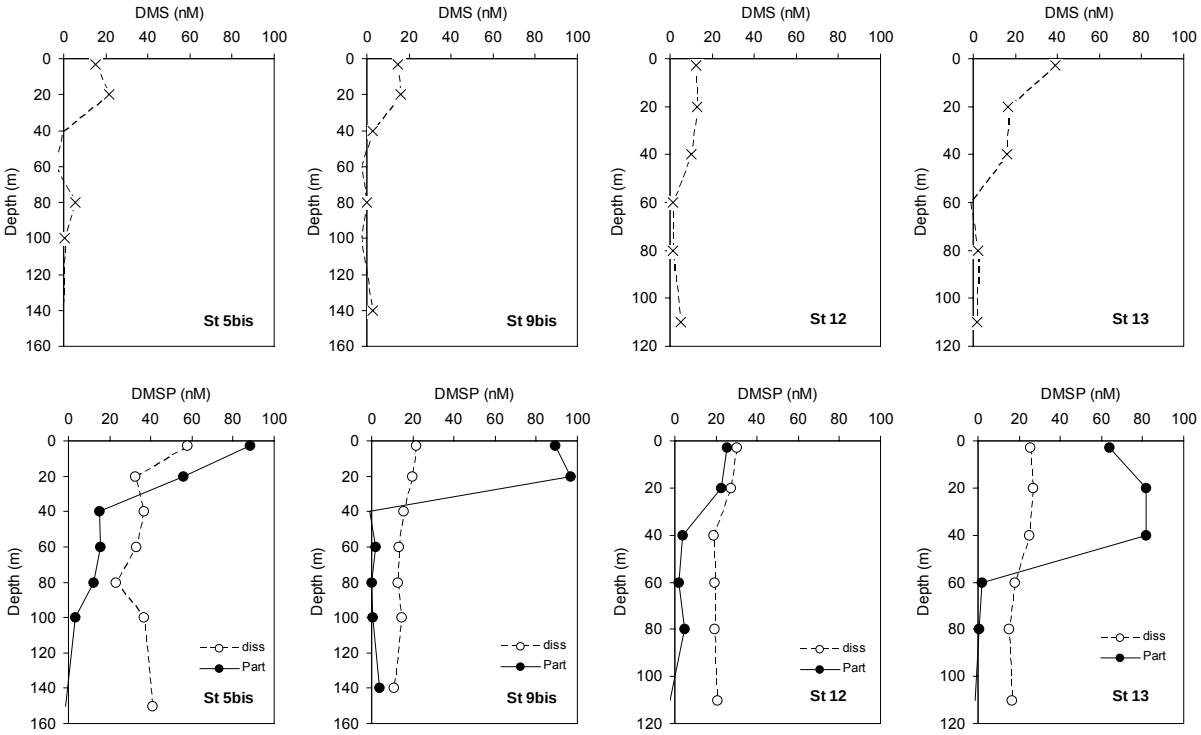


**Figure 52.** Vertical distributions of DMS, $DMS_d$ and $DMSP_p$ for May 2008 cruise in the Bay of Biscay. See Figure 6 for sampling locations.

Figure 52 shows the vertical distributions of DMS, $DMS_d$ and $DMSP_p$ at stations where coccolithophore were the dominant species (Figure 13c). High concentrations of the three species were observed in the upper 40m of the water column. Our DMS vaules agree with those reported by Uher et al. (2000) who found DMS concentrations in surface waters of the Celtic sea region in July 1995 ranging from 2.9 nM to 38.5 nM. Our $DMSP_p$ values (Figure 52) fall also within the range of those of an investigation devoted to the DMS biogeochemistry within a coccolithophore bloom in the North Sea (June 1999), where $DMSP_p$ concentrations reaching ~100 nM in the upper 40 m of the

water column were found (Archer et al., 2002). Our study confirms the important role of coccolithophores in the DMS cycling.

### *4.2.4 Influence of TEP on rain ratio PIC/POC*

#### *4.2.4.1 Distribution of POC and PIC*

Vertical profiles of concentrations of POC and PIC have been determined during the three cruises (Figures 53-55). As a general feature, POC and PIC concentrations were higher in the upper water column and decreased with depth. The organic fraction of carbon (POC) never exceeded 25 µmol $L^{-1}$ in the upper 40 m of the water column and decreased with depth. PIC were low compared to POC and presented maximum concentrations of 10 µmol $L^{-1}$ in surface waters.

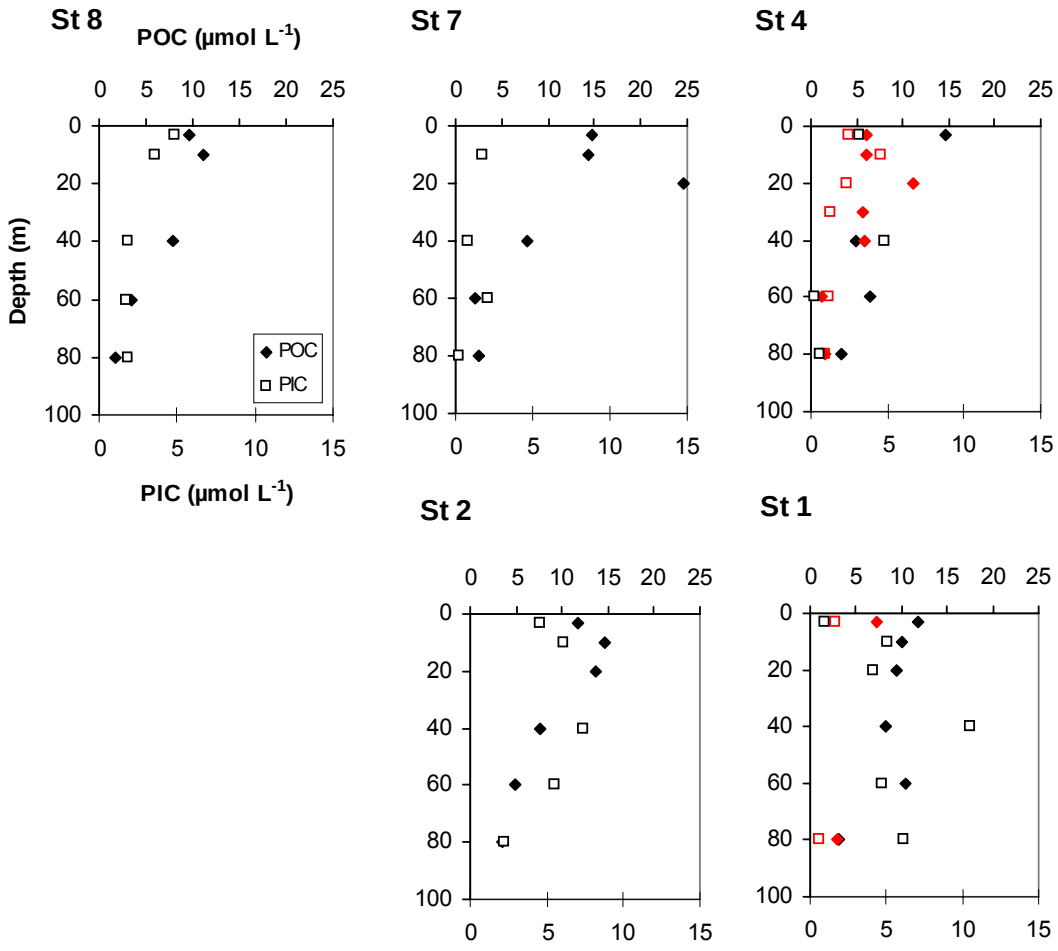


**Figure 53.** Vertical profiles of POC (black symbols) and PIC (open symbols) during the June 2006 cruise. Red symbols represent the revisited stations.

In June 2006 (Figure 53), higher PIC concentrations were found in the southern part of the survey area (stations 1 and 2) where coccolithophores were the major

contributor to the phytoplankton biomass (Figure 13a). At these stations, a low PIC:POC molar ratio (not shown) was found in surface and this ratio increased with depth to greater than 1 and even reached or exceeded 2 (stations 1, 2 and 4) below 40 m depth. The PIC:POC ratio in the photic layer ranged between 0.3 and 0.66, except at station 7 (~0.10) and in the surface sample at station 1 (~0.20).

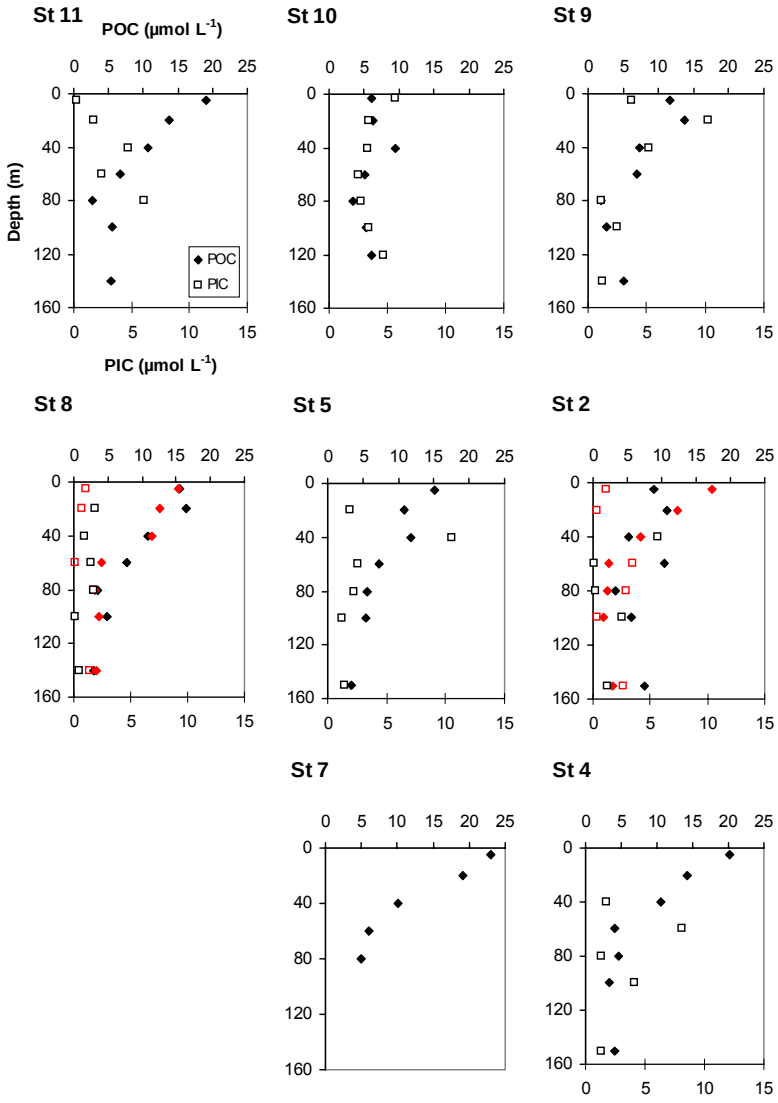


**Figure 54**. Vertical profiles of POC (black symbols) and PIC (open symbols) during the May 2007 cruise. Red symbols represent the revisited stations.

In May 2007, POC concentrations were contained between 6.1 µmol $L^{-1}$ at the surface of station 10 and 22.9 µmol $L^{-1}$ at the surface of station 7 (Figure 54, solid symbols). No increase in POC concentrations was observed at the revisited station 8b whereas an increase was observed at the revisited station 2b (8.9 to 17.3 µmol $L^{-1}$). Higher concentrations were observed at the surface of the station located along the shelf break (stations 4 and 7). The PIC concentrations ranged between 0.20 (station

11, 3 m) and 10.49 µmol $L^{-1}$ (station 5, 40 m) in the top 40 m (Figure 54, open symbols). The PIC:POC ratio (data not shown) in the top 20 m ranged between 0.01 (station 11, 5 m) and 0.93 with an average ratio of 0.27 (n = 14).

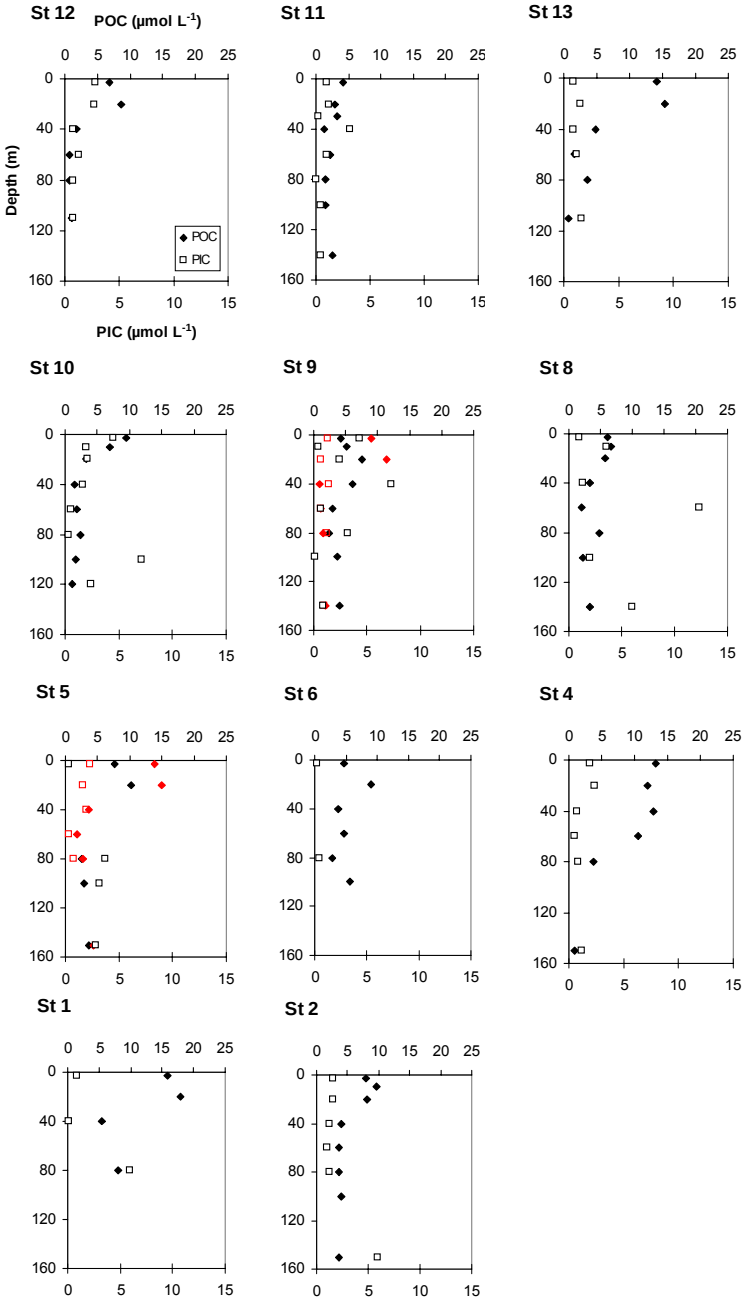


**Figure 55**. Vertical profiles of POC (black symbols) and PIC (open symbols) during the May 2008 cruise. Red symbols represent the revisited stations.

In May 2008, lower POC concentrations than during the two previous cruises were obtained and ranged in surface waters between 4.1 µmol $L^{-1}$ at station 11 and 15.8 µmol $L^{-1}$ at station 1 (Figure 55, filled symbols). PIC concentrations were also lower

than the two previous years and ranged between 0.23 µmol $L^{-1}$ at surface of the station 6 and 4.48 µmol $L^{-1}$ at surface of station 10 (Figure 55, open symbols). An increase in POC and PIC in surface waters was observed at the revisited station 5b suggesting the evolution of the bloom at this station which is accordance with the SEM images (Figure 30 a and b). The PIC:POC ratio (data not shown) in the top 20 m ranged between 0.04 (station 5, 3 m) and 0.99 (station 9, 3 m) with an average ratio of 0.28 (n = 24).

In general, POC concentrations agree with those determined during an early coccolithophorid bloom in the northern North Sea in June 1994 (16.6 to 19.1 µmol $L^{-1}$; Head et al., 1998; Marañon and González, 1997). The highest value (24.6 µmol $L^{-1}$) was close to those reported in a decaying bloom off Shetland in July 1993 (28 µmol $L^{-1}$; van der Wal et al., 1995). The PIC concentrations obtained in the northern Bay of Biscay in 2006 and 2007 were slightly higher than those reported in the northern North Sea in June 1994 (2.2 to 4.2 µmol $L^{-1}$, Head et al., 1998).

#### *4.2.4.2 Contributions of TEP-$C_{color}$ to POC*

TEP-$C_{color}$ showed the same evolution as POC concentrations. The relative contribution of the TEP-$C_{color}$ to POC was estimated for each depth by the molar ratio of TEP-$C_{color}$ to POC.

In 2007, the contribution of TEP-$C_{color}$ to POC ranged between 0.601% at 100 m depth at station 2 and 73% at 20 m depth at station 7. On average, in the photic zone, carbon content of TEP accounted for 9.3±3.2% (all stations except for stations 2b, 5b and 7, n=24) of the measured POC concentrations. Phytoplankton at stations 2b, 5b and 7 were dominated respectively by dinoflagellates, diatoms and coccolithophores. The percentage in the photic zone (from 3 m to 40 m) reached 21.9±6.9% at station 2b and 52±22% at station 7.

In 2008, the contribution of TEP-$C_{color}$ to POC accounted for 25.4±6.2% (average for stations until 20 m depth) for the stations (stations 2, 3, 4, 5, 5b, 6, 8) located near La Chapelle Bank and Meriadzek Terrace and for 26.4±8.5% for the stations (stations 12, 13 and 9b) located at Goban Spur during the second leg. The contribution of TEP-$C_{color}$ to POC in surface waters of stations 9, 10 and 11 averaged 75.2±14.1%.

Previous measurements conducted in the study area in June 2004 revealed an averaged TEP-$C_{color}$ of 2.42 ± 0.35 µmol C $L^{-1}$ (mean ± confidence interval at 95 %, n = 54) in the surface layer yielding to a contribution of TEP-$C_{color}$ to POC of 26 ± 4 % (TEP-$C_{color}$:POC, mean ± confidence interval at 95 %, n = 31) (Harlay et al., submitted). The concentrations of C and the contribution of TEP-$C_{color}$ to POC that we observed in May 2007 and May 2008 were in the same range and fall within the

range of previous studies which indicated a contribution of TEP-C to POC ranging between 17 % and 54 % (Mari, 1999).

## 4.3 Impacts of ocean acidification and climate change on coccolithophorid metabolism and TEP production

### *4.3.1 Influence of $pCO_2$/pH and temperature on calcification by selected coccolithophorid species using batch culture experiments*

#### *4.3.1.1 Development and decline of E. huxleyi during culture experiments*

As in the field, the growth of *E. huxleyi* led to an increase in Chl-a concentrations (Figure 56a) whose development during our batch cultures can be characterized in 4 phases: 1) a lag phase, 2) an exponential growth phase during which cell division occurs under nutrients-replete conditions, 3) a stationary phase where cell division is reduced and nutrients are depleted (Figure 56b) while cells continue to produce large amounts of coccoliths, followed by 4) the decline phase (De Bodt et al., 2008). TA was constant at the beginning of the experiment and decreased sharply from $d_{21}$ onwards (Figure 56c, solid triangles). Based on the TA anomaly calculation (Smith and Key 1975; Chisholm and Gattuso, 1991), the decrease in alkalinity by 1358 µmol $kg^{-1}$ at the end of the experiment corresponded to a precipitation of 67.9 mg $kg^{-1}$ of calcite. The production of calcite was detected on $d_{21}$, 5 days after the onset of *E. huxleyi*'s growth, which slowed down on $d_{43}$ (Figure 56c, open triangles). In addition, $TEP_{color}$ concentration was measured at the onset of the growth phase. It increased continuously during the course of the experiment, reaching a value of 3 219 µg X eq. $L^{-1}$ at the end of the experiment for the duplicate A (Figure 56d, solid triangles) and 7 090 µg X eq. $L^{-1}$ for the duplicate B (Figure 56d, solid triangles). During the exponential growth phase, POC concentrations were closely related to changes in PN yielding a POC:PN molar ratio of $6.42 \pm 0.06$ (n = 3), in good agreement with the Redfield ratio of 6.6 (Redfield et al., 1963). Ratios of POC:PN increased linearly after nutrient exhaustion, reaching a value of 27.6 at the end of the experiment (Figure 55e). This can be due to C overconsumption (Toggweiler, 1993), where photosynthesis still proceeds when nitrate or phosphate are depleted (Banse, 1994). A consequence for the excess of DIC uptake by phytoplankton after nutrient exhaustion is the release of dissolved organic matter (DOM) in the form of extracellular exudates (ie. polysaccharides) and the subsequent the formation of colloidal precursors that aggregate as TEP (Schartau et al., 2007). Moreover, a highly significant correlation was obtained between $TEP_{color}$ concentration and calcite concentration (Figure 56f) suggesting the occurrence of a common mechanism between the two processes. The formation of coccoliths requires the intracellular production of acidic polysaccharides. These polysaccharides accompany the

exocytosis of calcite plates and contribute to their aggregation in the coccosphere. Thus, calcification may be considered as a source of TEP precursors.

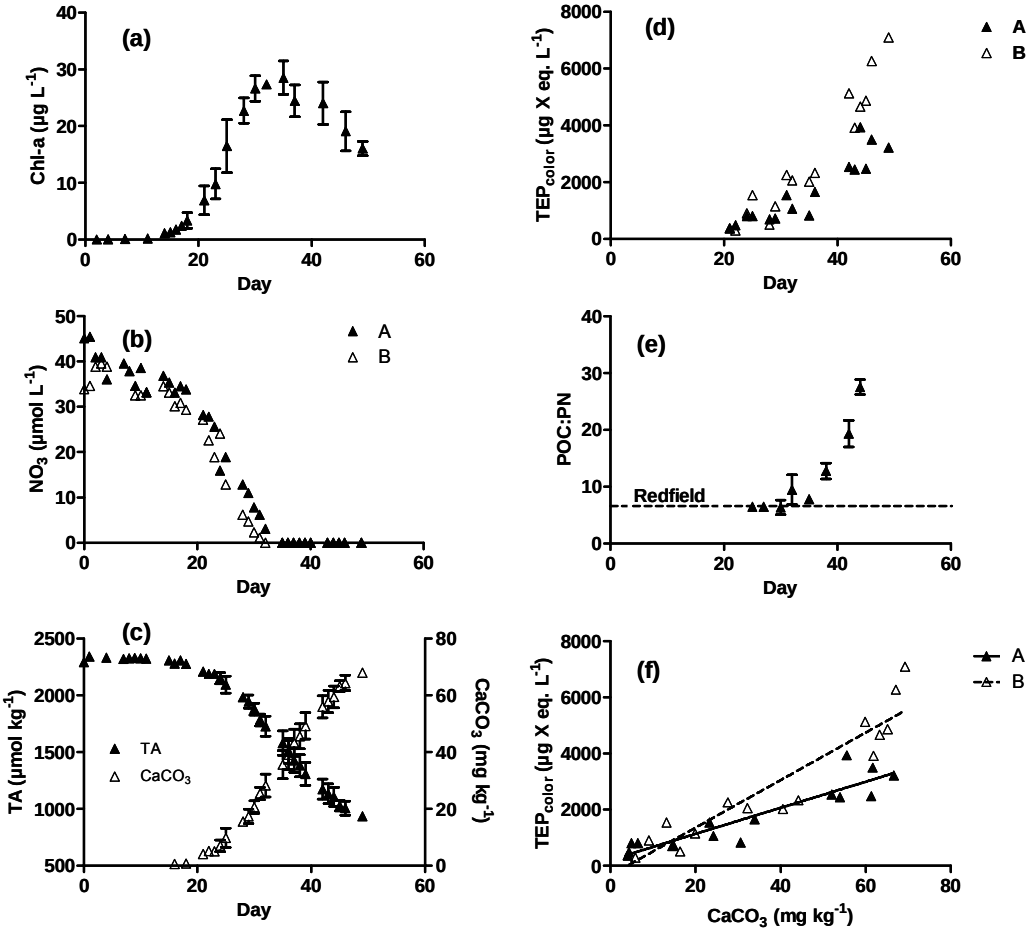


**Figure 56**. Evolution with time of (a) the Chl-a concentrations, (b) the nitrates ($NO_3$) concentrations, (c) the TA (solid triangles) and the calcite concentrations (open triangles), (d) the $TEP_{color}$ concentrations and (e) the POC:PN molar ratio. (f) $TEP_{color}$ concentrations as a function of calcite concentrations. The linear regression for the duplicate A (solid triangles) is shown with a straight line (n = 16, slope = 46.44±5.185, $R^2$ = 0.85, p<0.0001) and for the duplicate B (open triangles) with a dashed line (n = 14, slope = 84.62±8.24, $R^2$ = 0.88, p<0.0001). Errors bars represent the minimum and the maximum values.

### *4.3.1.2 Comparison of the E. huxleyi cultures at different initial $pCO_2$*

The $pCO_2$ (calculated from pH and TA) averaged 630 ppm initially in one culture experiment (Figure 57a, line) and 930 ppm in the other (Figure 57a, open diamonds). The variation of $pCO_2$ is influenced by the biological uptake of DIC during the exponential growth phase and by the calcification that releases $CO_2$.The initial decrease in $pCO_2$ in the culture @ 930 ppm could be attributed to the physical $CO_2$ outgassing in the absence of biological $CO_2$ uptake. The main influence of the $pCO_2$ between the two experiments is the delay for the initiation of the different processes, namely the onsets of photosynthesis (Figure 57b), calcification (Figure 57c) and TEP production (Figure 57d).

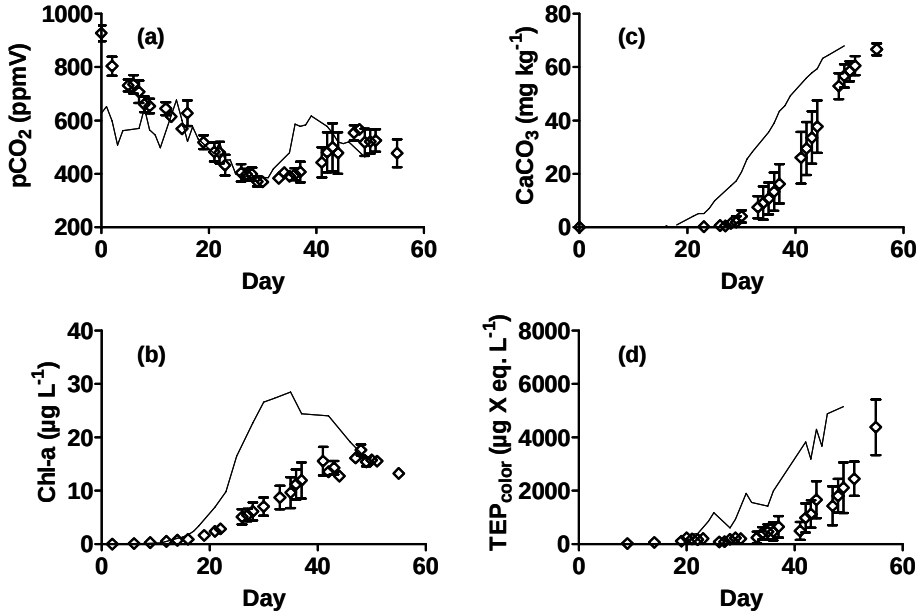


**Figure 57**. Evolution of (a) $pCO_2$, (b) Chl-a concentrations, (c) calcite concentrations and (d) $TEP_{color}$ concentrations for the two batch culture experiments. Lines represent the first culture @ 630 ppm and open diamonds the second culture @ 930 ppm.

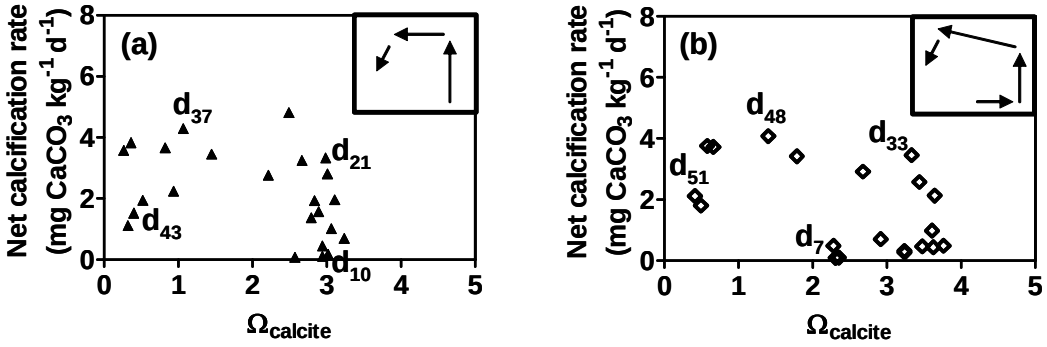


**Figure 58**. Evolution of the net calcification rate as a function of $\Omega_{cal}$ for (a) experiment 1 at an initial $pCO_2$ of 630 ppmV (solid triangles) and (b) experiment 2 at an initial $pCO_2$ of 930 ppmV (open diamonds).

Furthermore, the net calcification rate was plotted versus the $\Omega_{cal}$ (Figure 58). Calcification began at an initial $\Omega_{cal}$ of 3 (@ 630 ppm, Figure 58a) or at a value greater than 3 (@ 930 ppm, Figure 58b). Constant rates were observed at a $\Omega_{cal}$ varying between 3 and 1 and the net calcification rate decreased after saturation was reached ($\Omega_{cal} \leq 1$). Our results show that calcification could occur when $\Omega_{cal}$ was near 1. Moreover, the net calcification rate decreased only when the $\Omega_{cal}$ fell below 1. When $\Omega_{cal}$ is far above 1, one should not expect dissolution of $CaCO_3$ to occur and TA consumption should be due to calcification only. In contrast, when seawater is close to calcite saturation or is under-saturated with respect to calcite, dissolution

becomes important and the variations of TA cannot be used to estimate calcification but may be rather considered as the net result of dissolution and calcification. Thus, $CaCO_3$ accumulation corresponds to the net concentration of biogenic calcite present in solution.

#### *4.3.1.3 Cultures of E. huxleyi under different $pCO_2$/temperature conditions*

Cultures were carried out at 3 different $pCO_2$; low $CO_2$ (~180 ppm), present $CO_2$ (~380 ppm) and future $CO_2$ (~750 ppm) at 13°C and at 18°C for the present and the future $CO_2$ conditions. We studied the individual and combined effects of increased $pCO_2$ and T on the POC and PIC production (ULB), the PIC:POC ratio and on the coccolith morphology (UGent).

##### *4.3.1.3.1 Effect of $CO_2$ and/or temperature on the POC and PIC production ratios and on the PIC:POC ratio*

Differences in the Δ[POC]:Δ[cell], in the Δ[PIC]:Δ[cell] and in the PIC:POC ratio was observed between the culture experiments (Figure 59).

At 13°C and at 18°C, higher cell abundance-normalized POC levels was found in the future $CO_2$ compare to the present $CO_2$ treatment (t-test, $p<0.05$). Nevertheless, this ratio was higher in the low $CO_2$/13°C than in the present $CO_2$/13°C treatment. A two-way ANOVA between present and future $CO_2$ conditions indicated a significant effect of $pCO_2$ ($p<0.005$) while the effect of T was not significant ($p=0.1208$).

At 13°C, the highest Δ[PIC]:Δ[cell] ratio was found in the low $CO_2$ treatment and was significantly different from the present $CO_2$ or from the future $CO_2$ treatment (t-test, $p<0.05$) (Figure 59b). Both $pCO_2$ and temperature had a significant effect on the Δ[PIC]:Δ[cell] ratio in the present and future $CO_2$ treatments (two-way ANOVA, $p<0.05$ and $p<0.05$, respectively), although no interaction was found between both variables ($p=0.06$).

Like the cell abundance-normalized PIC, the PIC:POC ratio was lower in the future $CO_2$/13°C treatment than in the present or in the low $CO_2$/13°C treatment (one-way ANOVA, $p<0.05$, Figure 59c). At 18°C, the PIC:POC ratio is also lower in the future than in the present $CO_2$ treatment (t-test, $p<0.05$). No interactive effect of the $pCO_2$ and the temperature was found (two-way ANOVA, $p=0.09$) but a significant effect of the $pCO_2$ ($p<0.0001$) and of temperature ($p<0.05$) was found on the PIC:POC ratio.

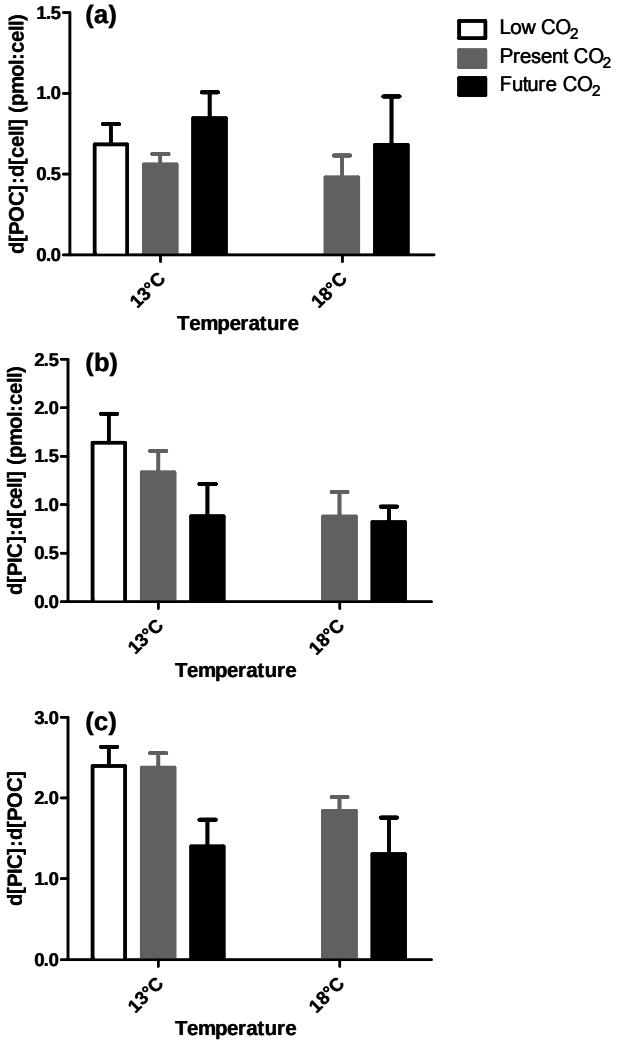


**Figure 59**. Ratio of the (a) POC and (b) PIC content per cell and SD during the batch culture experiments. (c) Cellular PIC:POC ratios in each treatment of $pCO_2$ and temperature.

#### *4.3.1.3.2 Effect of $CO_2$ and/or temperature on coccolith morphology*

A minimum of 100 coccoliths (attached onto the coccosphere, so at least 50 coccospheres) per $CO_2$ and temperature treatment duplicate were analyzed with a Jeolscan SEM (JSM 5600 LV). Categorization of attached coccoliths was preferred to loose coccoliths of unknown age and dissolution status. Coccoliths were classified according to a scale of four categories (Figure 60). The first category corresponds to normal coccoliths with all segments connected and forming an oval ring. The second one corresponds to slightly malformed coccoliths; in this category less than 5 segments are not well connected to others. The third category corresponds to malformed coccoliths where more than 5 segments are unconnected or not entirely formed. The fourth one corresponds to fragmented coccoliths; in this category parts of the coccolith are missing.

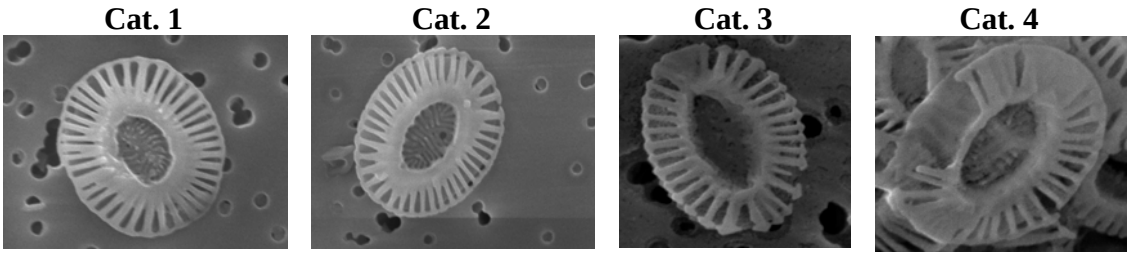


**Figure 60**. Images of the four categories of coccoliths morphology from normal coccoliths (cat. 1) to fragmented coccoliths (cat. 4)

SEM analysis revealed variable degrees of coccolith malformation. Coccoliths were classified at the end of the exponential growth phase for each treatment according to the scale (Figure 60). A significant effect of $CO_2$ treatments on the coccolith morphology was found at 13°C (Kruskal-Wallis test, $p<0.0001$) as well as at 18°C (Mann-Whitney U test, $p<0.0001$) while temperature did not significantly affect coccolith morphology (Mann-Whitney U test, $p_{present}=0.4090$, $p_{future}=0.1915$) (Figure 61). The share of normal coccoliths was more important in the cultures with low $CO_2$/13°C conditions than at present $CO_2$ conditions. The lowest percentage of normally formed coccoliths was observed in the future $CO_2$ treatments. The percentage malformed coccoliths increased with increasing $pCO_2$.

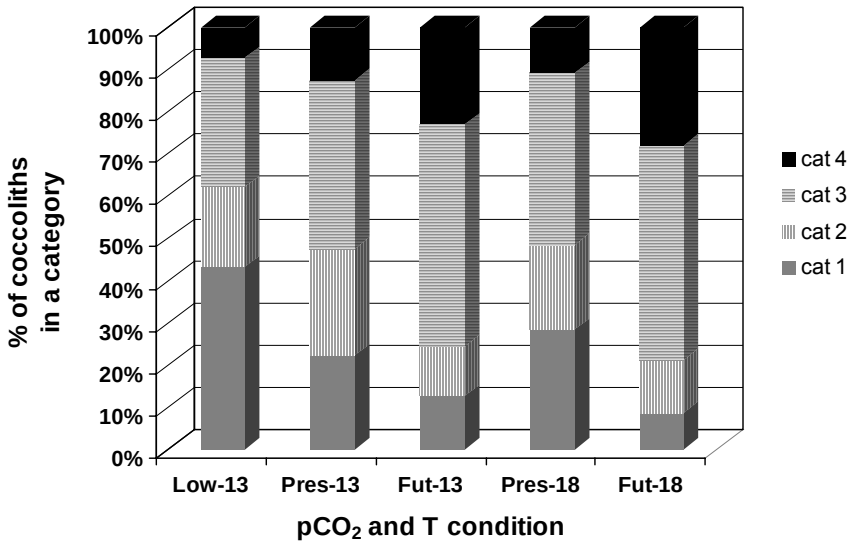


**Figure 61**. Percentage of coccoliths per category for each treatment of $pCO_2$ and temperature.

Testing the effect of increasing $pCO_2$ on *E. huxleyi* is well studied, results showed some differences depending on the experimental design used. Nevertheless, except for the paper of Iglesias-Rodriguez et al. (2008), it is generally accepted that *E. huxleyi* calcification decreases with increasing $pCO_2$ (Riebesell et al. 2008). To simulate our different treatment of $pCO_2$, the bubbling of gases at fixed $CO_2$ concentrations was used and we obtained similar results than Riebesell et al. (2000) or Zondervan et al. (2001) who used an addition of acid/base.

In addition to the $pCO_2$, we also investigated the effect of temperature on bloom variables. The calcification per cell decreased from the present $CO_2$/13°C to the future $CO_2$/18°C treatment, yet no significant interacting effect of $pCO_2$ and temperature on calcification was found. While no significant effect of temperature was observed on the POC production per cell, calcification per cell decreased by 34% in the culture at present $CO_2$ and by 7% in the one at future $CO_2$ with a temperature increase of 5°C. The latter result was not found by Feng et al. (2008) who also studied the interactive effect of $pCO_2$ (375 ppmV and 750 ppmV) and temperature (20 and 24°C) at two different irradiances (50 and 400 µmol $m^{-2}$ $s^{-1}$) using semi-continuous laboratory cultures. In analogy to this study, they observed a reduction in the cell abundance-normalized PIC with increasing $pCO_2$ but only at high irradiance (400 µmol $m^{-2}$ $s^{-1}$).

In parallel to the decrease in Δ[PIC]:Δ[cell] ratio with increasing $pCO_2$, an increase in the share of malformed coccoliths was observed in our experiments which was in agreement with Riebesell et al. (2000) and Langer et al. (2006).

The ratio of the PIC concentration per cell was shown to be lower at future $CO_2$/18°C. This could lead to a smaller ballast effect and thus a reduction of C export in the absence of a net effect on POC production which was highlight by a lower PIC:POC ratio. Lower PIC:cell ratios are expected at future $pCO_2$ and are reflected in the deteriorated coccolith morphology, while no effect of temperature on the coccolith morphology was observed. The sole future increase in $pCO_2$ may thus have a larger negative impact on the calcification phase of *E. huxleyi* than its interaction with temperature or the increase in temperature alone.

### *4.3.2 Influence of $pCO_2$/pH and temperature on TEP dynamics by selected coccolithophorid species using chemostat experiments*

#### *4.3.2.1 Laboratory chemostat experiments*

In order to investigate the effect of ocean acidification and warming on calcification and growth of the coccolithophore *E. huxleyi*, two chemostat experiments were conducted at the AWI.

We followed the growth of a calcifying strain of *Emiliania huxleyi* by the use of a chemostat system at two dilution rates (0.3 and 0.1 $d^{-1}$). Three different $CO_2$ concentations and two different temperatures were applied (300 µatm $CO_2$ at 14°C , 550 µatm $CO_2$ at 14°C ,900 µatm $CO_2$ at 14 and 900 µatm $CO_2$ at 18°C), with $pCO_2$ being perturbed by aeration..

Throughout the course of the experiment TEP-C concentration increased significantly in all treatments ($R^2$= 0.77, n= 24; Figure 62). Thereby, the variance from the mean value in 900 µatm treatment was significantly different from the 300 and 550 µatm $CO_2$ treatments (P= 0.005), indicating higher TEP accumulation at high $CO_2$ concentration. In contrast, the comparison of the two temperature treatments of the high $CO_2$ cultures showed no significant difference (P= 0.16; n= 12).

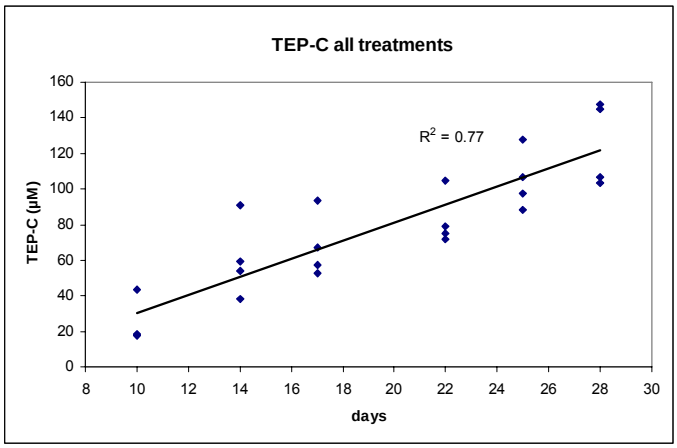


**Figure 62.** Accumulation of TEP-C in the course of the chemostat experiment.

Throughout the experiment, the average TEP-C concentration of all treatments increased by about 100 µM, while the average DOC concentration decreased by about 140 µM. Again, changes in DOC and TEP-C in the 900 µatm $CO_2$ treatments differed from the 300 and 550 µatm $CO_2$ treatments. The TEP-C increase under high $CO_2$ conditions (900 µatm 14 and 18°C cultures) was higher than the decrease in DOC, while the draw down of DOC exceeded TEP-C accumulation under low and moderate $CO_2$ concentrations (300 and 550 µatm $CO_2$ at 14°C) (Table 7).

On the last sampling day, the relative proportion of acidic sugars in particulate polysaccharides was 0.14 % for the 900_14 and 900_18 cultures, and therefore almost twice as high as observed in the 300 µatm $CO_2$ treatment (0.8 %).

During this chemostat experiment, TEP increased continuously, while cell growth exhibited steady states for each dilution rate. Hence, the accumulation of TEP throughout the experiment likely involved processes operating in addition to net production of TEP by *E. huxleyi*. The increased TEP formation determined at high $CO_2$ may be explained by two mechanisms. First, an increased TEP production in

response to rising $pCO_2$.. Alternatively, lowered pH as induced by rising $CO_2$ in seawater directly affected the structure of the exopolymeric matrix and thewith TEP formation rates as suggested by Dogsa et al. (2005) and Mari (2008). Thus both, lowered pH and high $CO_2$ treatment potentially changed the equilibration between TEP-precursors and TEP for the benefit of TEP formation

**Table 7.** Carbon budgets for the 300, 550 and 900 µatm $CO_2$ treatments.Increase in TEP-C is lower than the DOC decrease for the present day cultures, while the TEP-C increase in the future ocean cultures is enhanced compared to the DOC draw down.

| | Increase in TEP-C (µM) | Decrease in DOC (µM) |
|---|---|---|
| 300 &550 µatm $CO_2$ | 116 | 229 |
| 900 µatm $CO_2$ | 87 | 58 |

### *4.3.2.2 On-board chemostat experiment, Bay of Biscay 2006*

To describe the influence of $CO_2$ concentration on coccolithophores, specifically on the kinetics of polysaccharide exudation and TEP production, an on-board chemostat study was performed during the cruise 2006. The chemostat system during the Bay of Biscay cruise applied 4 different $CO_2$ concentrations corresponding to ~180 µatm (glacial), ~370 µatm, ~750 µatm, and ~1400 µatm (Figure 63). $CO_2$ concentration in each reservoir was regulated by aeration with the defined $CO_2$/air mixtures. The experiments were performed in duplicate bottles of 2.0 L and at an irradiance of 200 µmol photons $m^{-2}$ $s^{-1}$ with a 16:8 light:dark cycle, and two different flow rates (0.6 and 0.13 $d^{-1}$) for 4 days each.

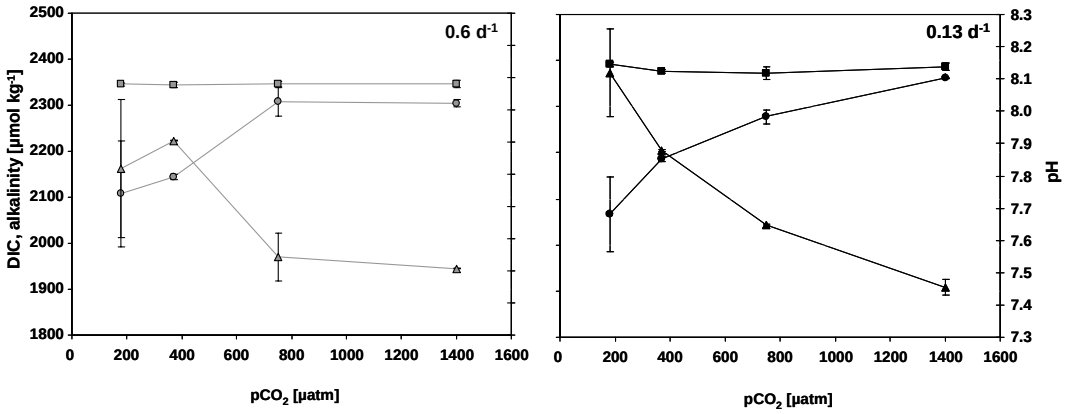


**Figure 63.** Seawater carbonare chemistry in the on-board chemostat experiment at high (grey) and low (black) flow rate. Circles: dissolved inorganic carbon (DIC), squares: alkalinity, triangles: pH.

The temperature was kept at values of 16±2°C by placing the bottles in a 400L reservoir with surface seawater exchange. The chemostat bottles were filled at Station 2, where the highest abundance of coccolithophores during the Belgica 2006 cruise was observed.

Samples were taken twice for analyses of the following variables: TA and DIC to describe the carbonate system; TPC, POC, PON, POP and TEP for particulate components; DOC and sugar composition to describe the dissolved components; bacterial cell abundances, growth rates, and enzymatic activities to describe the microbial system and SEM, light microscopy and chlorophyll *a* to describe the phytoplankton compartment. Results indicate a response of the plankton community to $CO_2$ at low flow rates, when nutrients in the incubation bottles were depleted. Here, net production of POM, such as POC and TEP decreased significantly with increasing $CO_2$ (Figures 64 and 65).

This result differs from previous publications that showed increased biomass production by marine phytoplankton with $CO_2$ availability (e.g. Engel, 2002, Rost et al., 2003, Riebesell et al., 2007). However, as our results also indicated that bacterial biomass production (BBP) under nutrient deplete conditions increase with $CO_2$, we conclude that the response to ocean acidification may depend on the ecosystem status, i.e. between dominance of autotrophic or heterotrophic communities.

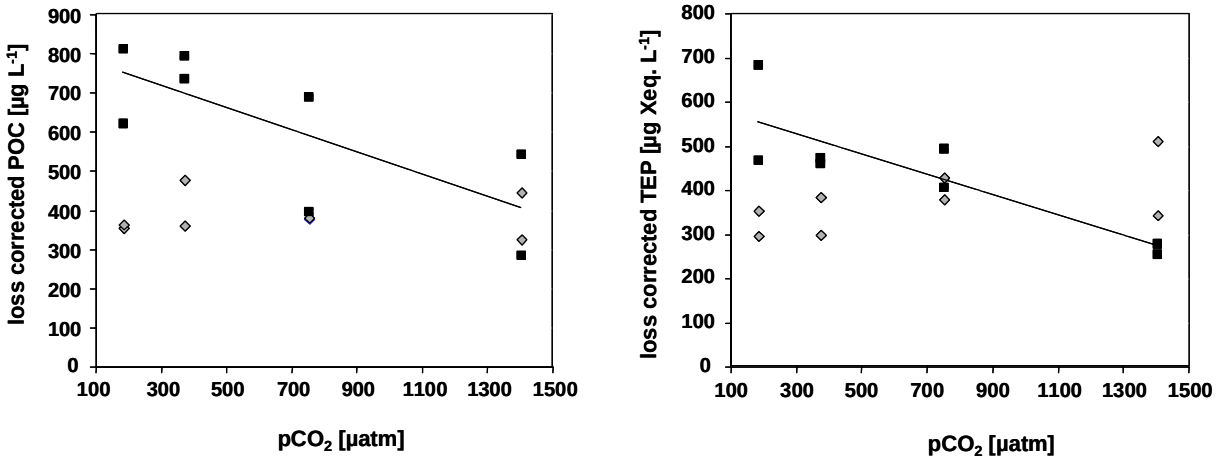


**Figure 64**. Concentration of particulate organic carbon (POC) and transparent exopolymer particles (TEP) at high (grey diamonds) and low (black squares) flow rate. Values have been loss corrected for dilution due to different flow rates. A significant decrease of POC and TEP with increasing $CO_2$ concentration was observed only under nutrient depletion (POC: $r^2$=0.55, p=0.03; TEP: 0.73, p=0.01).

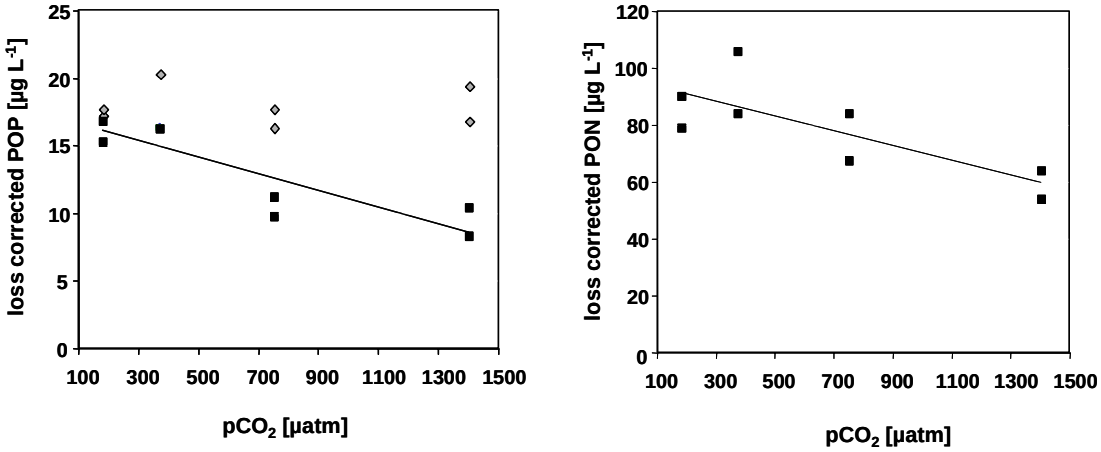


**Figure 65**. Concentration of particulate organic phosphorous (POP) and nitrogen (PON) at high (grey diamonds) and low (black squares) flow rate. Values have been loss corrected for dilution due to different flow rates. A significant decrease of POP and PON with increasing $CO_2$ concentration was observed only under nutrient depletion (POP: $r^2$=0.79, p=0.003; PON: 0.61, p=0.002).

### *4.3.2.3 Influence of $pCO_2$ on aggregate formation*

The influence of $CO_2$ on the aggregation and sinking behaviour of the coccolithophore *Emiliania huxleyi* (PML B92/11) during a laboratory experiment. Aggregation of the cells was promoted using roller tables. Size and settling velocity of aggregates were determined during the incubation using video image analysis. The results show that that more cells aggregated in the high-$CO_2$ incubations (Figure 66).Moreover, $CO_2$ induced changes in the inorganic carbon to organic carbon ratio (PIC/POC) influence the porosity and hence the sinking velocity of aggregates of Emiliania huxleyi (Figure 67). Average sinking velocity was highest for low $CO_2$ aggregates (~ 1292 m $d^{-1}$) that also had the highest PIC/POC ratio. Lowest PIC/POC ratios and lowest sinking velocity (~ 366 m $d^{-1}$) at comparable sizes were observed for aggregates of the high $CO_2$ treatment. Aggregates of the high $CO_2$ treatment showed an excess density about one order of magnitude lower (~ 4.2 x $10^{-4}$ g $cm^{-3}$) when compared to aggregates from the medium and low $CO_2$ treatments (~ 1.7 g x $10^{-3}$ $cm^{-3}$). Thus, the amount of calcite in aggregates is crucial for the degree of ballasting effect. In the high $CO_2$ treatment, aggregates with lower calcite content had higher bacterial abundance, suggesting enhanced bacterial degradation. Thus, our findings indicate that a $CO_2$ induced reduction of calcite content aggregates could affect the vertical export of organic matter in the ocean, particularly in areas dominated by coccolithophores blooms.

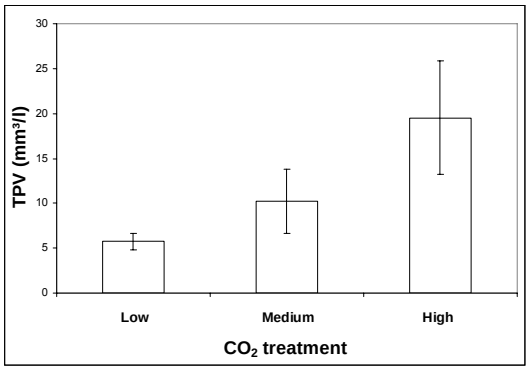


**Figure 66.** Total volume of biogenic material included in aggregates as detected by the Coulter Multisizer in the size range 2-60 µm ESD for incubations at different $pCO_2$ (n=3 for each $pCO_2$).

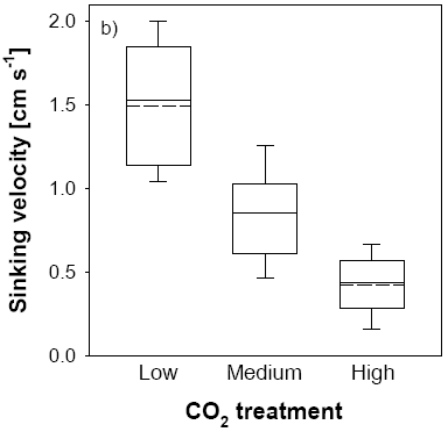


**Figure 67**. Box plot of sinking velocity of aggregates during the course of the roller table experiments. Aggregates formed from *E. huxleyi* cells were grown in batch cultures at different $pCO_2$.

## 4.4 Development and parameterisation of a mechanistic model to simulate the coccolithophorid bloom reproduced in mesocosm experiments

### *4.4.1 Simulations of "present day" mesocosms of the Bergen 2001 experiment*

Figure 68 compares model outputs with the data collected during the Bergen 2001 mesocosm experiment for biomass in carbon of *E. huxleyi*, TEP, TA and pH. The model represents the evolution of *E. huxleyi* carbon biomass in the range of mesocosms 5 and 6, and in particular the timing and value of the peak as well as the bloom termination phase. The differences noted with mesocosm 4 are due to the presence of another bloom of *Micromonas* at the beginning of the experiment which delayed the development of *E. huxleyi*. The dynamics of TEP is quite well reproduced showing that the model proposed by Engel et al. (2004a) is appropriate to describe the aggregation of DOC to form TEP. The model shows that the TEP production needs to be sustained by the DOC present in the environment in addition to the one produced by cellular excretion.

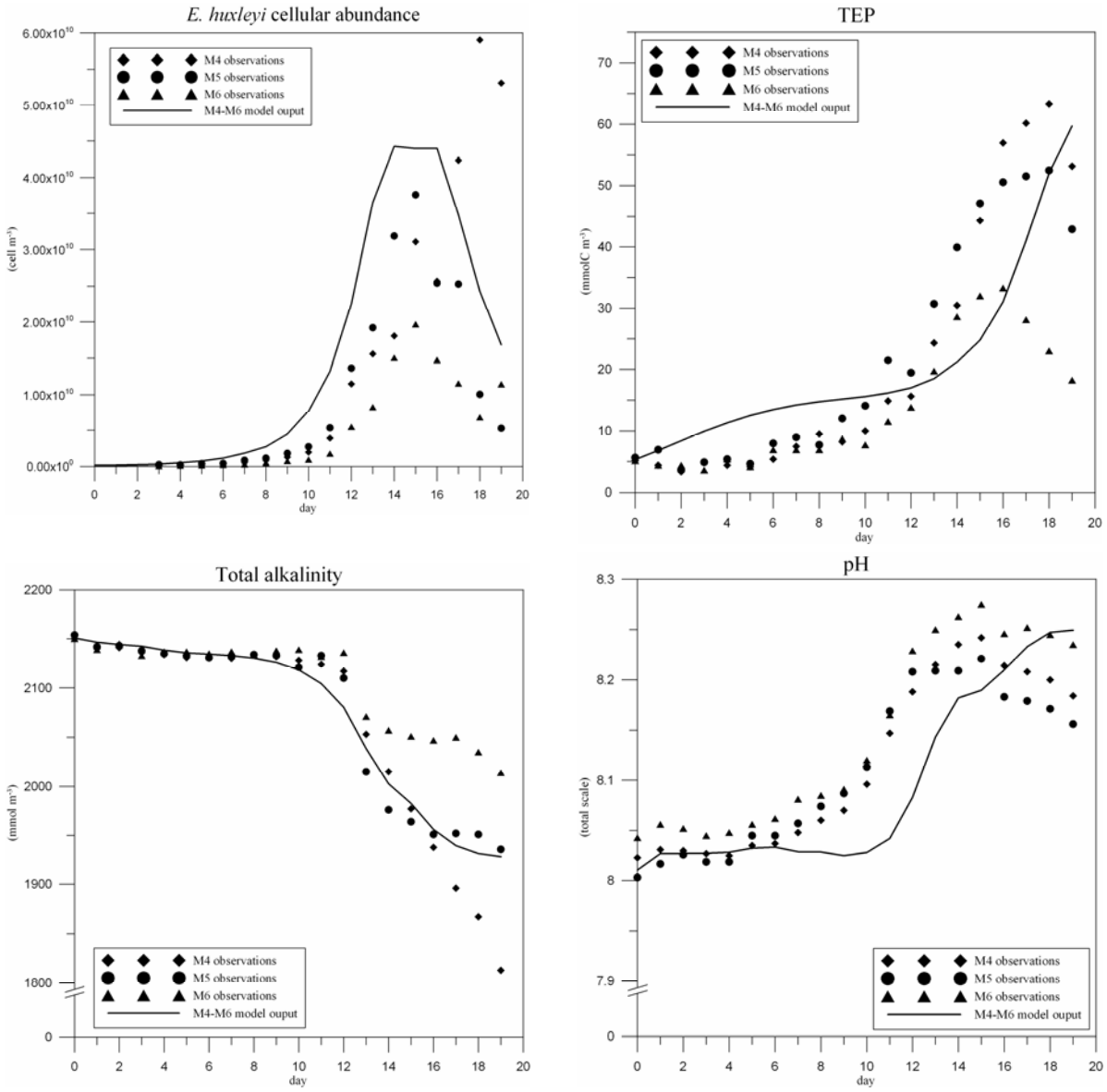


**Figure 68.** Model simulations for a) *E. huxleyi* carbon biomass (in mmolC $m^{-3}$), b) TEP concentration (in mmolC $m^{-3}$), c) TA, and d) pH, and observations obtained during the 2001 Bergen mesocosm experiment (Engel et al., 2005; Dellile et al., 2005) for mesocosm 4,5,6 which were submitted to present day atmospheric $pCO_2$. The biomass of *E. huxleyi* in carbon was computed from data on cells enumeration using a conversion factor of a content of 4-15 x $10^{-12}$ gC per cell (Tyrrell and Taylor, 1996).

The TA avolution simulated by the model lies within the ranges of observed values in the three mesocosms, showing a good representation of calcification in the model. The model represents the calcification as a function of primary production instead of biomass of *E. huxleyi* as usually established in other models. The pH is slightly underestimated by the model due to a small overestimation of the DIC concentration.

### *4.4.2 Simulations of "year 2100" mesocosms of the Bergen 2001 experiment*

Observations revealed a great divergence between *E. huxleyi* carbon biomasses. Moreover, blooms were not terminated by viral attack (as in the "present day" mesocoms, see above) except in mesocosm 2 (Figure 69). The model however reproduces a viral attack which was responsible for the collapse of the biomass around day 15, slightly earlier in comparison with observations from mesocosm 2. The cellular carbon content coefficient has a direct impact on the model outputs when the phytoplankton growth is duly terminated by a viral attack. The overall pattern of inorganic nutrients (nitrate and phosphate) was similar to "present day $pCO_2$" conditions for the model as well as the observations. The three mesocosms exhibited very similar evolutions for the nitrate concentrations since nitrate is the limiting nutrient in the model: modelled nitrate is entirely consumed around day 13. There was an evidence of photosynthetic activity of phytoplankton other than *Emiliania huxleyi* (*Micromonas*) between day 1 and day 6. This activity independent of *E. huxleyi* was not represented by the model. In the model, bacteria and *E. huxleyi* were in competition for phosphorous since day 9. This modelled DIP continued to decrease after the depletion of nitrate, while it increased in the observations. Dynamics of DIC were similar between the three replicates till day 14. After day 15, the evolution of DIC diverged between mesocosms, reflecting the differences formerly noted for the cellular biomasses. Disregarding the sidestep caused by the initial consumption of DIC by *Micromonas*, the modelled DIC is very close to the observations. At the end of the simulation, modelled DIC remained steady. Contrarily to the observations, the modelled DOC evolution is composed of two distinct phases. During the first one, from day 1 till day 12, the modelled DOC remained quasi steady. During the second one, from day 13 till the end of the simulation, the modelled DOC increased sharply. Increase of modelled DOC relies mainly on semi-labile pool of DOC, which was massively provided by the products of cellular DOC extra excretion during the *Emilinia huxleyi* photosynthesis, under nutrient limitation. Modelled TEP reflects the dynamics of cellular DOC extra excretion, that is a function of the cellular C:N ratio. Consequently, modelled formation of TEP only increases after nitrate depletion.

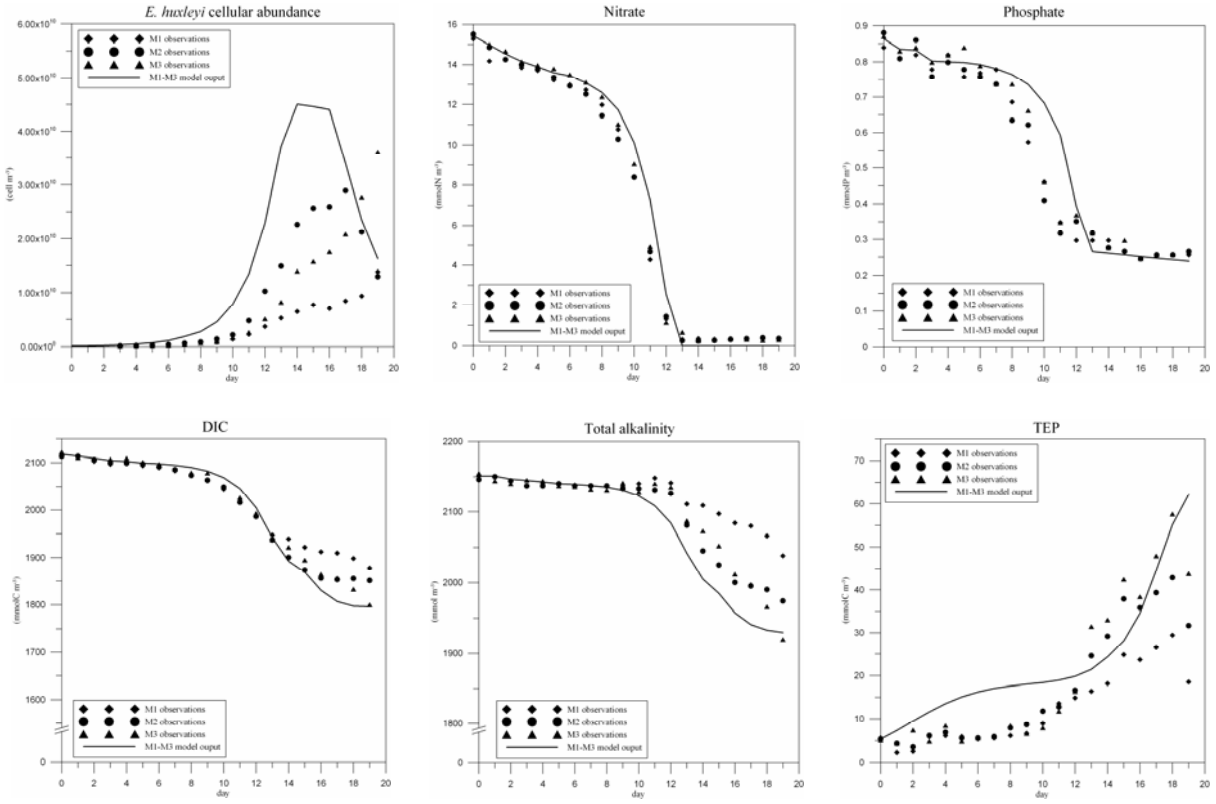


**Figure 69.** Comparison of model output and observations for the "year 2100" mesocosms of the Bergen 2001 experiment.

## 5. CONCLUSIONS AND POLICY SUPPORT

The accumulation of anthropogenic $CO_2$ has altered carbonate chemistry in surface waters (ocean acidification) since pre-industrial times and is expected to continue to do so in the coming centuries (Orr et al., 2005). Changes in the carbonate chemistry of surface waters related to ocean acidification can alter the rates and fates of primary production and calcification of numerous marine organisms and communities (Kleypas et al., 2006; Doney et al., 2009). Such changes can provide either positive or negative feedbacks on increasing atmospheric $CO_2$ by modifying the flux of $CO_2$ between the ocean and the atmosphere. Several manipulative experiments to test the effect of ocean acidification on coccolithophorids have shown that calcification would decrease in future, while export of organic carbon could increase (Riebesell et al., 2000; Engel et al., 2004b; Delille et al., 2005; Riebesell et al., 2007). However, for a robust and credible implementation in mathematical models of such feedback mechanisms to allow the projection of a plausible future evolution of marine carbon biogeochemistry under global change, it is required to understand present-day biogeochemistry and ecology of pelagic calcifying communities under field conditions ("the real world"). This can only be achieved with comprehensive and multidisciplinary studies of carbon cycling during coccolithophorid blooms in natural conditions such as the one carried out during the PEACE project.

Among the PEACE project findings that are relevant to policy makers and the scientific community at large related to ocean acidification and effects on pelagic calcifying communities and related feedbacks, we can highlight the following:

- The spatial and temporal (short-term and interannual) dynamics of phytoplankton blooms and associated bacterial communities at the shelf break in the Northern Bay of Biscay are complex and the underlying mechanisms are not completely understood. In general, however, stratification of the water column and concomitant changes in abiotic (e.g. nutrients, temperature) conditions and biotic processes (e.g. lysis, grazing, exudates) appear to have a strong influence on the dynamics of the microbial communities.
- Results of our field biogeochemical studies showed that during blooms of coccolithophorids, the Bay of Biscay acted as a sink for atmospheric $CO_2$. Hence, the present-day balance of organic carbon fixation to inorganic carbon production during coccolithophorid blooms does not lead to a significant accumulation of $CO_2$ that would reverse the direction of the air-sea $CO_2$ flux (i.e. from a sink to a source of atmospheric $CO_2$).
- Our cruise data also showed that the impact of calcification on decreasing the $CO_2$ sink in the Bay of Biscay is variable, but on average it is relatively small, ~12%. This implies that the potential feedback on atmospheric $CO_2$ of the projected decrease in

pelagic calcification due to $CO_2$ "production" resulting from biogenic $CaCO_3$ precipitation would probably be minor.

- Measured rates of benthic $CaCO_3$ dissolution over the continental shelf represent ~1% of the pelagic calcification rates. This implies a decoupling of calcification by coccolithophores and the dissolution of $CaCO_3$ in the sediments. PIC produced by coccolithophores is either stored in the sediments or exported out of the system, but does not seem to be significantly dissolved in the sediments.
- Field biogeochemical investigations allowed a better understanding of the TEP dynamics under naturally occurring bloom conditions :
  - Dissolved acidic sugars are an important source for TEP production during coccolithophorid blooms in the Bay of Biscay
  - Analysis of size spectrum of particules suggests the assembly of lager particles from smaller ones by aggregation.
- Laboratory experiments showed new results that should contribute to a better understanding of the future response of C cycling in pelagic calcifying communities to ocean acidification and other global change factors (e.g. temperature):
  - Calcification per cell decreased by 34% in the culture at present-day $pCO_2$ and by 7% in the one at future $pCO_2$ with a temperature increase of 5°C
  - Changes in polysaccharide composition indicate that the surplus of free glucose generated by higher glucosidase rates was efficiently metabolized by bacterioplankton and that the bacterial substrate supply was improved under simulated future-ocean pH conditions.
  - Lowering of pH potentially changed the equilibrium between TEP-precursors and TEP for the benefit of TEP formation. Further investigations are needed to explore the underlying mechanisms of increased TEP formation in response to increasing $pCO_2$
  - Net production of POM, such as POC and TEP, decreased significantly with increasing $pCO_2$ in contrast to previous studies. This is due to the increase of bacterial biomass production under nutrient deplete conditions with increasing $pCO_2$, suggesting that the response to ocean acidification may depend on the ecosystem status, i.e. between dominance of autotrophic or heterotrophic communities.
  - Rising $pCO_2$ induced a decrease in the PIC:POC ratio and reduced the sinking velocity of aggregates of *E. huxleyi*. Our findings therefore suggest a reduced deep-export of organic matter in the ocean, if $pCO_2$ in seawater further increases.

Overall, these results show that the understanding of the effects of ocean acidification on marine biogeochemistry, carbon cycling and potential feedbacks on increasing atmospheric $pCO_2$ is still in its infancy. Further research is required to reduce uncertainties and gain knowledge on the underlying mechanisms before a robust and credible implementation in mathematical models can be made to allow the projection of a plausible future evolution of carbon biogeochemistry under global change. Such future research will require a multitude of approaches, such as a combination of laboratory experiments, field measurements and modelling as carried out in the framework of the PEACE project.

## 6. DISSEMINATION AND VALORISATION

The dissemination and valorisation of the PEACE project can be summarized as follows:

- 4 Master theses and 2 Bachelor theses
- 6 PhD theses, 4 pending defence and 2 defended
- 17 peer review publications, 4 published, 13 in press, submitted or pending submission
- 47 presentations at international meetings, among which : ASLO Aquatic Sciences Meeting (January 2009), Second International Symposium on the Ocean in a High $CO_2$ World (October 2008), Advances in Marine Ecosystem Modeling Research symposium (July 2008), 4 EGU General Assembly (April 2009, April 2008, April 2007, April 2006), Joint IMBER/LOICZ Continental Margins Open Science Conference (September 2007), IUGG XXIV General Assembly (July 2007), and SOLAS Open Science Conferences (March 2007, November 2009)
- The coordinator and some PIs of PEACE co-signed the Monaco Declaration 2009 (http://www.igbp.net/documents/MonacoDeclaration2009.pdf)
- Project's internet site (http://www.co2.ulg.ac.be/peace/) that presents the project to the general public and to the scientific community

# 7. PUBLICATIONS

## 7.1. Publications of the teams

### *7.1.1 Peer review*

Biermann, A., Engel, A. (2009) Effect of $CO_2$ on the properties and sinking velocity of aggregates of the coccolithophore *Emiliania huxleyi, submitted to Biogeosciences.*

Borges A.V., L.-S. Schiettecatte, G. Abril, B. Delille & F. Gazeau (2006) Carbon dioxide in European coastal waters, Estuarine, Coastal and Shelf Science, 70(3), 375-387.

Borges A.V. (submitted) Present day carbon dioxide fluxes in the coastal ocean and possible feedbacks under global change.

Borges A.V. & N. Gypens (submitted) Carbonate chemistry responds more strongly to eutrophication than ocean acidification in the coastal zone.

Davoult D., Harlay J., and Gentil F. (2009) Contribution of a dense population of the brittle star *Acrocnida brachiata* (Montagu) to the biogeochemical fluxes of $CO_2$ in a temperate coastal ecosystem. *Estuaries and Coasts, in press,* DOI 10.1007/s12237-009-9216-2.

De Bodt C., Q. d'Hoop, J. Harlay & L. Chou (submitted) Calcification and transparent exopolymer particles (TEP) production in batch cultures of *Emiliania huxleyi* initially exposed to different future $pCO_2$. *Journal of Experimental Marine Biology and Ecology.*

### *7.1.2. Others*

#### *Master Theses*

d'Hoop, Q. (2006) Implication dans les changements climatiques de la production de particules exopolymériques transparentes (TEP) chez le coccolithophore *Emiliania huxleyi*, Mémoire de licence en sciences géographiques, Université Libre de Bruxelles, 159p.

Joassin, P. (2006) A 0D coupled biochemical model developped for the study of an experimental bloom of *Emiliania huxleyi* coccolithophorid phytoplankton, DEA thesis, University of Liège, 100p.

Perrault N. (2007) Effets de la $pCO_2$ sur la calcification du coccolithophore *Emiliania huxleyi* dans la perspective des changements climatiques. Travail de fin d'études, Bioingénieur en chimie et bioindustries, Université Libre de Bruxelles.

Steen F. (2007). Microplankton diversiteit in een coccolithoforenbloei. Bachelorproef Universiteit Gent, 53p.

Sollberger S. (2009) Impact of the variations of $pCO_2$ on coccolithophorid Emiliania huxleyi during a mesocosm bloom experiment and its direct contribution to carbon export, Master II thesis, University of Liège, 89 pp.

#### *Bachelor Theses*

Steen F. (2007). Microplankton diversiteit in een coccolithoforenbloei. Bachelorproef Universiteit Gent, 53p.

Breine, N. (2009). Dynamiek van fytoplankton groei en microzooplankton begrazing tijdens een coccolithoforenbloei in de Golf van Biskaye (NO Atlantische Oceaan). Bachelorproef Universiteit Gent, 22p.

***PhD Theses***

De Bodt C. (expected January 2010) Pelagic calcification and fate of carbonate production in marine systems. PhD thesis, Université Libre de Bruxelles.

Harlay J. (2009) Biogeochemical study of coccolithophorid blooms in the context of climate change, PhD thesis, Université Libre de Bruxelles, 500 pp

Koch, S. (2007) Growth and calcification of the coccolithophore Emiliania huxleyi under different $CO_2$ concentrations. Diploma thesis, University of Oldenburg

Piontek J. (2009) Effects of temperature and pCO2 on the degradation of organic. PhD thesis. Universität Bremen. 201pp.

Suykens S. (expected December 2009), Carbon dynamics in the in the Northeast European continental margin (Northern Bay of Biscay) during coccolithophore blooms, PhD thesis, University of Liège

Van Oostende, N. (expected 2$^{nd}$ half 2010) Microbial community dynamics and interactions between C-rich exudates, prokaryotic consumption and protozoan grazing in natural and experimental coccolithophore blooms.

## 7.2. Co-publications

### *7.2.1. Peer review*

Borchard C., A.V. Borges, N. Händel, A. Engel (in preparation) Description of a novel chemostat system for investigating elevated carbon dioxide and temperature effects on marine phytoplankton physiology.

De Bodt C., N. Van Oostende, K. Sabbe and L. Chou (in preparation) Phytoplankton cell lysis during coccolithophorid blooms in the northern Bay of Biscay.

De Bodt C., N. Van Oostende, J. Harlay, K. Sabbe and L. Chou (in preparation) Individual and combined effects of $pCO_2$ and temperature on *Emiliania huxleyi* calcification: Study of the calcite production, the coccolith morphology and the coccosphere size. To be submitted to Biogeosciences by end September.

Engel A., Schulz K. G., Riebesell U., Bellerby R., Delille B. & Schartau M. (2008) Effects of CO2 on particle size distribution and phytoplankton abundance during a mesocosm bloom experiment (PeECE II), Biogeosciences, 5, 509-521

Godoi R.H.M., K. Aerts, J. Harlay, R. Kaegi, Chul-Un Ro, L. Chou, R. Van Grieke (2009), Organic surface coating on Coccolithophores - Emiliania huxleyi: Its determination and implication in the marine carbon cycle, Microchemical Journal, 91:266–271, doi: 10.1016/j.microc.2008.12.009

Harlay J., C. De Bodt, A. Engel, S. Jansen, Q. d'Hoop, J. Piontek, N. Van Oostende, S. Groom, K. Sabbe & L. Chou (2009) In-situ abundance and size distribution of transparent exopolymer particles (TEP) in a coccolithophorid bloom in the northern Bay of Biscay (June 2006), Deep-Sea Research part I, 56: 1251–1265

Harlay J., L. Chou, C. De Bodt, N. Van Oostende, J. Piontek, K. Suykens, A. Engel, K. Sabbe, S. Groom & A.V. Borges (submitted) Biogeochemistry and carbon budget of a coccolithophorid bloom in the northern Bay of Biscay (June 2006).

Harlay J., A.V. Borges, C. Van Der Zee, B. Delille, R.H.M. Godoi, L.-S. Schiettecatte, N. Roevros, K. Aerts, P.-E. Lapernat, L. Rebreanu, S. Groom, M.-H. Daro, R. Van Grieken & L. Chou (submitted) Biogeochemical study of a coccolithophorid bloom in the northern Bay of Biscay (NE Atlantic Ocean), in June 2004

Joassin P., B. Delille, K. Soetaert, A.V. Borges, L. Chou, A. Engel, J.-P. Gattuso, J. Harlay, U. Riebesell, K. Suykens & M. Gregoire (submitted) A mathematical modelling of blooms of the coccolithophore Emiliana huxleyi occurring in a mesocosm experiment

Suykens, K. et al. (in preparation) Benthic remineralization in the Northeast European continental margin (Northern Bay of Biscay)
Suykens, K. et al. (in preparation) Dissolved inorganic carbon dynamics and air-sea carbon dioxide fluxes during coccolithophore blooms in the Northeast European continental margin (Northern Bay of Biscay)
Van Oostende, N. et al. (in preparation). Microbial community dynamics in a coccolithophorid bloom in the Northern Bay of Biscay (June 2006).
Van Oostende, N. et al. (in preparation). Interannual variation in bacterial and phytoplankton dynamics in coccolithophorid blooms in the Northern Bay of Biscay (2006-2008).

### *7.2.2 Others*

Monaco Declaration 2009 : http://www.igbp.net/documents/MonacoDeclaration2009.pdf

## 7.3 Other activities

### *7.3.1 Internet site*

The project's internet website went on-line on day 1 of project and has been updated regularly. The web-site has public pages that present the project to the general public and to the scientific community. It contains also a restricted page that has been actively used for the exchange of data, documentation and information within the network (partners, follow-up committee members and BSP).

### *7.3.2 Presentations at international meetings*

**2009**

Biermann, A., Engel, A. (2009). Effect of CO2 on the properties and sinking velocity of aggregates of the coccolithophore Emiliania huxleyi., ASLO Aquatic Sciences Meeting 2009, 25.-30. January, Nice, France.
Borchard C. , N. Händel, A.V. Borges & A. Engel, A new chemostat system to investigate combined temperature and CO2 effects on marine phytoplankton species, ASLO Aquatic Sciences Meeting, Nice, France, 25-30 January 2009
Chou L., J. Harlay, C. De Bodt, N. Roevros, A.V. Borges, K. Suykens, B. Delille, K. Sabbe, N. Van Oostende, A. Engel, J. Piontek, C. Borchard, Nicole Händel and S. Groom (2009) Role of pelagic calcification and export of carbonate production in climate change. SOLAS Open Science Conference, Barcelona, Spain, 16 - 19 November 2009, poster presentation.
De Bodt C., J. Harlay, N. Roevros & L. Chou, Cell lysis during the coccolithophorid blooms in the Northern Bay of Biscay, ASLO Aquatic Sciences Meeting, Nice, France, 25-30 January 2009
De Bodt, C., N. Van Oostende, J. Harlay, N. Roevros, K. Sabbe and L. Chou. Study of the combined effect of $pCO_2$ and temperature on the coccolithophore *Emiliania huxleyi*. Goldschmidt conférence, 21-26 June 2009, Davos, Switzerland.
Engel, A.(2009). Will the biological pump respond to ocean acidification? Gordon Research Conferences; Chemical Oceanography; Process, Dynamics, and Change in the Anthropocene Ocean; 2.-7.8.2009, Tilton, NH, USA.
Engel, A., Biermann, A., Szlosek, J., Abramson, L., Lee, C. (2009). Role of biogenic minerals in particle aggregation processes and potential sensitivities to ocean acidification, ASLO Aquatic Sciences Meeting 2009, 25.-30. January, Nice, France.

Händel N., J. Piontek, J. Harlay, C. de Bodt & Chou, Dynamics of polysaccharides and transparent exopolymer particles durind a coccolithophorid bloom in the Bay of Biscay, ASLO Aquatic Sciences Meeting, Nice, France, 25-30 January 2009

Harlay J., Borges A.V., De Bodt C., Suykens K., Roevros N., d'Hoop Q., Groom S. & L. Chou, Towards a comprehensive C-budgeting approach of a coccolithophorid bloom in the Northern Bay of Biscay (June 2006), ASLO Aquatic Sciences Meeting, Nice, France, 25-30 January 2009

Piontek, J., Händel, N., Borchard, C., Lunau, M., Chou, L., Engel, A. (2009). The significance of bacterial polysaccharide degradation for carbon export, today and in the future ocean, ASLO Conference, Nice, 25-30 January, 2009.

Suykens K., B. Delille & A. V. Borges, Dissolved inorganic carbon dynamics in the Bay of Biscay (June 2006 – May 2007 – May 2008) Preliminary results, 41st International Liège Colloquium on Ocean Dynamics, Liège, 4-8 May 2009

Suykens K., B. Delille & A. V. Borges, Benthic dissolved inorganic carbon dynamics in the Bay of Biscay (June 2006 - May 2007 - May 2008), VLIZ Young Scientist Day, 6 March 2009, Brugge, Belgium

Suykens K., B. Delille & A. V. Borges, Surface dissolved inorganic carbon dynamics in the Bay of Biscay (June 2006 - May 2007 - May 2008), VLIZ Young Scientist Day, 6 March 2009, Brugge, Belgium

Van Oostende N., Boschker H.T., Middelburg J.J., Vyverman W., & Sabbe K.. How do bacteria influence the extracellular carbohydrate pool in experimental /Emiliania huxleyi /blooms?, ASLO Aquatic Sciences Meeting, Nice, France, 25-30 January 2009

**2008**

Chou L., J. Harlay , C. De Bodt, N. Roevros, A.V. Borges, K. Suykens, B. Delille, K. Sabbe, N. Van Oostende, A. Engel, J. Piontek, N. Händel, S. Groom & S. Schmidt (2008) Biogeochemistry of Coccolithophore Blooms along the Continental Margin of the Northern Bay of Biscay, Eur-Oceans Final Meeting, Rome, 25-27 November 2008

Chou L. , J. Harlay, C. De Bodt, N. Roevros, A.V. Borges, K. Suykens, B. Delille, K. Sabbe, N. Van Oostende, A. Engel, J. Piontek, C. Borchard, N. Händel, S. Schmidt & S. Groom, Biogeochemical investigations of coccolithophore blooms along the continental margin of the northern Bay of Biscay: highlights of the PEACE project, Second International Symposium on the Ocean in a High CO2 World, Monaco, 6-8 October 2008

Engel, A.(2008). Testing the effects of ocean acidification on marine plankton: What can we expect in the future?, SOMAS Special Seminar, Stony Brook University, Stony Brook, USA.

Händel, N., Piontek, J., Wohlers, J., Riebesell, U., Engel, A. (2008). Dynamics of dissolved neutral and acidic sugars in seawater, Ocean Science Meeting, March 2-7, 2008, Orlando, Florida.

Joassin P., Delille B., Soetaert K., Borges A.V., Chou L., Engel A., Gattuso J.-P., Harlay J., Riebesell U., Suykens K. & M. Gregoire, A mathematical modelling of bloom of the coccolithophore Emiliania huxleyi in a mesocosm experiment, Advances in Marine Ecosystem Modeling Research (AMEMR) symposium, Plymouth, United Kingdom, 23-26 July 2008

Piontek, J., Händel, N., Lunau, M., Borchard, C., Engel, A. (2008). Effects of ocean acidification on the bacterial degradation of organic matter, Second International Symposium on the ocean in a high-CO2 world, October 6-9, 2008, Monaco.

Suykens K., B. Delille & A.V. Borges, Surface dissolved inorganic carbon dynamics in the Bay of Biscay (June 2006 - May 2007), EGU General Assembly, Vienna, Austria, 13 - 18 April 2008

Suykens K., B. Delille & A.V. Borges, Benthic dissolved inorganic carbon dynamics in the Bay of Biscay (June 2006 - May 2007), EGU General Assembly, Vienna, Austria, 13 - 18 April 2008

Van Oostende N., W. Vyverman, J. Harlay, C. De Bodt, L. Chou, K. Suykens, A.V. Borges, J. Piontek, A. Engel, & K. Sabbe. Coccolithophore bloom dynamics shape bacterioplankton communities in the northern Bay of Biscay, 12th International Symposium on Microbial Ecology (ISME 12), Cairns, Australia, 17-22 August 2008.

**2007**

Biermann, A., Engel, A. (2007).Effect of CO2 on the properties and sinking velocity of aggregates of the coccolithophore Emiliania huxleyi, 97th annual meeting GV, Bremen, Germany.

Borges A.V., Present day CO2 cycle in the coastal ocean and possible evolution under global change, Joint IMBER/LOICZ Continental Margins Open Science Conference, September 17- 21, 2007, Shanghai, China

De Bodt C., Q. d'Hoop, J. Harlay & L. Chou. Calcification and transparent exopolymer particles (TEP) production in batch cultures of Emiliania huxleyi exposed to different $pCO_2$, EGU General Assembly, 15-20 April 2007, Vienna, Austria . Poster presentation.

Engel A., R. Bellerby,. B. Delille, K. Schulz, U. Riebesell, M. Shartau, 2007. Effect of CO2 concentration on suspended particle dynamics during a mesocosm bloom experiment (PeeceII), European Geosciences Union General Assembly 15-20 April 2007, Vienna, Austria, oral presentation

Harlay J., C. De Bodt, Q. D'Hoop, A.V. Borges, B. Delille, K. Suykens, N. Van Oostende, K. Sabbe, N. Roevros, S. Schmidt, S. Groom & L. Chou, Biogeochemistry of a late coccolithophorid bloom at the continental margin of the Bay of Biscay, International Union of Geodesy and Geophysics XXIV General Assembly, 2-13 July 2007, Perugia, Italy

Harlay J., C. De Bodt, Q. D'Hoop, A.V. Borges, K. Suykens, N. Van Oostende, K. Sabbe, N. Roevros, S. Groom, & L. Chou, Biogeochemistry of a late marginal coccolithophorid bloom in the Bay of Biscay, 15-20 April 2007, EGU General Assembly, Vienna, Austria, oral presentation

Joassin P., Borges A.V., Chou L., Delille B., Engel A., Harlay J., Jacquet S., Riebesell U., Rochelle-Newall E., Zondervan I., Soetaert K., Gattuso J.-P. & M. Gregoire, A dynamic model of an experimental bloom of coccolithophores Emiliania huxleyi, The 6th European Conference on Ecological Modelling,Trieste, Italy, November 27-30 2007

Koch S., N. Händel & A. Engel, Testing the effects of $pCO_2$ on the coccolithophore Emiliania huxleyi during different growth stages, EGU General Assembly, Vienna, April 2007

Lunau M., S. Koch, J. Piontek, N. Händel & A. Engel, Investigating the effects of changes in $CO_2$ concentration on marine plankton dynamics with chemostat systems, 42nd EMBS, Kiel, August 2007

Piontek J., N. Händel, M. Lunau & A. Engel, Investigating the effects of changing $CO_2$ concentration on a natural marine plankton community using a chemostat system, IUGG XXIV General Assembly, Perugia, July 2007Suykens K., B. Delille & A. V. Borges, Dissolved inorganic carbon dynamics in the Bay of Biscay (June 2006), 15-20 April 2007, EGU General Assembly, Vienna, Austria, poster presentation

Suykens K., B. Delille & A. V. Borges, Biogeochemical carbon cycle in a coccolithophorid bloom, VLIZ Young Scientist Day, 2 March 2007, Brugge, Belgium, poster presentation

Suykens K., B. Delille & A. V. Borges, Dissolved inorganic carbon dynamics in the Bay of Biscay (June 2006), International Union of Geodesy and Geophysics XXIV General Assembly, 2-13 July 2007, Perugia, Italy

Suykens K., B. Delille & A. V. Borges, Surface dissolved inorganic carbon dynamics in the Bay of Biscay (june 2006-may 2007), CARBOOCEAN Annual Meeting, 4 -7 December 2007, Bremen, Germany

Thomas H., F. Prowe, S. van Heuven, Y. Bozec, H.J.W. de Baar, L.-S. Schiettecatte, K. Suykens, M. Koné, A.V. Borges, I.D. Lima & S.C. Doney, Rising CO2 conditions and ocean acidification - a severe threat to high latitude coastal ecosystems, Joint IMBER/LOICZ Continental Margins Open Science Conference, September 17- 21, 2007, Shanghai,

ChinaPiontek J., N. Händel & A. Engel, Effects of rising temperature and $pCO_2$ on bacterial degradation processes in the future ocean, EGU General Assembly, Vienna, April 2007

Van Oostende N. & K. Sabbe, 2007. Bacterial community structure during a coccolithophorid bloom in the Northern Bay of Biscay. *VLIZ 7th young scientists' day, March 2nd Brugge, Belgium.*

**2006**

Borges A.V., L. S. Schiettecatte, G. Abril, B. Delille & F. Gazeau, Carbon dioxide in European coastal waters, Open Science Conference on the GHG Cycle in the Northern Hemisphere organised by CarboEurope-IP, CarboOcean and NitroEurope-IP, 14-18 November 2006, Sissi-Lassithi, Crete, Greece, poster presentation

Borges A.V., L.-S. Schiettecatte, G. Abril, B. Delille & F. Gazeau, Carbon dioxide in European coastal waters, EGU General Assembly, 02–07 April 2006, Vienna, Austria (Geophysical Research Abstracts, Vol. 8, 05270, 2006), poster presentation.

De Bodt C., Q. d'Hoop, J. Harlay & L. Chou. Calcification and transparent exopolymer particles (TEP) production in batch cultures of Emiliania huxleyi exposed to different $pCO_2$, CARBOOCEAN 2nd annual meeting, 4-8 December 2006, Gran Canaria. Oral presentation

Thomas, H., F. Prowe, S. van Heuven, Y. Bozec, H.J.W. de Baar, L.-S. Schiettecatte, K. Suykens, M. Koné, A.V. Borges, I.D. Lima, S.C. Doney, Rising CO2 conditions and ocean acidification - a severe threat to high latitude coastal ecosystems,First IGBP–SCOR FTI Workshop on "Ocean Acidification - modern observations and past experiences", 28 - 30 September 2006, Lamont-Doherty Earth Observatory of Columbia University, U.S.A., oral presentation

## 8. ACKNOWLEDGMENTS

The scientists involved in the PEACE project are grateful to the officers and crewmembers of the *RV Belgica* for their logistic support during the cruises, to Joan Backers, Jean-Pierre De Blauw and Gregory Deschepper of the Unit of the North Sea Mathematical Models for their support in data acquisition during the cruises, to Steve Groom (RSG, PML) for providing remote sensing images during the cruises. AVB is a research associate at the FRS-FNRS. This study is financed by the Belgian Science Policy Office (BELSPO) under contract numbers SD/CS/03A&B in the framework of the Science for a Sustainable Development (SSD) programme (Climate). Besides BELSPO, this work has been carried out also with the support from Helmholtz Association (contract no. HZ-NG-102), EU FP6 IP CarboOcean (contract no. 511176–2), EU FP6 NoE EUR–OCEANS (contract no. 511106-2) and Institute for the Promotion of Innovation through Science and Technology in Flanders (IWT-Vlaanderen). The present study contribute to the the EU FP7 IP EPOCA (contract no. 211384). This is also a Belgian contribution to the SOLAS initiative.

# 9. REFERENCES


Agusti S., M. P. Satta, M. P. Mura and E. Benavent (1998) Dissolved esterase activity as a tracer of phytoplankton lysis: Evidence of high phytoplankton lysis rates in the northwestern Mediterranean. Limnol. Oceanogr. 43: 1836-1849.

Agusti S. and C. M. Duarte (2000) Strong seasonality in phytoplankton cell lysis in the NW Mediterranean littoral. Limnol. Oceanogr. 45(4): 940-947.

Agusti S. and C. M. Duarte (2002) Addressing uncertainties in the assessment of phytoplankton lysis rates in the sea. Limnol. Oceanogr. 47: 921-924.

Alldredge A.L., U. Passow and B.E. Logan (1993) The abundance and significance of a class of large, transparent organic particles in the ocean. Deep Sea Research Part I: Oceanographic Research Papers 40: 1131-1140.

Anderson L.A. and Sarmiento J.L. (1994) Redfield ratios of remineralization determined by nutrient data analysis. Glob. Biogeochem. Cycles 8, pp. 65–80.

Archer S.D., Smith G.C, Nightingale P.D., Widdicombe C.E., Tarran G.A., Rees A.P. and Burkill P.H. (2002) Dynamics of particulate dimethylsulphoniopropionate during a Lagrangian experiment in the northern North Sea. Deep-Sea Research II 49: 2979–2999.

Armstrong R.A., C. Lee, J. I. Hedges, S. Honjo, and S. G. Wakeham (2002) A new mechanistic model for organic carbon fluxes in the ocean based on the quantitative association of POC with ballast minerals. Deep-Sea Research Part II 49: 219-236.

Arrigo K.R. (2007) Carbon cycle - marine manipulations. Nature 450:491-492.

Banse K. (1994) Uptake of inorganic carbon and nitrate by marine plankton and the Redfield ratio. Global Biogeochemical cycles 8: 81-84.

Benner R. (2002) Chemical composition and reactivity. In (Eds) Hansell, D., Carlson, C., A. Biogeochemistry of marine dissolved organic matter. Academic Press.

Berelson W. M., W. M. Balch, R. Najjar, R. A. Feely, C. Sabine, and K. Lee (2007) Relating estimates of $CaCO_3$ production, export, and dissolution in the water column to measurements of $CaCO_3$ rain into sediment traps and dissolution on the sea floor: A revised global carbonate budget, Global Biogeochem. Cycles, 21, GB1024, doi:10.1029/2006GB002803.

Bode A., M.T. Alvarez-Ossorio and N. Gonzalez (1998) Estimations of mesozooplankton biomass in a coastal upwelling area off NW Spain. Journal of Plankton Research, 20(5): 1005-1014.

Bollmann J., M.Y. Cortés, A.T. Haidar, B. Brabec, A. Close, R. Hofmann, S. Plama, L. Tupas and H.R. Thierstein (2002) Techniques for quantitative analyses of calcereous marine phytoplankton. Marin Micropaleontology 44 : 163-183.

Boström K.H., K. Simu, A. Hagström and L. Riemann (2004) Optimization of DNA extraction for quantitative marine bacterioplankton community analysis. Limnology and Oceanography: Methods, 2: 365-373.

Brewer P.G. and Goldman J.C. (1976) Alkalinity changes generated by phytoplankton growth. Limnology and Oceanography, 21: 108-117.

Brezenski M. (1985) The Si:C:N ratio of marine diatoms: Interspecific variability and the effect of some environmental variables. J. Phycol., 21: 347-357.

Brussaard C. P. D., R. Riegman, A. A. M. Noordeloos, G. C. Cadée, H. Witte, A. J. Kop, G. Nieuwland, F. C. van Duyl and W. M. Balch (1995) Effects of grazing, sedimentation and phytoplankton cell lysis on the structure of a coastal pelagic food web. Marine ecology progress series 123: 259-271.

Brussaard C. P. D., Gast G. J., van Duyl F. C. and Riegman R. (1996) Impact of phytoplankton bloom magnitude on a pelagic microbial food web. Marine ecology progress series 144: 211-221.

Calbet A. and Landry M. R. (2004) Phytoplankton growth, microzooplankton grazing, and carbon cycling in marine systems. Limnol. Oceanogr. 49: 51-57.

Carlson C.A. (2002) Production and removal processes. Chap 4 in "Biogeochemistry of marine dissolved organic matter". Academic Press, ISBN 0-12-323841-2, p 91-139.

Charlson R.J., J.E. Lovelock, M.O. Andreae and S.G. Warren (1987) Oceanic phytoplankton, atmospheric sulfur, cloud albedo and climate. Nature, 326, 655-661.

Chrisholm J.R.M. and Gattuso J.-P. (1991) Validation of the alkalinity anomaly technique for investigating calcification and photosynthesis in coral reef communities. Limnol. Oceanogr. 36: 1232–1239.

De La Rocha C. L. and U. Passow (2007) Factors influencing the sinking of POC and the efficiency of the biological carbon pump. Deep Sea Research Part II 54: 639-658.

Delille B., Harlay J., Zondervan I., Jacquet S., Chou L., Wollast R., Bellerby R.G.J., Frankignoulle M., Borges A.V., Riebesell U. and Gattuso J-P. (2005) Response of primary production and calcification to changes of $pCO_2$ during experimental blooms of the coccolithophorid Emiliania huxleyi. Global Biogeochemical Cycles, Col.19, GB2023.

de Wilde P. A. W. J., G. C. A. Duineveld, E. M. Berghuis, M. S. S. Lavaleye and A. Kok (1998) Late-summer mass deposition of gelatinous phytodetritus along the slope of the N.W. European Continental Margin. Progress in Oceanography 42: 165-187.

Dickson A. G. and F. J. Millero (1987) A comparison of the equilibrium constants for the dissociation of carbonic acid in seawater media. Deep-Sea Res. 34, 1733-1743. (Corrigenda. Deep-Sea Res. 36, 983).

Dogsa I., Kriechbaum M., Stopar D. and Laggner P. (2005) Structure of bacterial extracellular polymeric substances at different pH values as determined by SAXS. Biophysical Journal 89:2711-2720.

Doney S. C., V. J. Fabry, R. A. Feely and J. A. Kleypas (2009) Ocean acidification: the other $CO_2$ problem, Ann. Rev. Mar. Sci. 1: 169-192.

Ducklow H.W. and Carlson C.A. (1992) Oceanic bacterial production. Adv Microb Ecol 12:113-181.

Egge, J. K., and D. L. Aksnes. (1992) Silicate as regulating nutrient in phytoplankton competition. Marine ecology progress series 83: 281-289.

Egge J. K. and Heimdal B. R. (1994) Blooms of Emiliania huxleyi in mesocosm experiment; effects of nutrient supply in different N:P ratios. Sarsia 79, 333-348.

Eilers P. H. C. and Peeters J. C. H. (1988) A model for the relationship between light intensity and the rate of photosynthesis in phytoplankton. Ecol. Model. 42, 199-215.

Engel A. (2000) The role of transparent exopolymer particles (TEP) in the increase in apparent particle stickiness (alpha) during the decline of a diatom bloom. Journal of Plankton Research 22(3): 485-497, 0142-7873.

Engel A. (2002) Direct relationship between $CO_2$ uptake and transparent exopolymer particles production in natural phytoplankton 24 (1): 49-53.

Engel A., B. Delille, S. Jacquet, U. Riebesell, E. Rochelle-Newall, A. Terbrüggen and I. Zondervan (2004a) TEP and DOC production by Emiliania huxleyi exposed to different $CO_2$ concentrations: A mesocosm experiment, Aquatic Microbial Ecology, 34(1):93-104.

Engel A., U. Thoms, U. Riebesell, E. Rochelle-Newall and I. Zondervan (2004b) Polysaccharide aggregation as a potential sink of marine dissolved organic carbon. Nature 428: 929– 932.

Engel A. (2004c) Distribution of transparent exopolymer particles (TEP) in the northeast Atlantic Ocean and their potential significance for aggregation processes. Deep-Sea Research Part I 51: 83-92.

Engel A., I. Zondervan, K. Aerts, L. Beaufort, A. Benthien, L. Chou, B. Delille, J.-P. Gattuso, J. Harlay, C. Heemann, L. Hoffmann, S. Jacquet, J. Nejstgaard, M.-D. Pizay, E. Rochelle-Newall, U. Schneider, A. Terbrueggen A. and U. Riebesell (2005) Testing the direct effect of $CO_2$ concentration on a bloom of the coccolithophorid Emiliania huxleyi in mesocosm experiments, Limonology and Oceanography, 50(2): 493-507.

Engel A. (2009) Determination of marine gel particles. In: O. Wurl (ed), Practical guidelines for the analysis of seawater, CRC Press, Boca Raton.

Engel A. and Händel N. (submitted) Simultaneous determination of the neutral-, amino-, and acidic sugar composition of polysaccharides in seawater using High Performance Anion Exchange Chromatography with Pulsed Amperometric Detection, submitted to Limnology & Oceanography Methods.

Feng Y., Warner M. E., Zhang Y., Sun J., Fu F.-X., Rose J. M. and Hutchins D. A. (2008) Interactive effects of increased $pCO_2$, temperature and irradiance on the marine coccolithophore Emiliania huxleyi (Prymnesiophyceae). Eur. J. Phycol. 43: 87-98.

Fernandez E., P. Boyd, P. M. Holligan and D. Harbour (1993) Production of organic and inroganic carbon within a large-scale coccolithophore bloom in the northeast Atlantic Ocean. Marine ecology progress series 97: 271-285.

Frankignoulle M., Borges A. and R. Biondo (2001) A new design of equilibrator to monitor carbon dioxide in highly dynamic and turbid environments, Water Research, 35(5): 1344-1347.

Frankignoulle M. and A.V. Borges (2001) European continental shelf as a significant sink for atmospheric carbon dioxide, Global Biogeochemical Cycles, 15(3): 569-576.

Fraser J.H. (1968) Smaller mesozooplankton: Report of Working Party 2, in: (1968) Zooplankton sampling: review papers of the proceedings of the symposium on the hydrodynamics of zooplankton sampling. Monographs on oceanographic methodology (UNESCO, Paris), 2: 153-159.

Gasol J.M. and P.A. Del Giorgio (2000) Using flow cytometry for counting natural planktonic bacteria and understanding the structure of planktonic bacterial communities. Scientia Marina 64: 197-224

Gazeau F., Smith S.V., Gentili B., Frankignoulle M. and Gattuso J-P (2004) The European Coastal zone: characterization and first assessment of ecosystem metabolism. Estuarine Coastal and Shelf Science, Vol.60, 673-694.

Gehlen M., R. Gangstø, B. Schneider, L. Bopp, O. Aumont, and C. Ethe (2007) The fate of pelagic $CaCO_3$ production in a high $CO_2$ ocean: a model study, Biogeosciences, 4, 505–519.

Gibb S.W., D.G. Cummings, X. Irigoien, R.G. Barlow, R. Fauzi and C. Mantoura (2001) Phytoplankton chemotaxonomy of the northeastern Atlantic. Deep-Sea Research II 48 : 795-823.

Gran G. (1952) Determination of the equivalence point in potentiometric titrations of seawater with hydrochloric acid. Oceanologica Acta 5, 209–218.

Grasshoff K., Ehrhardt M. and Kremling K. (1983) Methods of seawater analysis. Verlag Chemie.

Hales B. (2003) Respiration, dissolution, and the lysocline, Paleoceanography, 18(4), 1099, doi:10.1029/2003PA000915, 2003.

Harlay J., A. V. Borges, C. Van der Zee, B. Delille, R.H.M.Godoi, L.-S., Schiettecatte, N. Roevros, K. Aerts, P.-E., Lapernat, L. Rebreanu, S. Groom, M.-H. Daro, R. Van Grieken and L. Chou. Biogeochemical study of a coccolithophorid bloom in the northern Bay of Biscay (NE Atlantic Ocean), in June 2004. Submitted to Progress in Oceanography.

Harlay J., C. De Bodt, A. Engel, S. Jansen, Q. d'Hoop, J. Piontek, N. Van Oostende, S. Groom, K. Sabbe and L. Chou (2009) Abundance and size distribution of transparent exopolymer particles (TEP) in a coccolithophorid bloom in the northern Bay of Biscay. Deep-Sea Research Part I 56: 1251-1265.

Head R. N., D.W. Crawford, J. K. Egge, R. P. Harris, S. Kristiansen, D. J. Lesley, E. Marañón, D. Pond and D. A. Purdie (1998) The hydrography and biology of a bloom of the coccolithophorid Emiliania huxleyi in the northern North Sea. Journal of SEA research 39: 255-266.

Hillebrand H., C.-D. Dürselen, D. Kirschtel, U. Pollingher, T. Zohary (1999) Biovolume calculation for pelagic and benthic microalgae. Journal of Phycology 35 : 403-424.

Holligan P.M., Fernandez E., Aiken J., Balch W.M., Boyd P., Burkill P.H., Finch M., Groom S.B., Malin G., Muller K., Purdie D.A., Robinson C., Trees C.C., Turner S.M. and van der Wal P. (1993) A biogeochemical study of the coccolithophore, Emiliania huxleyi, in the North Atlantic. Global Biogeochemical Cycles, Vol. 7, 4, 879-900.

Hoppe H.G. (1983) Significance of Exoenzymatic Activities in the Ecology of Brackish Water - Measurements by Means of Methylumbelliferyl-Substrates. Mar Ecol Prog Ser 11:299-308.

Huskin I., E. Lopez, L. Viesca and R. Anadon (2006) Seasonal variation of mesozooplankton biomass, abundance and copepod grazing in the central Cantabrian Sea (southern Bay of Biscay). Scienta Marina, 70S1: 119-130.

Iglesias-Rodriguez M. D., P. R. Halloran, R. E. M. Rickaby, I. R. Hall, E. Colmenero-Hidalgo, J. R. Gittins, D. R. H. Green, T. Tyrrel, S. W. Gibbs, P. von Dassow, E. Rehm, E. V. Armbrust, and K. P. Boessenkool (2008) Phytoplankton calcification in a high-$CO_2$ world. Science 320: 336-340.

Jahnke R. A., D. B. Craven, D. C. McCorkle and C. E. Reimers (1997) $CaCO_3$ dissolution in California continental margin sediments: The influence of organic matter remineralization, Geochim. Cosmochim. Acta, 61, 3587– 3604, 1997.

Jahnke R.A. and Jahnke D.B. (2000) Rates of C, N, P and Si recycling and denitrification at the US Mid-Atlantic continental slope depocenter, Deep Sea Research Part I, 47(8): 1405-1428.

Joint I., Wollast R., Chou L., Batten S., Elskens M., Edwards E., Hirst A., Burkill P. H., Groom S., Gibb S., Miller A., Hydes D. J., Dehairs F., Antia A. N., Barlow R., Rees A., Pomroy A., Brockmann U., Cimmings D., Lampitt R., Loijens M., Mantoura F., Miller P., Raabe T., Alvarez-Salgado X., Stelfox C. and Woolfenden J. (2001) Pelagic production at the Celtic Sea shelf break. DSR Part II 48, 3049-3081.

Key R. M., A. Kozyr, C. L. Sabine, K. Lee, R. Wanninkhof, J. L. Bullister, R. A. Feely, F. J. Millero, C. Mordy and T.-H. Peng (2004) A global ocean carbon climatology: Results from Global Data Analysis Project (GLODAP), Global Biogeochem. Cycles, 18, GB4031, doi:10.1029/2004GB002247.

Kirchman D.L. (1992) Incorporation of thymidine and leucine in the subarctic Pacific: application to estimating bacterial production. Mar Ecol Prog Ser 82:301-309.

Klaas, C. and Archer D.E. (2002) Association of sinking organic matter with various types of mineral ballast in the deep sea: Implications for the rain ratio. Global Biogeochemical cycles 16: 63-1-63-14.

Kleypas, J. A., R. A. Feely, V. J. Fabry, C. Langdon, C. L. Sabine and L. L. Robbins (2006) Impacts of Ocean Acidification on Coral Reefs and Other Marine Calcifiers: A Guide for Future Research,

report of a workshop held 18–20 April 2005, St. Petersburg, FL, sponsored by NSF, NOAA, and the U.S. Geological Survey.

Knap, A. H., Michaels, A. E., Close, A., Ducklow, H. W. and Dickson, A. G (1996) Protocols for the Joint Global Ocean Flux Study (JGOFS) core measurements. [19]. 1996. Bergen, Norway, UNESCO. JGOFS Report.

Koroleff F. (1969) Direct determination of ammonia in natural waters as indophenol blue, Int. Council Expl. Sea, 9, 19-22.

Lampert L., B. Quéguiner, T. Labasque, A. Pichon and N. Lebreton (2002) Spatial variability of phytoplankton composition and biomass on the eastern continental shelf of the Bay of Biscay (north-east Atlantic Ocean). Evidence for a bloom of Emiliania huxleyi (Prymnesiophyceae) in spring 1998. Continental Shelf Research 22: 1225-1247.

Landry M. R. and R. P. Hassett (1982) Estimating the grazing impact if marine micro-zooplankton. Marine biology 67: 283-288.

Langer G., M. Geisen, K.-H. Baumann, J. Kläs, U. Riebesell, S. Thoms and J. R. Young (2006) Species-specific responses of calcifying algae to changing seawater chemistry. Geochemistry Geophysics Geosystems 7: 1-12.

Latasa M. (2007) Improving estimations of phytoplankton class abundances using CHEMTAX. Marine Ecology Progress Series 329: 13-21.

Lessard E. J., Merico A. and Tyrrell T. (2005) Nitrate : phosphate ratios and Emiliania huxleyi blooms. Limnol. Oceanogr. 50, 1020-1024.

Logan B. E., U. Passow, A. L. Alldredge, H. P. Grossard and M. Simon (1995) Rapid formation and sedimentation of larges aggregates is predictable from coagulation rates (half-lives) of transparent exopolymer particles (TEP). Deep Sea Research Part II 42: 203-214.

Lohse L., W. Heldera, E.H.G. Eppinga and W. Balzerb (1998) Recycling of organic matter along a shelf-slope transect across the N.W. European Continental Margin (Goban Spur), Progress in Oceanography 42, 77–110.

Mackey M.D., D.J. Mackey, H.W. Higgins, S.W. Wright (1996) CHEMTAX - a program for estimating class abundance for chemical markers: application to HPLC measurements of phytoplankton. Marine Ecology Progress Series 114 : 265-283.

Marañón E. and N. Gonzalez (1997) Primary production, calcification and macromolecular synthesis in a bloom of the coccolithophore Emiliania huxleyi in the North Sea. Marine ecology progress series 157: 61-77.

Margalef R. (1997) Our biosphere. Ecology Institute, Oldendorf/Luhe, Germany.

Mari X. (1999) Carbon content and C:N ratio of transparent exopolymeric particles (TEP) produced by bubbling exudates of diatoms. Mar Ecol Prog Ser 183: 59-71.

Mari X. (2008) Does ocean acidification induce an upward flux of marine aggregates? Biogeosciences Discuss., 5, 1631–1654, 2008.

Mehrbach C., Culberson C. H., Hawley J. E. and Pytkowicz R. M. (1973) Measurement of the apparent dissociation constants of carbonic acid in seawater at atmospheric pressure. Limnol. Oceanogr., 18 (6), 897-907.

Menden-Deuer S. and E.J. Lessard (2000) Carbon to volume relationships for dinoflagellates, diatoms, and other protist plankton. Limnology and Oceanography 45(3) : 569-579.

Merico A., Tyrrell T., Lessard E., Oguz T., Stabeno P., Zeeman S. and Whitledge T. (2004) Modelling phytoplankton succession on the Bering Sea shelf: Role of climate influences and trophic interactions in generating Emiliania huxleyi blooms 1997-2000. Deep Sea Research Part I: Oceanographic Research Papers 51: 1803-1826.

Millero F. J., Lee K. and Roche M. P. (1998) Distribution of alkalinity in the surface waters of the major oceans. Marine Chemistry 60(1-2): 111-130.

Murata A. and Takizawa T. (2002) Impact of coccolithophorid bloom on the $CO_2$ system in surface waters of the eastern Bering Sea shelf. Geophysical Research Letters, Vol. 29, 11, 1547.

Muyzer G., E. De Waal and A.G. Uitterlinden (1993) Profiling of complex microbial populations by denaturing gradient gel electrophoresis analysis of polymerase chain reaction-amplified genes coding for 16S rRNA. Applied and Environmental Microbiology, 59(3): 695-700.

Olson B.M. and S.L. Strom (2002) Phytoplankton growth, microzooplankton herbivory and community structure in the southeast Bering Sea: insight in the formation and temporal persistence of an Emiliania huxleyi bloom. Deep-Sea Research II, Vol. 49, 5969-5990.

Orr J. C., V. J. Fabry, O. Aumont, L. Bopp, S. C. Doney, R. A. Feely, A. Gnanadesikan, N. Gruber, A. Ishida, F. Joos, R. M. Key, K. Lindsay, E. Maier-Reimer, R. Matear, P. Monfray, A. Mouchet, R. G. Najjar, G. K. Plattner, K. B. Rodgers, C. L. Sabine, J. L. Sarmiento, R. Schlitzer, R. D. Slater, I.

J. Totterdell, M. F. Weirig, Y. Yamanaka and A. Yool. (2005) Anthropogenic ocean acidification over the twenty-first century and its impact on calcifying organisms. Nature 437: 681-686.

Paasche E. (2002) A review of the coccolithophorid Emiliania Huxleyi (Prymnesiophyceae), with particular reference to growth, coccolith formation, and calcification-photosynthesis interactions. Phycologia 40: 503-529.

Pakulski and Benner (1994) Abundance and distribution of carbohydrates in the ocean. Limn. Oceanogr., 93, 930-940.

Passow U. and A. L. Alldredge (1995) A dye-binding assay for the spectrophotometric measurement of transparent exopolymer particles (TEP). Limnol.Oceanogr. 40: 1326-1335.

Passow U., Shipe R.F., Murray A., Pak D.K., Brzezinski M.A. and Alldredge A.L. (2001) The origin of transparent exopolymer particles (TEP) and their role in the sedimentation of particulate matter. Continental Shelf Research 21(4): 327-346.

Passow U. (2002) Transparent exopolymer particles (TEP) in aquatic environments. Progress In Oceanography 55(3-4): 287-333.

Pingree R. D. and Le Cann B. (1989) Celtic and Armorican slope and shelf residual currents. Progress In Oceanography 23, 303-338.

Pingree R.D. and Le Cann B. (1990) Structure, strength and seasonality of the slope currents in the Bay of Biscay region. Journal of the Marine Biological Association of the UK, 70, 857-885.

Pingree R. D. and New A. L. (1995) Structure, seasonal development and sunglint spatial coherence of the internal tide on the Celtic and Armorican shelves and in the Bay of Biscay. DSR Part I 42, 245-284.

Pingree R. D., Sinha B. and Griffiths C. R. (1999) Seasonality of the European slope current (Goban Spur) and ocean margin exchange. Cont. Shelf Res. 19, 929-975.

Quian M., Mopper K. (1996) Automated High-Performance, High-Temperature Combustion Total Organic Carbon Analyzer. Anal. Chem. 68, 3090-3097.

Ramus J. (1977) Alcian blue: A quantitative aqueous assay for algal acid and sulfated polysaccharides. J. Phycol. 13, 345-348.

Redfield A. C., Ketchum B. M. and Richards F. A. (1963) The influence of organism on the composition of seawater, In N. M. Hill (eds.), The Sea, 2nd ed. Wiley, pp. 26-77.

Rees A. P., Woodward E. M., Robinson C., Cummings D. G., Tarran G. A., and Joint I. (2002) Size-fractionated nitrogen uptake and carbon fixation during a developing coccolithophore bloom in the North Sea during June 1999. Deep Sea Research Part II: Topical Studies in Oceanography 49, 2905-2927.

Reimers, C. E., H. A. Stecher III, G. L. Taghon, C. M. Fuller, M. Huettel, A. Rusch, N. Ryckelynck and C. Wild (2004) In situ measurements of advective solute transport in permeable shelf sands. Continental Shelf Research, 24: 183-201.

Riebesell U., I. Zondervan, B. Rost, P. D. Tortell, R. Zeebe and F. M. M. Morel (2000) Reduced calcification of marine plankton in response to increased atmospheric $CO_2$. Nature 407: 364– 367.

Riebesell U., K. G. Schulz, R. G. J. Bellerby, M. Botros, P. Fritsche, M. Meyerhofer, C. Neill, G. Nondal, A. Oschlies, J. Wohlers and E. Zollner (2007) Enhanced biological carbon consumption in a high $CO_2$ Ocean. Nature 450: 545-548.

Riebesell U., R. Bellerby, A. Engel, V. J. Fabry, D. A. Hutchins, T. B. H. Reusch, K. G. Schulz and F. M. M. Morel (2008) Comment on "Phytoplankton Calcification in a high-$CO_{2\ world}$". Science 322: 1466b-.

Riegman R., W. Stolte, A. A. M. Noordeloos and D. Slezak (2000) Nutrient uptake and alkaline phosphatase (APase) activity of Emiliania huxleyi (Prymnesiophyceae) during growth under N and P limitation in continuous cultures. J. Phycol. 36: 87-96.

Riegman R., J. D. L. van Bleijswik and C. P. D. Brussaard (2002) The use of dissolved esterase activity as a tracer of phytoplankton lysis. Limnol. Oceanogr. 47: 916-920.

Riegman R. and C. Winter (2003) Lysis of plankton in the non-stratified southern North Sea during summer and autumn 2000. Acta Oecologica 24: S133-S138.

Rost B., U. Riebesell, S. Brukhardt and D. Slütemeyer (2003) Carbon acquisition of bloom-forming marine phytoplankton. Limnol. Oceanogr. 48: 55-57.

Rusch, A., M. Huettel, C. Wild and C. E. Reimers (2006) Benthic oxygen consumption and organic matter turnover in organic-poor, permeable shelf sands. Aquatic Geochemistry, 12: 1-19.

Sapp M., A. Wichels, K.H. Wiltshire, & G. Gerdts (2007a) Bacterial community dynamics during the winter-spring transition in the North Sea. FEMS Microbiology Ecology 59: 622-637.

Sapp M., A.S. Schwaderer, K.H.Wiltshire, H.G.Hoppe, G. Gerdts & A. Wichels (2007b) Species-specific bacterial communities in the phycosphere of microalgae? Microbial Ecology 53: 683-699.

Sautour B., F.Artigas, A.Herbland and P. Laborde (1996) Zooplankton grazing impact in the plume of dilution of the Gironde estuary (France) prior to the spring bloom. Journal of Plankton Research, 18(5): 835-853.

Schartau M., A. Engel, J. Schröter, S. Thoms, C. Völker and D. Wolf-Gladrow (2007) Modelling carbon overconsumption and the formation of extracellular particulate organic carbon. Biogeosciences 4: 433-454.

Shanks A. L. and Edmondson E. W. (1989) Laboratory-made artificial marine snow: A biological model of the real thing. Mar. Biol. 101. 4: 463-470.

Smith D.C. and Azam F. (1992) A simple, economical method for measuring bacterial protein synthesis in seawater using $^{3}$H-leucine. Mar Microb Food Webs 6:1007-114.

Smith S.V. and Key G.S. (1975) Carbon dioxide and metabolism in marine environments. Limnol. Oceanogr. 20, pp. 493–495.

Stefels J. (2000) Physiological aspects of the production and conversion of DMSP in marine algae and higher plants. Journal of Sea Research 43 (3–4), 183–197.

Stelfox-Widdicombe C. E., E. S. Edwards, P. H. Burkill and M. A. Sleigh (2000) Microzooplankton grazing activity in the temperate and sub-tropical NE Atlantic: summer 1996. Marine ecology progress series 208: 1-12.

Suffrian K., P. Simonelli, J. C. Nejstgaard, S. Putzeys, Y. Carotenuto and A. N. Antia (2008) Microzooplankton grazing and phytoplankton growth in marine mesocosms with increased $CO_2$ levels. Biogeosciences 5: 1145-1156.

Takahashi T., Olafsson J., Goddard J., Chipman D. W. and Sutherland S. C. (1993) Seasonal variation of $CO_2$ and nutrients in the high-latitude surface oceans: A comparative study. Global Biogeochemical Cycles, 7, 843-878.

The Royal Society. Ocean acidification due to increasing atmospheric carbon dioxide. [Policy Report 12/05]. (2005) London. The Royal Society.

Toggweiller J. (1993). Carbon overconsumption. Nature 363, 210-211.

Trimmer M., Gowen R.J., Stewart B.M. and Nedwell D.B. (1999) The spring bloom and its impact on benthic mineralization rates in western Irish Sea sediments. Marine Ecology Progress Series, Vol. 185, 37-46.

Tyrrell T. and Taylor A. H. (1996) A modelling study of Emiliania huxleyi in the NE Atlantic. Journal of Marine Systems 9: 83-112.

Uher G., G. Schebeske, R.G. Barlow, D.G. Cummings, R.F.C. Mantoura, S.R. Rapsomanikis, M.O. Andreae (2000) Distribution and air–sea gas exchange of dimethyl sulphide at the European western continental margin. Marine Chemistry 69, 277–300.

Utermöhl H. (1958) Zur Vervollkommung der quantitative Phytoplankton Methodik. Mitteilungen Internationale Vereinigung für Theoretische und Angewande Limnologie, Vol. 9, 1-38.

van Boekel W. H. M., F. C. Hansen, R. Riegman and R. P. M. Bak (1992) Lysis-induced decline of a Phaeocystis spring bloom and coupling with the microbial foodweb. Marine ecology progress series 81: 269-276.

Van den Meersche K., Middelburg J., Soetaert K., van Rijswijk P. H. B. and Heip C. (2004) Carbon-nitrogen coupling and algal-bacterial interactions during an experimental bloom: Modeling a $^{13}$C tracer experiment. Limnol. Oceanogr., 49(3): 862-878.

van der Wal P., R. S. Kempers and M. J. W. Veldhuis (1995) Production and downward flux of organic matter and calcite in a North Sea bloom of the coccolithophore Emiliania huxleyi. Marine ecology progress series 126: 247-265.

Wanninkhof R. (1992) Relationship between wind speed and gas exchange over the ocean. Journal of Geophysical Research 97(C5):7373-7382.

Wishner K.F., M.M. Gowing and C. Gelfman (1998) Mesozooplankton biomass in the upper 1000 m in the Arabian Sea: overall seasonal and geographic patterns, and relationship to oxygen gradients. Deep Sea Research II, 45: 2405-2432.

Wollast R. and L. Chou (2001) The carbon cycle at the ocean margin in the northern Bay of Biscay. Deep-Sea Research Part II 48(14-15):3265-3293.

Wright S.W., S.W. Jeffrey (1997) High resolution system for chlorophylls and carotenoids of marine phytoplankton. In: Jeffrey SW, RFC Mantoura, SW Wright (eds.) Phytoplankton pigments in oceanography: a guide to advanced methods. SCOR-UNESCO, Paris, pp. 327-341.

Yentsch C. S. and Menzel D. W. (1963) A method for the determination of phytoplankton chlorophyll and phaeophytin by fluorescence. Deep Sea Research and Oceanographic Abstracts 10(3): 221-231.

Zapata M., S.W. Jeffrey, S.W. Wright, F. Rodriguez, J.L. Garrido and L. Clementson (2004) Photosynthetic pigments in 37 species (65 strains) of Haptophyta: implacations for oceanography and chemotaxonomy. Marine Ecology Progress Series, 270: 83-102.

Zondervan I., R. E. Zeebe, B. Rost and U. Riebesell (2001) Decreasing marine biogenic calcification : A negative feedback on rising atmospheric $pCO_2$. Global Biogeochemical cycles 15: 507-516.